②

Final Report
SRO-IV PROGRAM
Contract No. N0014-85-K-0412

COHERENT STRUCTURES, CHAOS AND
THE ROLE OF MODERN DYNAMICS IN
TURBULENT SHEAR FLOWS

DTIC
ELECTE
APR 25 1990
S
D

Submitted to:

Dr. Michael M. Reischman
Office of Naval Research
Mechanics Division, Code: 1132F
800 N. Quincy Street
Arlington, VA 22217-5000

Principal Investigators:

Hermann F. Fasel
Department of Aerospace and
  Mechanical Engineering

Alan C. Newell
Department of Mathematics

MARCH 1, 1988 - FEBRUARY 28, 1989

ENGINEERING EXPERIMENT STATION
COLLEGE OF ENGINEERING AND MINES

THE UNIVERSITY OF ARIZONA

TUCSON, ARIZONA 85721

90 04 23 047

REPORT DOCUMENTATION PAGE

1a. REPORT SECURITY CLASSIFICATION	1b. RESTRICTIVE MARKINGS
Unclassified	

2a. SECURITY CLASSIFICATION AUTHORITY	3. DISTRIBUTION/AVAILABILITY OF REPORT
2b. DECLASSIFICATION/DOWNGRADING SCHEDULE	N/A

4. PERFORMING ORGANIZATION REPORT NUMBER(S)	5. MONITORING ORGANIZATION REPORT NUMBER(S)
	N/A

6a. NAME OF PERFORMING ORGANIZATION	6b. OFFICE SYMBOL (If applicable)	7a. NAME OF MONITORING ORGANIZATION
University of Arizona		N/A

6c. ADDRESS (City, State and ZIP Code)	7b. ADDRESS (City, State and ZIP Code)
Department of Aerospace & Mechanical Engrg. Tucson, Arizona 85721	

8a. NAME OF FUNDING/SPONSORING ORGANIZATION	8b. OFFICE SYMBOL (If applicable)	9. PROCUREMENT INSTRUMENT IDENTIFICATION NUMBER
Office of Naval Research		

8c. ADDRESS (City, State and ZIP Code)	10. SOURCE OF FUNDING NOS.			
Mechanics Division, Code 1513:LHO 800 N. Quincy Street Arlington, VA 22217-5000	PROGRAM ELEMENT NO.	PROJECT NO.	TASK NO.	WORK UNIT NO.

11. TITLE (Include Security Classification)
Coherent Structures, Chaos and the Role of Modern Dynamics in Turbulent Shear Flows

12. PERSONAL AUTHOR(S)
Hermann F. Fasel and Alan C. Newell

13a. TYPE OF REPORT	13b. TIME COVERED	14. DATE OF REPORT (Yr., Mo., Day)	15. PAGE COUNT
Final	FROM 3/1/88 TO 2/28/89	March 2, 1990	108

16. SUPPLEMENTARY NOTATION

17. COSATI CODES			18. SUBJECT TERMS (Continue on reverse if necessary and identify by block number)
FIELD	GROUP	SUB. GR.	

19. ABSTRACT (Continue on reverse if necessary and identify by block number)

In this report investigations are discussed that were carried out to shed light on the dynamics of coherent structures and to explore the role of modern dynamics in turbulent shear flows. Toward this end, a Proper Orthogonal Decomposition Technique was developed and applied to a forced plane mixing layer.

Further, theoretical studies were undertaken to understand the turbulent dissipation rates and the random occurrence of coherent events.

20. DISTRIBUTION/AVAILABILITY OF ABSTRACT	21. ABSTRACT SECURITY CLASSIFICATION
UNCLASSIFIED/UNLIMITED ☐ SAME AS RPT. ☐ DTIC USERS ☐	

22a. NAME OF RESPONSIBLE INDIVIDUAL	22b. TELEPHONE NUMBER (Include Area Code)	22c. OFFICE SYMBOL
Dr. Michael M. Reischmann, Code: N00014	(202) 696-4406	ONR

DD FORM 1473, 83 APR   EDITION OF 1 JAN 73 IS OBSOLETE.

TABLE OF CONTENTS

Accesion For	
NTIS CRA&I	☑
DTIC TAB	☐
Unannounced	☐
Justification	
By per call	
Distribution /	
Availability Codes	
Dist	Avail and / or Special
A-1	

a) SCIENTIFIC RESEARCH GOALS

The main objective of this research is to investigate the relationships between modern concepts of nonlinear dynamical systems, chaos theory and fully turbulent boundary layers. The approach that we are taking is to search for a connection between strange attractors and the large-scale coherent structures which appear to play a dominant role in the dynamics of turbulent shear flows. Within the framework of this research contract we are attacking the high Reynolds number turbulent boundary layer from two fronts: (i) From the lower Reynolds number transitional boundary layers, which have the proper flow geometry but a lower Reynolds number and therefore lower dimensional dynamics; and (ii) from the high Reynolds number free shear layer flows, which have a simpler flow geometry than the fully turbulent boundary layer, but for which the coherent structures and their dynamics appear to be much simpler. Because of the somewhat reduced complexity, investigating these flows first will offer a far better opportunity to establish a connection of transitional and/or turbulent behavior with low-dimensional strange attractors. With the experience and understanding gained from these simpler flows, we will then be in a position to successfully attack the fully turbulent boundary layer.

b) <u>MAJOR PROGRESS IN THE PAST YEAR</u>

Continuation of build-up and/or modification of various facilities for investigating coherent structures and their connection to chaos:

i) Shear-layer facility (water) with extensive use of various flow visualization techniques and advanced measurement techniques (LDV, particle tracking, etc.). (A. Glezer)

ii) Jet facility (air). (R. A. Petersen)

iii) Wind tunnel (air) for wake studies. (F. Champagne, I. Wygnanski)

iv) New water channel for investigation of boundary layer transition. (H. Fasel, A. Glezer, R. A. Petersen)

v) New versatile water channel for wakes (plane and axisymmetric), shear layers, etc. (F. Champagne, A. Glezer, R. A. Petersen, I. Wygnanski)

<u>Experimental Investigations</u>

- Connection between correlation dimension and large coherent structures in jet flows via the use of diagnostic tools. (R. Petersen, I. Wygnanski, H. Fiedler.)

- Application of the proper orthogonal decomposition technique to a harmonically forced plane mixing layer. (A. Glezer and A. Pearlstein)

<u>Theoretical Work in Progress</u>

- Dynamics and Stability of Soliton Solutions of the Damped and Driven Sine-Gordon Equation. (D. McLaughlin, A. Pearlstein)

- Development of Numerical Methods for Determining Dimensions,
  Attractors from "Real" Data (data from experiments, or Navier-
  Stokes simulations). (S. Lichter, D. Rand, A. Newell)

- Coherent Mode — Stochastic Mode Decomposition of Turbulent
  Fields. (A. Newell)

- Development of Navier-Stokes Methods for Investigating Dynamics
  of Coherent Structures in Free Shear Layers and Wakes. (H.
  Fasel)

- Development of Navier-Stokes Methods for Simulating Later
  Stages of Transition (appearance of random motion). (H. Fasel)

- Nonperiodic Flow Generated by an Oscillating Two-Dimensional
  Cylinder. (A. Pearlstein)

- Development of chaos diagnostic tools that incorporate spatial
  information (i.e., spatial coherence) and application to
  transitional and turbulent jets. (D. Rand, J. Caputo, R.
  Petersen)

c) PLANS FOR NEXT YEAR'S RESEARCH

All the work listed under b is in progress and will be
continued in the coming year.

Newly added activities will be:

- Chaos diagnostics and analysis of numerical data obtained from
  Navier-Stokes simulation of laminar-turbulent transition in
  boundary layers. (A. Glezer, A. Pearlstein, H. Fasel)

- Development of numerical model for simulations of transition
  and turbulence in axisymmetric jets (to allow direct comparison
  with jet experiments). (H. Fasel and R. Li)

- Phase space statistics analysis of data from jet experiments
  (R. Petersen)

(d,e,f,g) List of Publications, Reports, Presentations

List of Major Publications/Reports/Presentations of Participants in This Research

1. Papers Published in Refereed Journals:

H. Fasel

"Generation of Three-Dimensional, Spatially Amplified Disturbance Waves by Periodic Flowing and Suction in a Flat Plate Boundary Layer," with U. Konzelmann and U. Rist), ZAMM 67, p. 298, (1987).

"The Influence of Wall Temperature on the Development of Tollmien-Schlichting Waves in Boundary Layer Flows," (with H. Bestek and P. Dittrich), ZAMM 67, p. 256, (1987).

"Breakdown of a Two-Dimensional Laminar Separation Bubble in a Flat Plate Boundary Layer," (with K. Gruber), ZAMM 67, p. 286, (1987).

"Numerical Investigation of the Three-Dimensional Development in Boundary Layer Transition," (with U. Rist and U. Konzelmann), AIAA Paper 87-1203, (1987).

"Interaction Between a Tollmien-Schlichting Wave and a Laminar Separation Bubble," (with K. Gruber and H. Bestek), AIAA Paper 87-1256, (1987).

"Nonlinear Interactions of Two-Dimensional Tollmien-Schlichting Waves in a Flat Plate Boundary Layer,: (with J. Currle and A. Thumm), ZAMM 68 (to be published in 1988).

"Numerical Investigation of the Stability of Taylor Vortex Flow in a Wide Gap," (with J. A. Meyer), ZAMM 68 (to be published in 1988).

"Numerical Simulation of Subharmonic Resonance in Boundary Layer Transition," (with U. Konzelmann and U. Rist), ZAMM 68, (to be published in 1988).

"Numerical Simulation of the Boundary Layer Transition Process Near the Secondary Instability," (with U. Rist and U. Konzelmann), ZAMM 68, (to be published in 1988).

"Numerical Investigation of the Onset of Chaos in the Flow Between Rotating Cylinders," (with E. Laurien), ZAMM 68 (to be published in 1988).

A. Glezer

"On the Formation of Vortex Rings," accepted Phys. Fluids.

"On the Breakdown of the Wave Packet Trailing a Turbulent Spot in a Laminar Boundary Layer," (with Y. Katz, and I. J. Wygnanski), accepted J. Fluid Mechanics.

D. McLaughlin

"On the Weak Limit of Rapidly Oscillating Waves," (with L. Chierchia and N. Ercolani), to appear in *Duke Math. J.*, 1988.

"Geometry of the Modulational Instability. Part 1: Local Results; Part 2: Global Results," (with N. Ercolani and M. G. Forest) submitted to *Comm. Pure Appl. Math.*, 1988.
Part 1 also *Memoirs of the AMS*, 1988 and Part 2 *Memoirs of the AMS* 1988 and *Physica D* 1988 "Connection Between Homoclinic Structure of Isospectral Set, in Instabilities.

"Geometry of the Modulational Instability, Part 3: Homoclinic Orbits for the Period Sine-Gordon Equation," (with N. M. Ercolani and M. G. Forest) to appear *Physica D*, 1988.

"A Quasi-periodic Route to Chaos in a Near Integrable PDE," (with A. Bishop, M. G. Forest, and E. Overman), *Physics Lett. A*, Vol. 126. pp. 335-340, 1988.

"Stability and Bifurcation of Time-periodic Solutions of the Damped and Driven Sine-Gordon Equation," (with A. Pearlstein and G. Terrones) preprint, Univ. of Ariz., 1988.

"Stability and Bifurcation of Spatially Coherent Solutions of the Damped-Driven NLS Equation," (with G. Terrones and A. Pearlstein, in preparation.

"Notes on Melnikov Integrals for Models of the Driven Pendulum Chain," (with N. M. Ercolani and M. G. Forest) preprint, Univ. of Ariz., 1988.

"Chaos in a Perturbed Sine-Gordon Equation and in a Truncated Modal System," (with A. R. Bishop, R. Flesch, M. G. Forest, and E. A. Overman II) preprint, Los Alamos, 1987.

"Modal Representations of Chaotic Attractors for the Driven Damped Pendulum Chain," (with A. R. Bishop, M. G. Forest, and E. A. Overman II) preprint, Ohio State University , 1988.

"Finite Amplitude Modal Equations for Nearly Integrable PDE's," (with N. M. Ercolani and M. G. Forest) preprint, Ohio State University, 1988.

A. Newell

"Fixed Points and Chaotic Dynamics of an Infinite Dimensional Map," (with J. W. Moloney, H. Adachihara, and D. W. McLaughlin, *Chaos, Noise and Fractals*, pp. 137-186, 1987.

"A Calculus Curriculum for the Nineties," (with D. Lovelock) *Proceedings NRC-MAA "Calculus Curriculum."* Oct. 1987.

"Snell's Laws at the Interface Between Nonlinear Dielectrics," (with A. B. Aceves and J. V. Moloney), *Physics Letters A*, Vol. 129, No. 4, 1988, pp. 231-235.

"Reflection and Transmission of Self-focused Channels at Nonlinear Dielectric Interfaces, (with A. B. Aceves and J. V. Moloney).

"Trajectories of Surface Waves at the Interface Between Nonlinear Dielectrics (with A. Aceves and J. Moloney), submitted to Physics Review Letters.

"Wavenumber Selection of Convection Rolls in a Box," (with W. Arter and A. Bernoff), accepted Physics of Fluids Letters.

"Numerical Simulation of Rayleigh-Benard Convection in Shallow Tanks, (with W. Arter), accepted Physics of Fluids.

"Solitary Waves as Fixed Points of Infinite-Dimensional Maps for an Optical Bistable Ring Cavity: Analysis," (with H. Adachihara, D. W. McLaughlin, and J. V. Moloney), to appear J. of Mathematical Physics.

"Lax Pairs, Backlund Transformations and Special Solutions for Ordinary Differential Equations," (with J. D. Gibbon, M. Tabor, and Y. Zeng), to appear Nonlinearity.

"Turbulent Transport and the Random Occurrence of Coherent Events, (with D. Rand and D. Russell), to appear in special volume of Physica D. Nonlinear Phenomena, Sept. 1988.

"Theory of Beam Reflection, Transmission, Trapping, and Breakup at Nonlinear Optical Interfaces, (with A. B. Aceves and J. V. Moloney), to appear Optical Bistability I 1988.

"Turbulent Dissipation Rates and the Random Occurrence of Coherent Events," (with D. A. Rand and D. Russell), to appear Phys. Letters A.

A. Pearlstein

"Onset of Convection in Variable Viscosity Fluids: An Assessment of Approximate Viscosity-Temperature Relations," Physics of Fluids, 31, pp. 1380-1385, 1988.

"Stability of Free Convection Flows of Variable Viscosity Fluids in Vertical and Inclined Slots," (with Y,-M. Chen) accepted J. Fluid Mechanics.

"Temperature Distributions in a Laminar-Flow Tubular Photoreactor," (with F. Chen) accepted AIChE Journal.

"Low Peclet Number Heat Transfer in a Laminar Tube Flow Subjected to Axially Varying Wall Heat Flux," (with B. F. Dempsey) accepted J. Heat Transfer.

"Efficient Transformation of Certain Singular Polynomial Matrix Eigenvalue Problems," (with D. A. Goussis) accepted J. Computational Physics.

"Removal of Infinite Eigenvalues in the Generalized Matrix Eigenvalue Problem," (with D. A. Goussis) accepted J. Computational Physics.

2. Technical Reports:

H. Fasel

ONR Contract N00014-85-K-0412 yearly report, Mar. 1987

3. Presentations

a. Invited

. H. Fasel

"Navier-Stokes Simulations of Laminar-Turbulent Transition," International Symposium on Computational Fluid Dynamics, Sydney, Australia, 14-17 August 1987.

"Numerical Investigation of Stability and Transition in Shear Flows," Euromech Colloquium on Boundary Layer Instability and Transition, Exeter, England, 21-25 Sept. 1987.

"Numerical Investigation of Transition in Wall Bounded Sheer Flows," Calif. Inst. of Technology, April 1988.

"Numerical Simulation of Breakdown to Turbulence," Illinois Institute of Technology, Chicago, Ill., May 1988.

"Stability and Transition and Transition Control in Shear Flows," McDonnell Douglas Research Labs, St. Louis, Mo., May 1988.

A. Glezer

DARPA/URI-Brown/Yale Conference on Turbulent Structures in Free Shear Flows and Their Detection by Proper Orthogonal Decomposition, Newport, RI, June 1988.

Cornell University, Mechanical and Aerospace Engineering Seminar, March 1988.

Princeton University, Mechanical and Aerospace Engineering Seminar, Dec. 1987.

D. McLaughlin

Joint Summer Research Conferences in the Mathematical Sciences, University of Colorado, 1987.

Second Howard University Symposium on Nonlinear Semigroups, Partial Differential Equations, and Attractors, 1987.

Summer School, 2 weeks of lectures, Ravello, Italy, 1987.

Math Colloquium, University of California, Davis, 1988.

Nonlinear Science Colloquium, University of California, San Diego, 1988.

Nonlinear Schroedinger Conference, France, 1988.

"Critical Level Sets of Integrable PDE's," Solitons in Physics and Mathematics, Minneapolis, Minn., Sept. 1988.

A. Pearlstein

Gordon Research Conference on Oscillations and Dynamic Instabilities in Chemical Systems, Plymouth, NH, July 1988.

DARPA/URI-Brown/Yale Conference on Turbulence Structures in Free Shear Flows and Their Detection by Proper Orthogonal Decomposition, Newport, RI, June 1988.

University of California, San Diego, Dept. of Applied Mechanics and Engineering Science, Feb. 1988.

Yale University, Applied Mechanics Colloquium, Nov. 1987.

b. Contributed

H. Fasel

"Nonlinear Interactions of Two-Dimensional Tollmien-Schlichting Waves in a Flat Plate Boundary Layer," (with J. Currle and A. Thumm), GAMM Conference, Stuttgart, April 1987.

"Numerical Simulation of Subharmonic Resonance in Boundary Layer Transition," (with U. Konzelmann and J. Rist), GAMM Conference, Stuttgart, April 1987.

"Numerical Investigation of the Onset of Chaos in the Flow Between Rotating Cylinders," (with E. Laurien), GAMM Conference, Stuttgart, April 1987.

"Numerical Investigation of the Stability of Taylor Vortex Flow in a Wide Gap," (with J. A. Meyer), GAMM Conference, Stuttgart, April 1987.

"Numerical Simulation of the Boundary Layer Transition Process Near the Secondary Instability," (with U. Rist and U. Konzelmann), GAMM Conference, Stuttgart, April 1987.

"Interaction Between a Tollmien-Schlichting Wave and a Laminar Separation Bubble," (with K. Gruber and H. Bestek), AIAA 19th Fluid Dynamics, Plasma Dynamics and Lasers Conference, Honolulu, Hawaii, 8-10 June 1987.

"Numerical Investigation of the Three-Dimensional Development in Boundary Layer Transition," (with U. Rist and U. Konzelmann), AIAA 19th Fluid Dynamics, Plasma Dynamics and Lasers Conference, Honolulu, Hawaii, 8-10 Jun. 1987.

"Numerical Investigation of Unsteady Separation in Boundary Layers," APS/DFD Meeting, Eugene, OR, Nov. 1987.

A. Glezer

"Evolution of a Pulsed Two-Dimensional Disturbance Superimposed on an Excited Turbulent Plane Mixing Layer," (with X. Gu and I. J. Wygnarski) APS/DFD Meeting, Eugene, OR, Nov. 1987.

"Concurrent Streamwise and Spanwise Forcing of a Turbulent.Mixing Layer," (with K. J. Nygaard and I. J. Wygnanski) APS/DFD Meeting, Eugene, OR, Nov. 1987.

"Application of the Proper Orthogonal Decomposition Technique to an Anharmonically Forced Plane Mixing Layer," (with Z. Kadioglu and A. J. Pearlstein) APS/DFD Meeting, Eugene, OR, Nov. 1987.

A. Pearlstein

"The Onset of Instability Via Three-Dimensional Disturbances in Parallel Shear Flows," APS/DFD Annual Meeting, Eugene, OR, Nov. 1987

"Control of Planform Selection by Boundary Anisotropy," (with A. Oztekin APS-DFD Annual Meeting, Eugene, OR, Nov. 1987.

"Application of the Proper Orthogonal Decomposition Technique to an Anharmonically Forced Plane Mixing Layer," (with Z. Kadioglu and A. Glezer) APS-DFD Annual Meeting, Eugene, OR, Nov. 1987.

"Modeling of Mass Transfer Controlled Electrodeposition on Masked Substrates," AIChE Annual Meeting, New York, Nov. 1987.

h) List of Participants

Principal Investigators:

    H. F. Fasel, Professor of Aerospace & Mechanical Engineering

    A. E. Newell, Professor of Mathematics

Faculty:

    A. Glezer, Assistant Professor, Aerospace & Mechanical Engineering

    D. McLaughlin, Professor of Mathematics

    A. Pearlstein, Assistant Professor, Aerospace & Mechanical Engineering

    R. Petersen, Assistant Professor, Aerospace & Mechanical Engineering

    D. Rand, Professor, University of Warwick, England
        (visiting for three months)

    D. Russell, Center for Nonlinear Studies, Los Alamos, N.M.
        (Mathematics Department)

    R. Li, Post-doc Assistant, Aerospace-Mechanical Engineering

Graduate Students:
Aero-Mech. Engineering:
    G. Terrones
    Z. Kadioglu
    J. Powell
    D. Dratler
    A. Godil

Applied Math:
    M. Aksman
    J. Powell
    G. Solomon

Appendix: Description of Research

DETAILED DISCUSSION OF SOME RESEARCH IN PROGRESS

Application of the Proper Orthogonal Decomposition Technique to an Anharmonically Forced Plane Mixing Layer

A. Glezer and A. Pearlstein (with Z. Kadioglu)
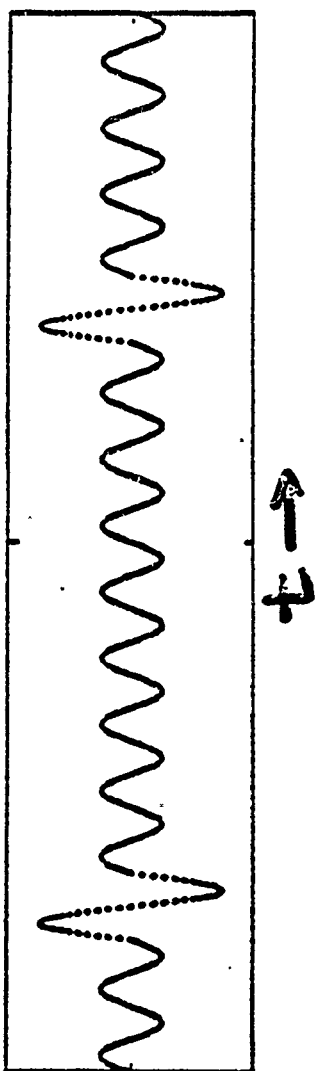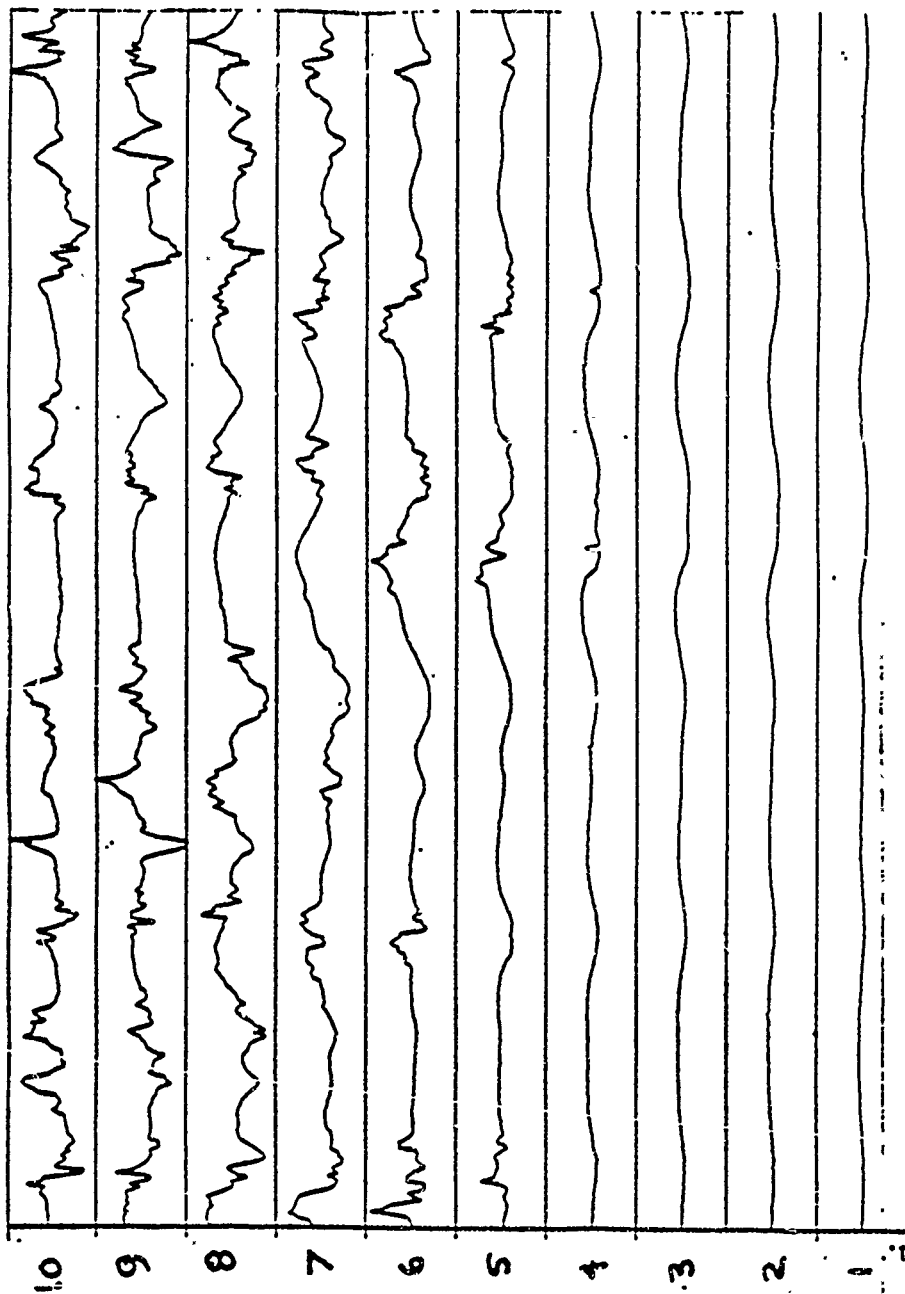
GOAL

Develop low order description of the dynamics of mixing layers.

MOTIVATION
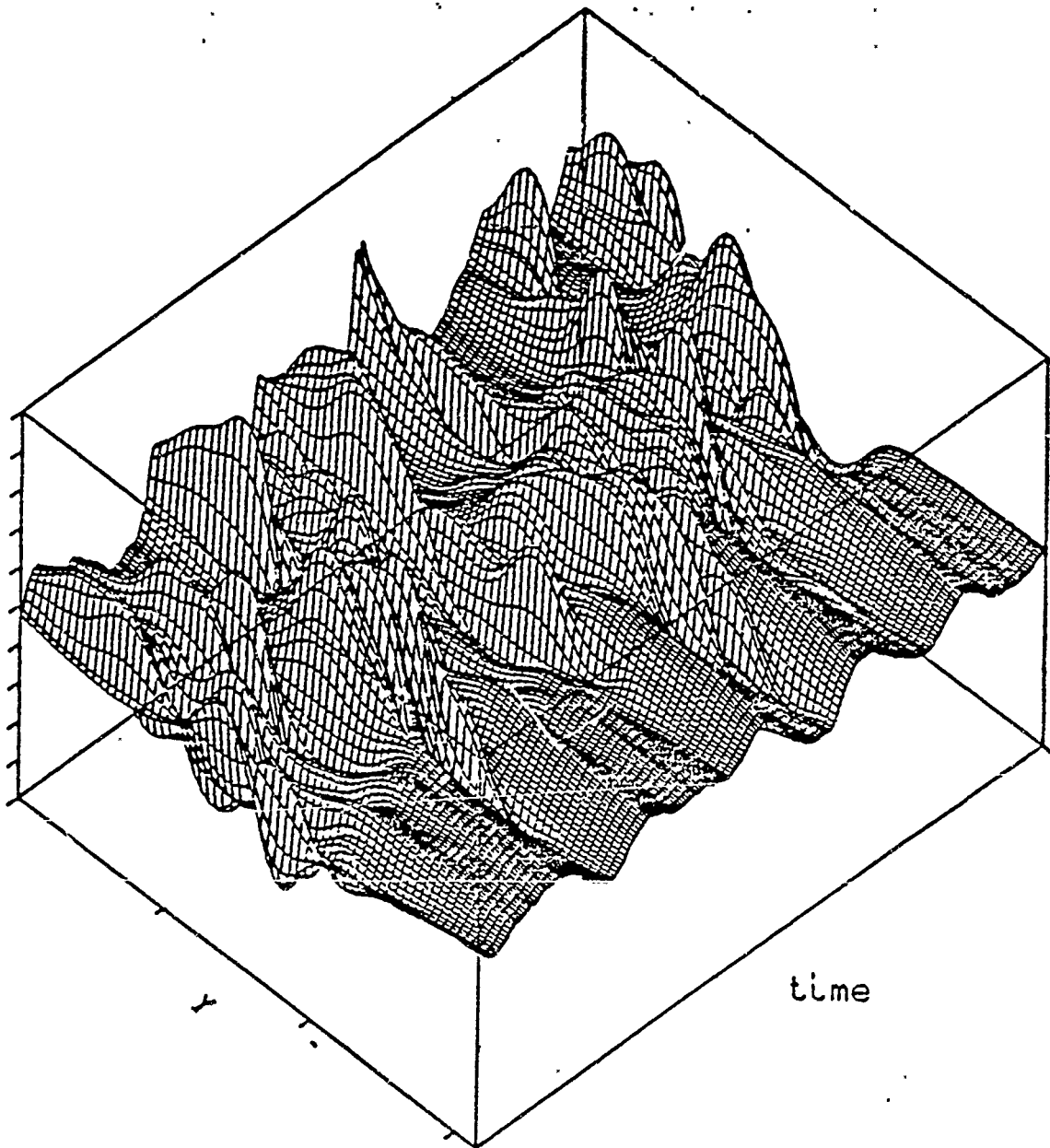
Improved controller design.

time →

Wire number

10 9 8 7 6 5 4 3 2 1

2
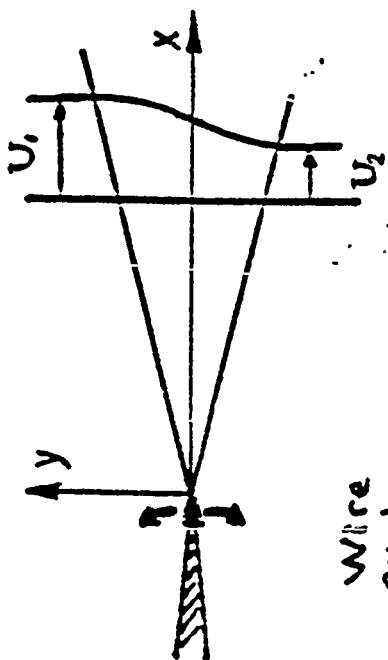
MEAN VELOCITY (mm/s)

MEAN VELOCITY (mm/s)

The avaliable data consists of 10 chanels of U(x,y,t)

Before Applying the P.O.D.

* Smoothing in time

* Piecewise polynomial fit in Y

* Subtract the mean velocity

the filtered velocity (u)(mm/s)

Y

time

4

APPLICATION OF THE P.O.D. TO THE DATA

Lumley(1967); Aubry, Holmes, Lumley & Stone (1986)

Previous applications have been to fully developed turbulent flows that are :

* Statistically Homogeneous in Two Directions
* Statistcally Stationary

DESCRIPTION OF THE P.O.D.

$$
A = \begin{pmatrix}
U(1,1) \dots\dots\dots\dots\dots\dots\dots\dots\dots U(1,n) \\
\dots\dots\dots\dots\dots\dots\dots\dots\dots\dots\dots\dots \\
\dots\dots\dots\dots\dots\dots\dots\dots\dots\dots\dots\dots \\
\dots\dots\dots\dots\dots\dots U(y,t)\dots\dots\dots\dots\dots \\
\dots\dots\dots\dots\dots\dots\dots\dots\dots\dots\dots\dots \\
U(m,1) \dots\dots\dots\dots\dots\dots\dots\dots\dots U(m,n)
\end{pmatrix}
$$

Singular Value Decomposition of A (SVD) is equivalent to computing the eigen values of $A \cdot A^T$

The eigen values measure energy or action in correponding eigen vectors (spatial modes) .

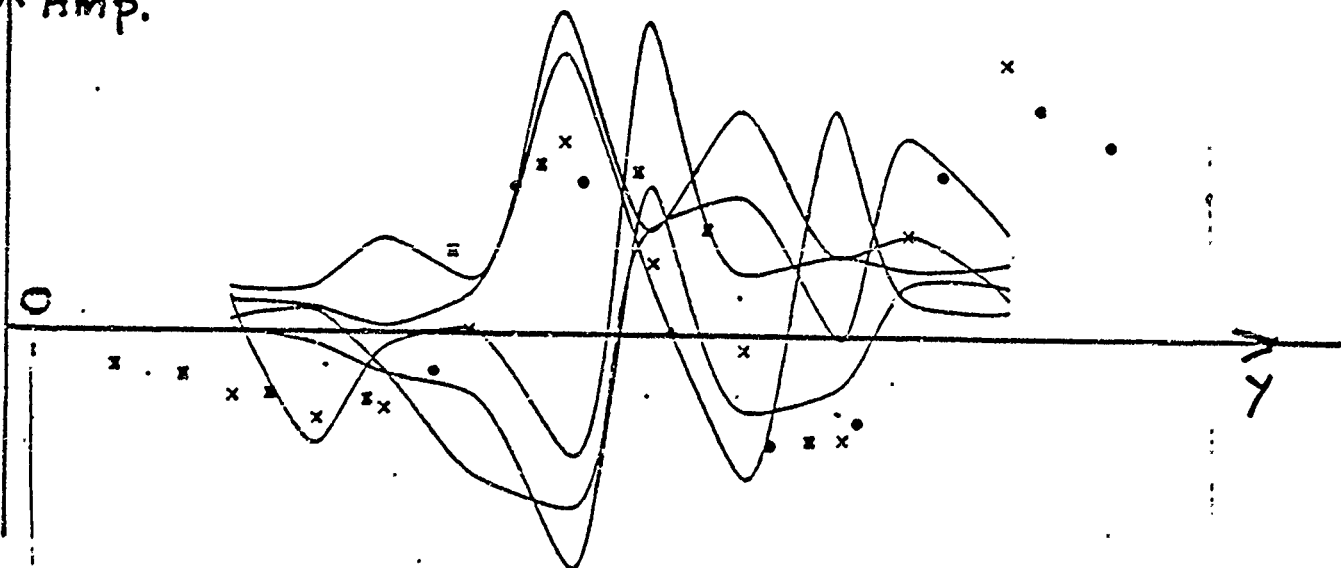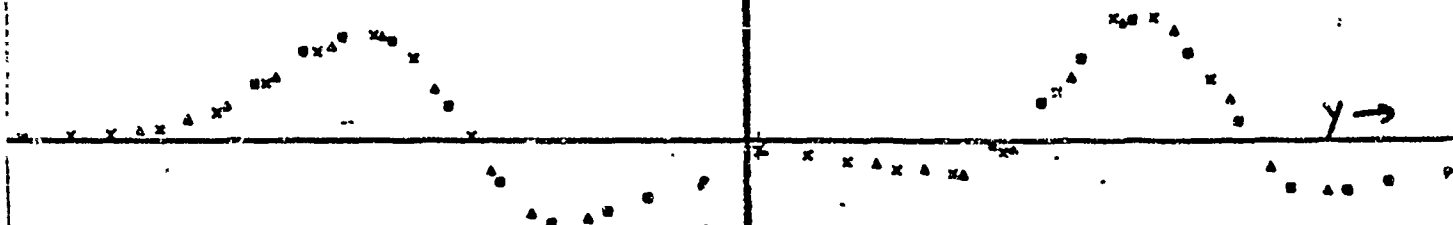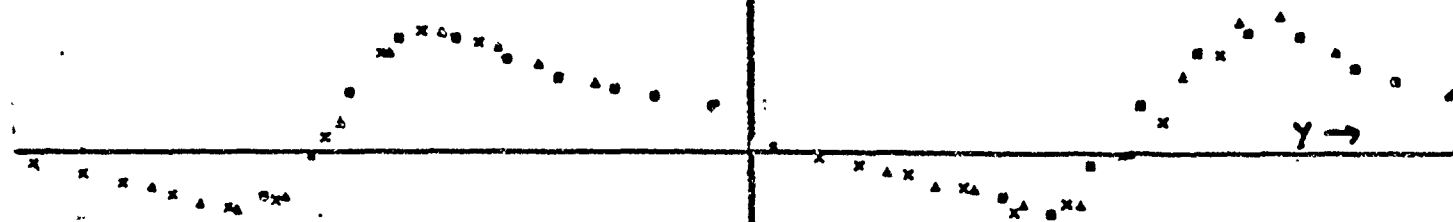Eigen vectors constitute an orthogonal basis for representing $U(x,y,t)$.
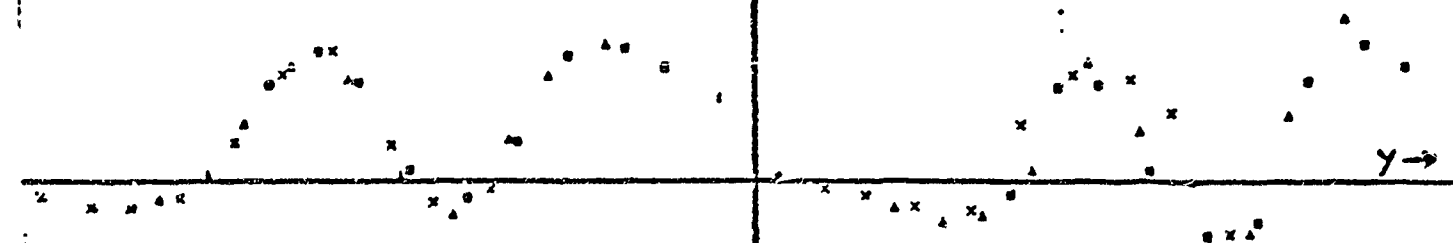
5
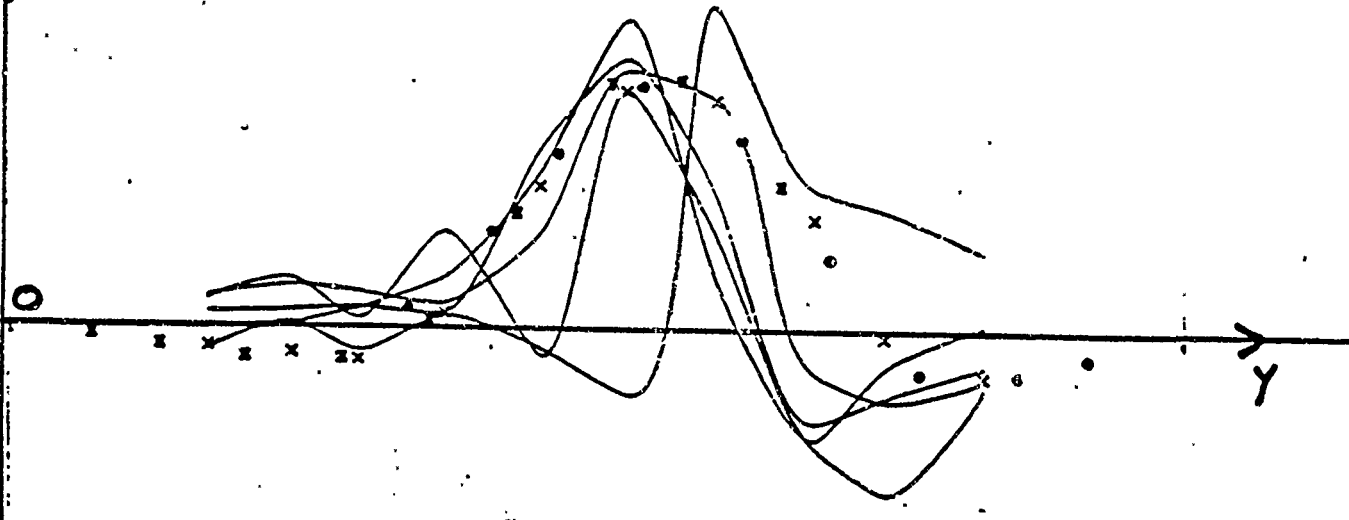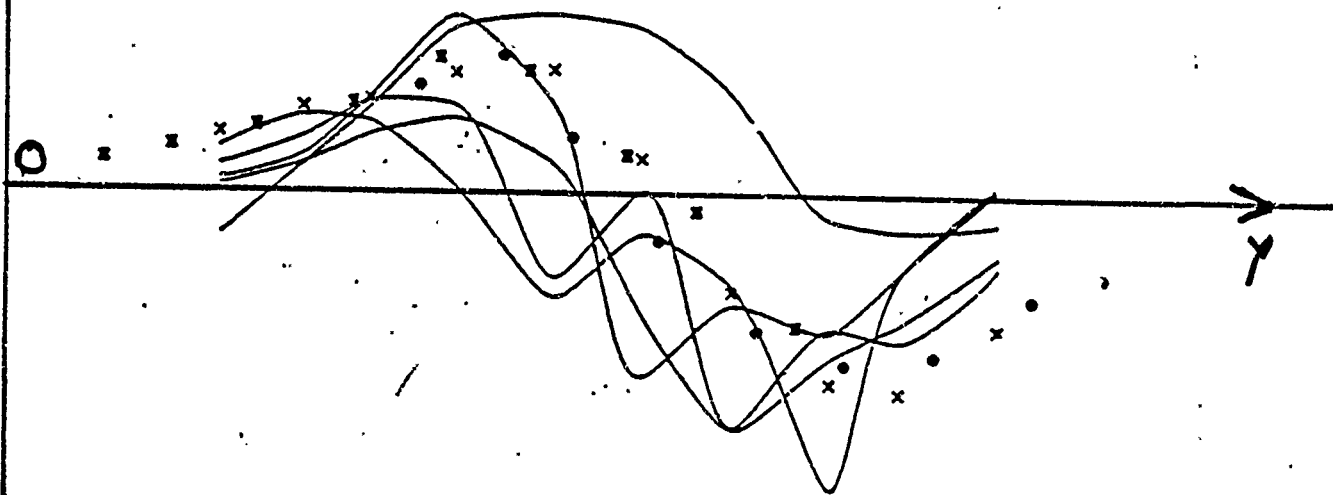
512 time points   64 time points

Amp.

Amp.

Amp.

Y→

Y→

Y→

cumulative energy in first n modes

o   n=1
△   n=2
+   n=3

energy (% of total)

wire number

8 time

cumulative energy in first n modes

o   n=1
△   n=2
+   n=3

10
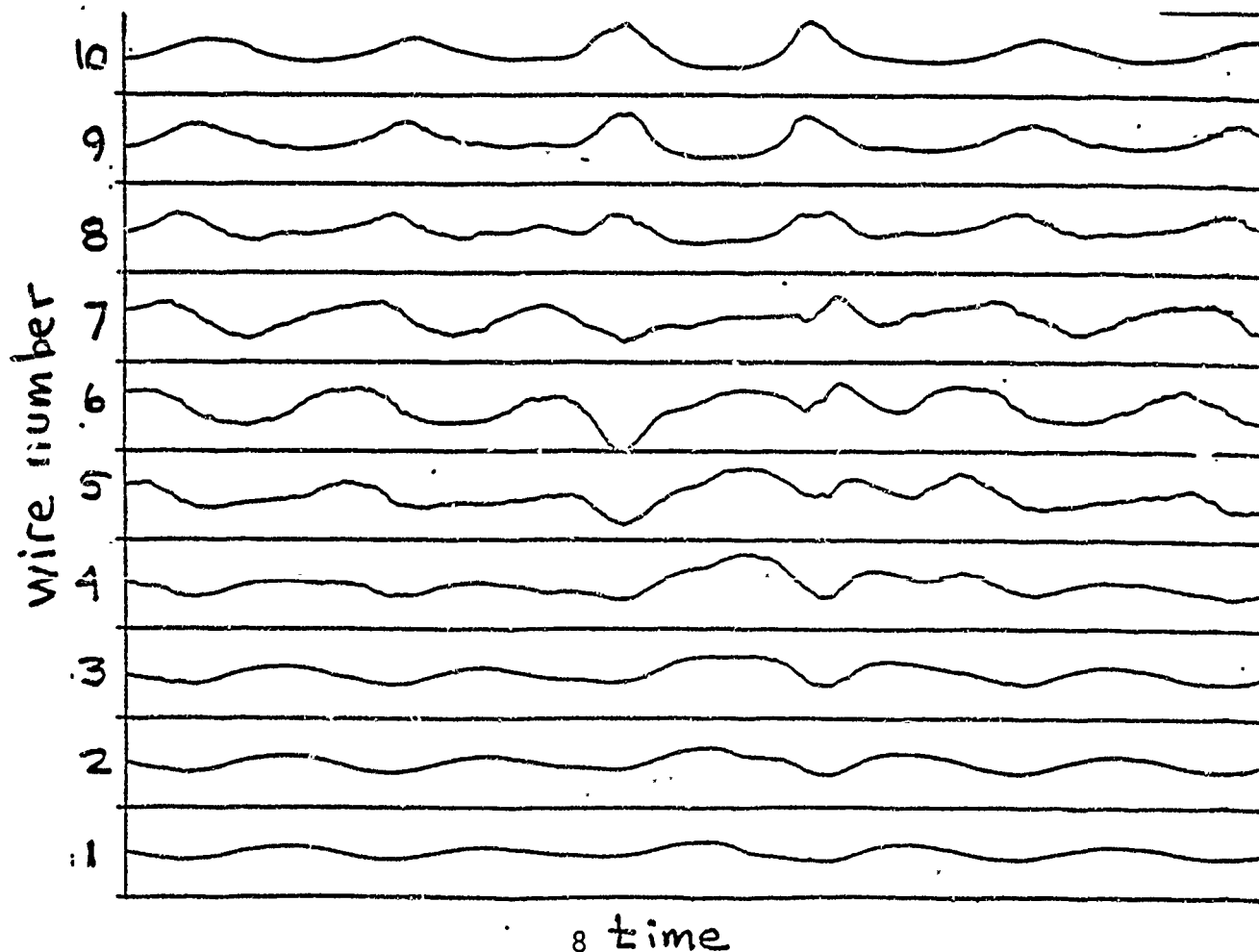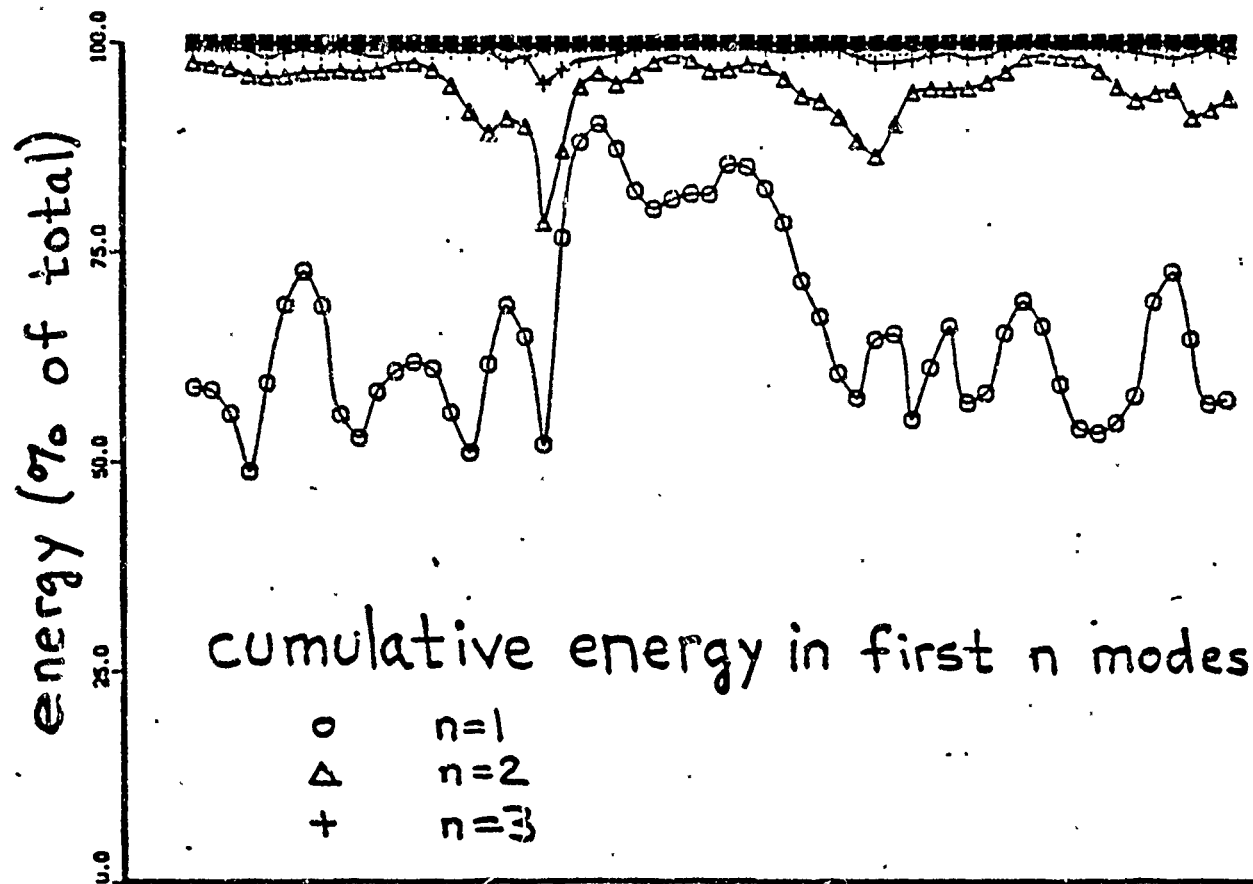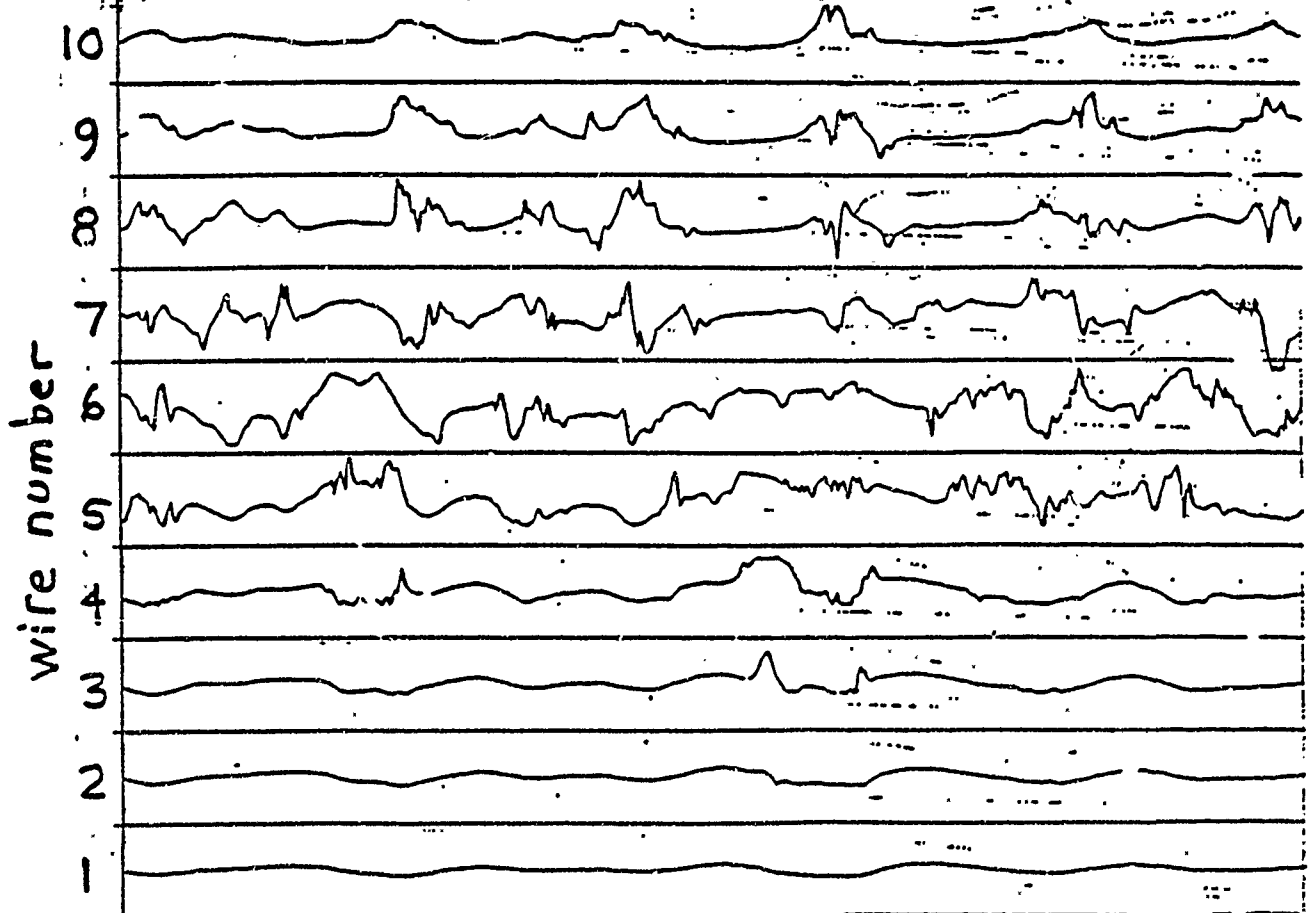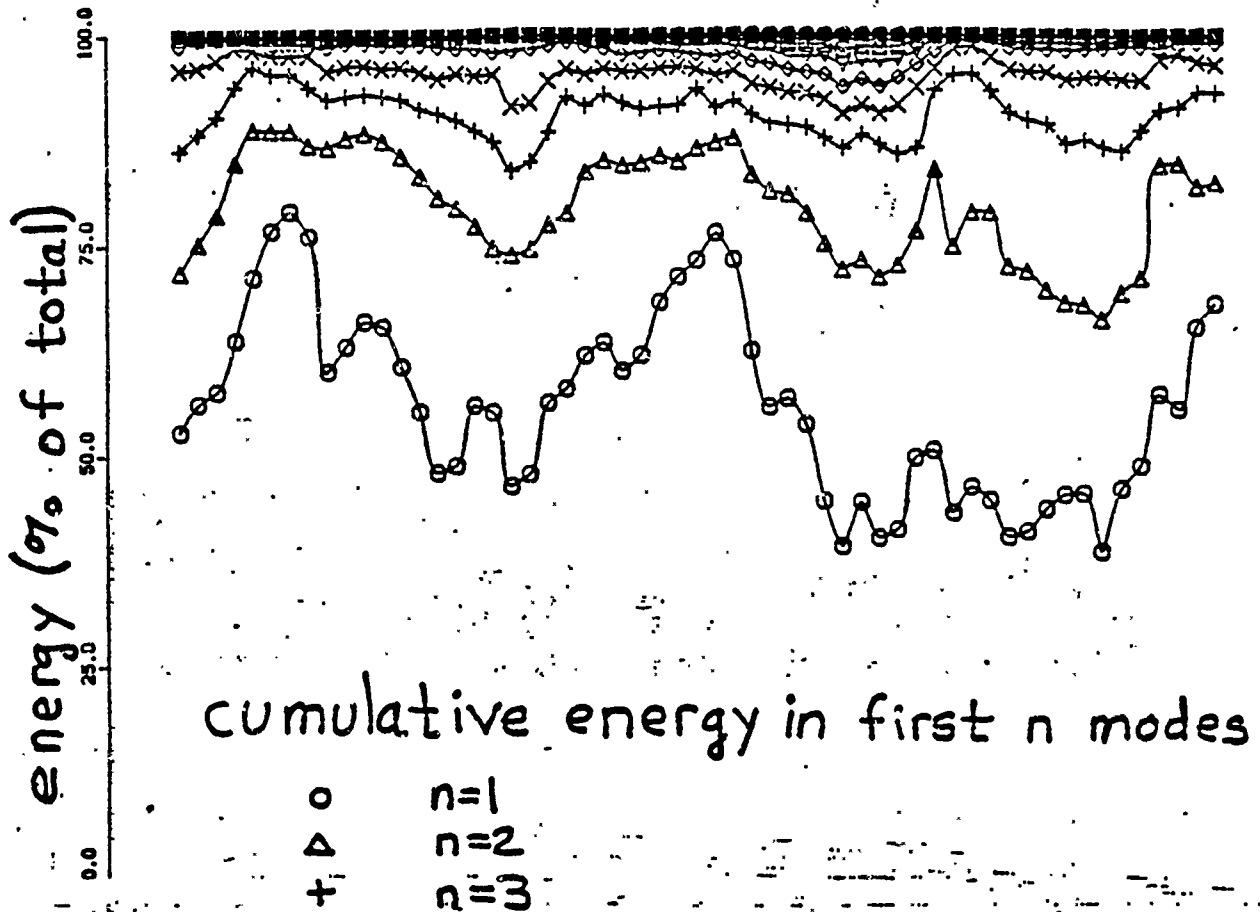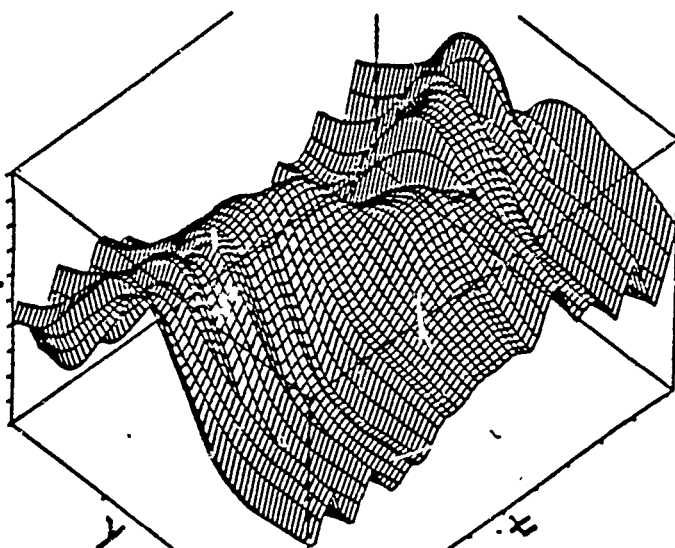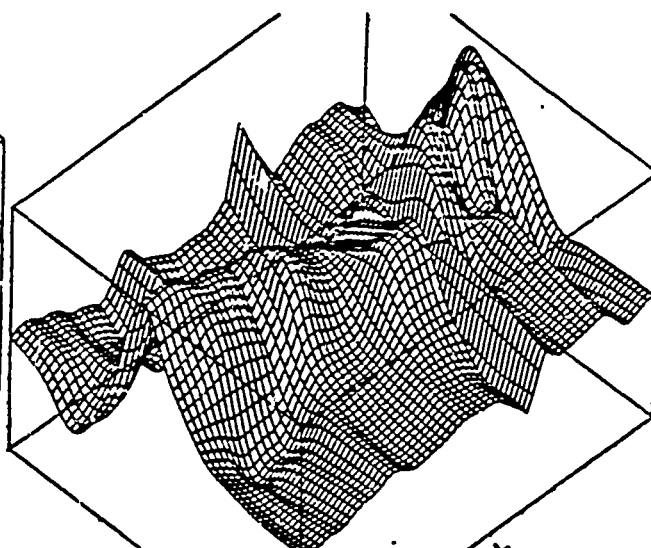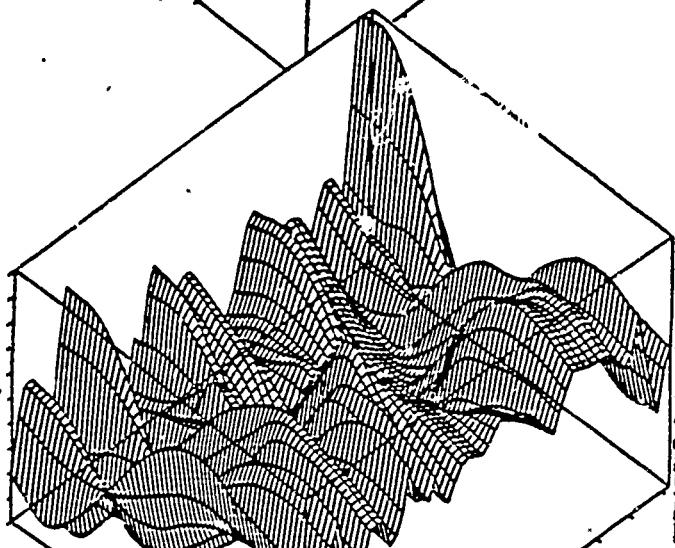
Conclusions

- Can apply POD to nonstationary, nonhomogenous turbulent flows

- Can represent flow by superposition of small number of POD modes

- Can use small part of temporal record to generate POD modes.

11

Turbulent Dissipation Rates
and the Random Occurrence of Coherent Events
by

Alan C. Newell, David A. Rand*, David Russell †
Department of Mathematics
University of Arizona
Tucson, AZ 85721

Abstract

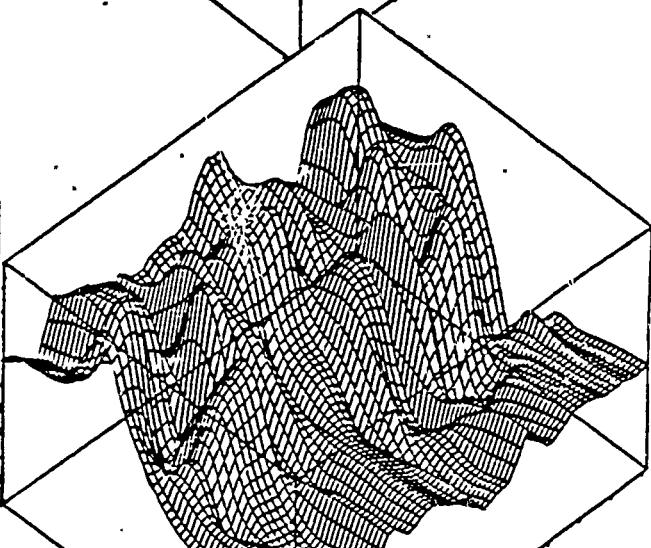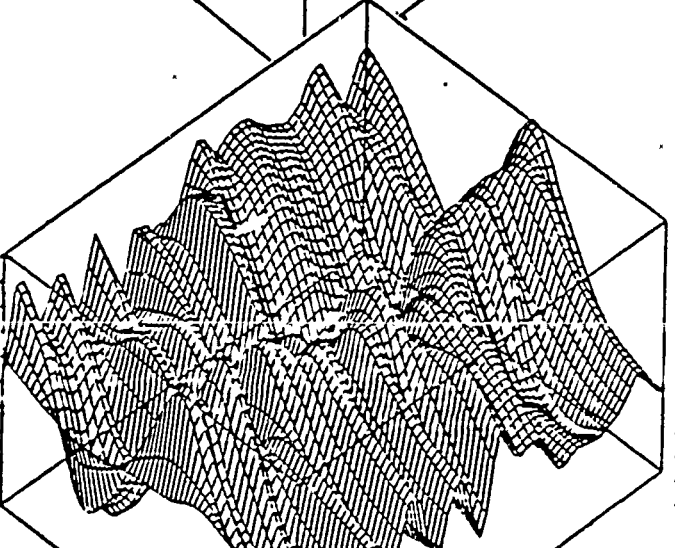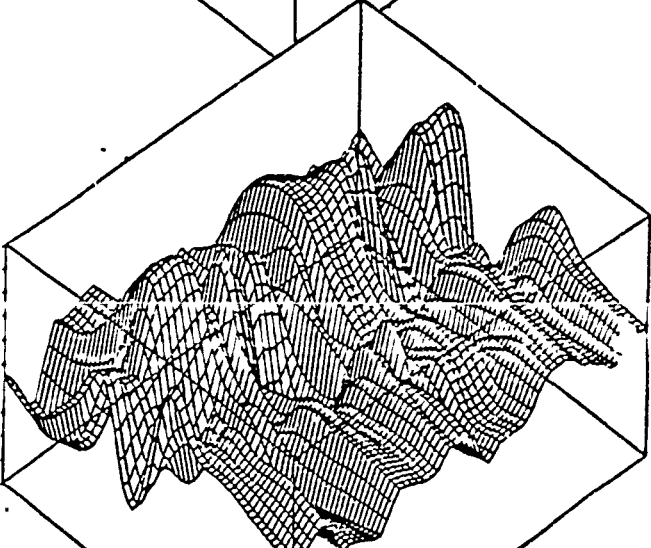In this letter, we suggest that the transport properties and dissipation rates of a wide class of turbulent flows are determined by the random occurrence of coherent events that correspond to certain orbits which we call homoclinic excursions in the high dimensional strange attractor. Homoclinic excursions are trajectories in the non-compact phase space that are attracted to special orbits which connect saddle points in the finite region of phase space to infinity and represent coherent structures in the flow field.

Introduction

It is generally accepted that turbulence in shear flows at Reynolds numbers of 10^3 and higher has a large number of active degrees of freedom. Although estimates of Lyapunov and Hausdorff dimensions are strictly upper bounds, the rapid loss of spatial correlations over distances of the Taylor microscale $R^{-\frac{1}{2}}$ and the broadband wavenumber spectrum suggest that many modes are playing an active role in the dynamics. The $R^{\frac{9}{4}}$ estimate [1], which is consistent with the intuitive idea of Landau that it is necessary to resolve a turbulent flow field in a box of volume V down to the Kolmogoroff inner scale of $(\nu^3/\varepsilon)^{\frac{1}{4}}$ (ν is kinematic viscosity, $\varepsilon = \nu \int_V |\nabla u|^2 d\bar{x}$ is the energy dissipation rate and is independent of ν for a large range of large Reynolds numbers), means that if R is 10^4, $R^{\frac{9}{4}}$ is a billion! It is unlikely that replacing the Navier-Stokes equations by a system of a billion o.d.e.s. will either bring much insight into the nature of turbulence or make it possible to calculate the invariant measure on the attractor needed to compute averages. Therefore, whereas the concept of a strange attractor on which the flow is everywhere unstable and ergodic is a valuable and necessary one, a new idea is needed if one is to be able to compute in a practical way average flow quantities and in particular those averages which represent transport properties, the flux of heat across a convection

*Present Address: Nonlinear Systems Laboratory, Warwick University, Coventry, CV4 7AL United Kingdom

† Present Address: Center for Nonlinear Studies, Los Alamos, NM 87545

layer, momentum across a boundary layer, angular momentum between cylinders rotating at different velocities, mass flux down a pipe or the amount of heavier fluid which falls through a lighter one. It is also important to calculate the dissipation rate which, in systems where energy is fed in at low wavenumbers and removed at high ones, is equivalent to computing the flux or cascade of energy across any middle wavenumber. One of the main goals of a turbulence theory is to predict the transport and the dissipation rate as a function of the applied stress. The purpose of this paper is to suggest one new avenue of approach to these problems of transport in physical and wave space.

The basic idea is fairly simple. There is some evidence that, in a variety of situations, transport is associated with organized flow structures. If this is the case, one would like to identify and isolate those parts of the attractor and those orbits in phase space which are the principal contributors to a particular flux. In this letter we focus on a class of such special orbits which connect saddle points in the finite part of phase space to infinity and which are the principal contributors to the dissipation rate. The ideas are first illustrated in terms of a simple, but nontrivial, example , the two dimensional forced, damped, nonlinear Schrödinger (NLS) equation

$$\psi_t - i\nabla^2\psi - i|\psi|^2\psi = F - D \tag{1}$$

which arises in models of Langmuir turbulence. Although this model is a poor approximation to the full Zakharov equations on several counts, it nevertheless retains the essential feature, emphasized for many years by Soviet colleagues [2], that, in the limit of strong ion damping, dissipation is mainly due to the collapse of filaments rather than energy transfer to high wavenumbers by resonant wave-wave interactions. The filaments are closely related to an exact, singular, localized solution of the unperturbed and conservative NLS equation (1), whose modulus has the shape

$$|\psi(\vec{x},t)| = \lambda^{-1}R(\eta) , \quad \eta = \lambda^{-1}|\vec{x} - \vec{x}_0| \tag{2}$$

near the blow-up point $\vec{x}_0$. In (2), $R(\eta)$ is the unique solution of $R'' + \eta^{-1}R' - R + R^3 = 0, R'(0) = 0, R(\infty) = 0$ without zeros in $(0,\infty)$ and $\lambda(t)$ is a time dependent function which becomes zero after a finite time t_0. The rate of collapse $\lambda(t)$ has not been yet satisfactorily determined. The two most recent efforts [3] both agree that it has be form $f(t)(t_0 - t)^{\frac{1}{2}}$ where $f(t)$ tends to zero very slowly (e.g.$(\ln(t_0 - t))^{-1}$ or $(\ln\ln(t_0 - t))^{-1}$) but differ on the exact asymptotic answer. A sufficient but not necessary condition for collapse is that the Hamiltonian $H = \int(|\nabla\psi|^2 - \frac{1}{2}|\psi|^4)d\vec{x}$ is negative. The negativity of H guarantees that $n_\psi = \int |\psi|^2 d\vec{x}$, also a constant of the motion for the NLS equation, is greater than the minimum power $p = 2\pi\int_0^\infty R^2\eta d\eta = 0.29$ needed to sustain collapse. If $n_\psi = p$, Weinstein [4] has shown that, if the solution blows up in finite time, then $\psi(\vec{x},t)$ converges to (2) in the H^1 norm. On the other hand, if $n_\psi < p$, global existence is assured

2

and no blow-up occurs. Our interest is in larger values of n_ψ. In particular, an initial condition which is a small perturbation of the unstable, monochromatic state $\psi = \psi_0 \exp(i\vec{k} \cdot \vec{x} + i(k^2 - |\psi_\iota|^2)t)$ in a square box of side length L with $\vec{k} = 2\pi L^{-1}(m,n)$, m,n integers ($m = n = 0$ corresponds to the $\vec{x}$ independent state) for which $n_\psi = |\psi_0|^2 L^2$ will develop approximately $n_\psi p^{-1}$ collapsing filaments, each having precisely the shape (2) near its collapse site $\vec{x}_0$ and time t_0. In the phase space of the unperturbed system, each collapsing filament will be represented by an orbit which joins the saddle point representing the unstable solution to infinity. We give these orbits a special name, heteroclinic connections to infinity or HCI's, because all orbits which escape to infinity are attracted to them even though the unperturbed system is conservative. In other words, all solutions of NLS which become singular in finite time have the shape (2) as they approach infinity. Of course, in the damped system, the singularity is never quite reached. Once the filament diameter is of the order of the Debye radius, Landau damping (represented by D in (1)) becomes important and the energy is transferred from the wavefield to electrons, a process know as burnout. The process of dissipation changes the attracting point at infinity to a repeller and the system returns to the finite part of phase space where it again comes under the influence of a saddle point and the cycle is repeated. We call these large excursions, from the finite part of phase space to the neighborhood of infinity and back again, homoclinic excursions. They are organized by the HCI's in the sense that as the trajectory approaches infinity, the corresponding solution in physical space approaches a very special shape and in particular the amount of energy it carries off to the dissipation cemetery at infinity is known. Before attempting to mathematize these notions any further, we present some numerical evidence to support our picture.

Numerical Results

We now turn to the main results of the numerical study. We integrated (1) using a split-step Fourier algorithm on a grid of $(128)^2$ points. The time step used was 10^{-4} and adequate to resolve the largest linear (k^2) and nonlinear ($|\psi|^2$) frequencies encountered in our simulations. Aliasing errors were judged to be insignificant by making spot comparisons with a dealiased code on a $(256)^2$ grid. More details are given in [5]. Energy is fed into the system at low k and removed at high k through F and D whose Fourier transforms are $\gamma_b(k)\psi_k$ and $\gamma_e(k)\psi_k$ respectively (ψ_k is the Fourier transform of $\psi(\vec{x},t)$). The support of $\gamma_b(k)$ is near $k = 0$ and the support of $\gamma_e(k)$ is beyond k_d where k_d is the Debye wavenumber. It turned out that in most of our simulations the global energy H (not a constant of motion for (1)) was positive during all time intervals in which there were collapse events. Figure 1 shows snapshots of $|\psi^2(\vec{x},t)|$ before, during and after the collapse. Figure 2 displays the instantaneous rate of dissipation $\gamma(t) \equiv 2\sum_{\vec{k}} \gamma_e(k)|\psi_k|^2$, its integral $\Gamma(t) \equiv -\int^t dt' \gamma(t')$, and the global maximum of $|\psi|^2$ over a time interval including several collapses in a strong-turbulent regime after transients have died out and

3

the system has reached a statistically steady state. $-\Gamma$ is just the energy lost due to dissipation as a function of time. Observe that a large fraction of the energy dissipation occurs in sudden jumps and is directly correlated to the collapse events. Energy $n_\psi \equiv \sum_{\vec{k}} |\psi_k|^2$ is considered to be dissipated due to collapse only if $\gamma > \gamma_0$, where γ_0 is a threshold parameter. If this inequality holds over the interval $[t_1, t_2]$, then the energy burnt out is $\Gamma(t_1) - \Gamma(t_2)$, and the total energy lost due to collapse for the entire simulation is the sum of all such differences. Denote this total energy lost due to collapse by δn_c and the total energy dissipated by δn. We have plotted the ratio $\delta n_c / \delta n$ as a function of γ_0 for several different turbulent regimes. As γ_0 decreases the ratio increases and is of course one at $\gamma_c = 0$. $\gamma_0 = 1$ was the smallest value that gave ratios judged to be free from contamination by non-collapse events for all cases studied, so it was chosen as the standard cut-off rate. With this choice of γ_0, as much as 80% of the total energy dissipated is dissipated by collapsing filaments in the most energetic case examined ($< n_\psi > \cong 10$). In the weakest case ($< n_\psi > \cong 5$) more than 70% of the dissipated energy was lost in burned out filaments. Furthermore, these estimates of the energy dissipation are conservative because we have not yet included the more gradual loss due to the decay of the high k remnant left over from the collapse. The reason for this remnant, peculiar to the nonlinear Schrödinger equation, is that a singular filament of this equation carries the minimum threshold energy p required to sustain collapse. (In contrast, the energy of a collapsing Zakharov filament, again a constant of the motion, can take on a continuous range of values above the critical threshold.) Therefore, when a significant portion of the filament's spectral energy lies in the dissipative range ($k > k_d$), some of its energy is lost, collapse is arrested and only a partial burnout occurs. It leaves behind a remnant in the form of broadened concentric cylindrical shells of field energy centered at the collapse site (see Figure 3). In order to follow the energy associated with the remnant, we monitored the field energy inside a small cell centered at the collapse site and observed that the burnout of the central part of the filament, or core, causes the fastest depletion of energy in the cell, but also that it is immediately followed by a slower depletion. The slower loss is primarily due to the fluxing of the remnant through the cell boundary. If we add the energy loss $rp, 0 < r \leq 1$, due to the burnout of the core to that carried out of the cell by the remnant, we obtain a total loss of energy in the cell very close to the total amount p carried by the collapsing filament. Figure 4 shows the disribution of r.

The remnant plays two roles in the dissipation process. First, it provides a nucleating center for new collapses, a fact we have verified by examining the spatial distribution of collapse sites. As a consequence the frequency of collapses increases. We found that for $\gamma_b(k) = 2\delta(k - 1)$ (the beam drives just the lowest wavenumber in the box), the distribution of collapse times is nearly Poisson with a mean time between events of $\omega_c^{-1} = < \tau > \simeq .08$. Second, the gradual damping of the remnant enhances the ambient dissipation rate $< \gamma_A >$ (i.e., the dissipation rate averaged over time intervals free from collapse) over that amount we would expect from other dissipative mechanisms. In order to verify this, we carried out the following

4

relaxation experiment. By changing the sign of the nonlinearity in equation (1) from plus to minus, we obtain a system with the same linear dispersion as the plus system and therefore presumably the same resonant wave interaction character but without the unstable modulational and nucleational instabilities (which will be discussed in the next section) and collapsing solutions. Initializing the two systems identically, we ran them with the forcing turned off ($\gamma_b = 0$) and compared their dissipation rates between collapses of the (+) system, before their energies had separated by more than 10% of the common initial value. The ambient dissipation rate of the (+) system was typically 50% greater than that of the non-collapsing (-) system while the collapse remnants were dissipated. Including collapse events in the tally, the (+) system lost energy three times as fast as the (-) system. We conclude, therefore, that the amount of energy dissipated by non-collapse events is at most one-quarter of the total energy dissipated. Therefore, the energy dissipation budget is as follows. The average total dissipation rate $< \gamma >= \omega_c < r > p + < \gamma_A >= \omega_c p < r > \frac{\delta n}{\delta n_c}$ since $\frac{\omega_c < r > p}{<\gamma>} = \frac{\delta n}{\delta n_c}$. $< \gamma >$ depends only on the mean turbulence level $< n_\psi >$ but, as we have pointed out, $< \gamma_A >$ and ω_c depend both on $< n_\psi >$ and the nature of the dissipation. The average function $< r >$ lost in burnout depends only on the latter. We plotted both $< \gamma >$ and ω_c as a function of $< n_\psi >$ and found that, as expected from above, the product $< \gamma > \omega_c^{-1}$ is almost independent of $< n_\psi >$. Futhermore it was equal to .13 which is equal to the product of p (which was .29), $< r >$ (which was .3) and $\frac{\delta n}{\delta n_c}$ (which was about 1.3). Graphs showing the loss of energy from a small cell surrounding the collapsing filament, $\frac{\delta n_c}{\delta n}$ as a function of γ_0, $< \gamma >$ and ω_c as a function of $< n_\psi >$, the distribution of collapse times, the angle-averaged correlation function and actual trajectories illustrating homoclinic excursions will be given elsewhere [5].

Whereas these results confirm the thesis that coherent collapse events dominate dissipation, the expense involved in two dimensional experiments did not allow us to run a sufficient number of simulations in order to determine in what limit, if any, $\frac{\delta n_c}{\delta n}$ approaches unity. In connection with this question, and in parallel with the ideas of DiPerna and Majda [6], one would also like to develop the notion of a weak solution in which solutions of the undamped equations could be continued beyond the collapse time by simply deleting the collapsed filament and lowering the L_2 norm of the solution by a fixed amount. In order to examine these questions, we simulated the one dimensional nonlinear Schrödinger and Zakharov models with quintic nonlinearities on grids of 1024 and 256 points respectively. Aliasing errors were removed by smoothly interpolating ψ onto a grid of 8×1024 or 256 points before forming the nonlinear frequency $|\psi|^4$. The results for NLS showed that, for the same turbulence levels, the percentage of the dissipation rate accounted for by collapses rose from 59% at $k_d = 128$ (where, because the dissipation effects are clearly felt in the early stages, there are many failed attempts to form collapsing filaments), to 72% for $k_d = 256$, to 82% for $k_d = 512$. The average loss of energy per collapse decreases with k_d (the amount of energy greater than k_d in the Fourier transform

5

of the collapsing filament decreases with increasing k_d) but the frequency of events increases proportionately so that the average dissipation rate remains the same. The evidence clearly suggests that in the large k_d limit, all the energy dissipated is dissipated by collapse events which occur infinitely often with infinitesemal losses of energy per event.

A much more striking result was obtained when we ran the very same experiment on the Zakharov model

$$\psi_t - i\psi_{xx} + i\rho\psi = F - \varepsilon D \tag{3}$$

$$\rho_{tt} + 2\nu \circ \rho_t - \rho_{xx} = (|\psi|^4)_{xx} \tag{4}$$

where F and D are as before and $2\nu \circ \rho_t$ is a convolution integral modelling ion damping. The ion acoustic field $\rho(x,t)$ is no longer slaved to the electric field intensity (for NLS, ρ in the equation (3) is replaced by $-|\psi|^4$). Therefore, during collapse, in which the fields take on a self-similar form close to (2) but in which the inertial acceleration ρ_{tt} is also important, the cavity formed by the ion field encourages total burnout of the filament (see Figure 5). We found that when $\varepsilon = 1, k_d = 32, < n_\psi > = 1.625$, the average energy $< r > p$ lost per event was 1.95, the average time between events was .83 and $\frac{\delta n_c}{\delta n}$ was 92%. (For the Zakharov model, the amount of energy carried in the filament, a constant of the motion for the unperturbed equations, can take on a range of values greater than the threshold value $p = .43$ in this case. Thus $r > 1$). The distribution of r rose sharply after $r = 1$, had a mean of 1.95/.43 and had a relatively long tail. Also, we observed that all the collapses occurred in 9 nonoverlapping sites, were driven by the nucleational instability (see the section after next for discussion), and the sites drifted about the box. When we increased k_d to 64, $< n_\psi > = 1.8$, the frequency of events increased to $(.69)^{-1}$ (there were 287 events in 198 time units) and the distribution of r came closer to one. The average energy lost per event was 1.57 units and $\frac{\delta n_c}{\delta n}$ was 95%. (In contrast, at the same parameter values and over 100 time units, the NLS model had 972 events with an average energy loss of .09 and $\frac{\delta n_c}{\delta n}$ was 72%.) Further, when we decreased ε to $\frac{1}{4}$ (again $k_d = 64$), the distribution of r came closer to threshold and $\frac{\delta n_c}{\delta n}$ was 98%. Also, for $\varepsilon = 1$, when k_d was increased to 128, $\frac{\delta n}{\delta n}$ was 98%. This leads us to conjecture that as k_d increases and ε decreases, the distribution of r will cluster about one, and that each collapsing event will burn off exactly the threshold energy $p = .43$. In this asymptotic limit, the weak solution of the unforced, undamped equation in which the turbulence eventually decays, is found by simply removing the collapsing filament from the field and reducing the L_2 norm by p. (The weak limit, i.e. $\psi(x, 0)$ is the weak limit of $\psi(x, \lambda)$ as $\lambda \to 0$ if $\int \varphi(x)\psi(x, 0)dx = \lim_{\lambda \to 0} \int \varphi(x)\psi(x, \lambda)dx$ where φ is smooth, of a collapsing filament is zero because it oscillates very fast and its width decays at a faster rate than its amplitude increases). We will report more details elsewhere. We are also currently testing some ideas concerning the estimation of the frequency of events.

6

Coherent Events

Our picture, then, is that in this and a wide variety of similar situations, the dissipation rate is governed by *the random occurrence of coherent events*. In order to compute a good approximation to the dissipation rate, one need only know the following information; (i) the nature of the homoclinic excursion (equivalently the spatial and temporal shape of the coherent structure) and the energy lost in the cycle and (ii) the average frequency of occurrence. Although finding approximations to these quantities will not in general be an easy task, it should be considerably simpler than finding the complete statistics on the turbulent flow. Further, this picture suggest that the most natural decomposition of the turbulent field is one in which the field is divided into low dimensional, organized structures (the collapsing filaments) and a high dimensional component consisting of chaotic fluctuations in the field during intervals when no collapse events occur. In phase space, the high dimensional component will cause the homoclinic excursion to fluctuate chaotically about the HCI but, because in physical space these fluctuations represent chaotic behavior away from the collapse site, it is reasonable to expect that their effects can be captured using low order statistics and that they will not appreciably affect the dissipation rate.

One would like to understand better the low dimensionality and attractive nature of the organized, singular structures. Why is it that the only structures through which the $\psi(\vec{x}, t)$ field becomes singular are relatively simple? We have no mathematically rigorous or even plausibly compelling argument but suggest that this is a very important question to answer. Our own attempt at an answer is incomplete but stresses the importance of the scaling symmetry which the NLS (and Zakharov) equation enjoys: if $\psi(\vec{x}, t)$ is a solution, so is $\varphi(\vec{x}, T)$ where $\varphi = \lambda^{-1}\psi$, $\vec{X} = \lambda^{-1}\vec{x}$, $T = \lambda^{-2}t$ which suggests the family $\psi = \lambda^{-1}R(\lambda^{-1}|\vec{x}|)\exp(-i\lambda^{-2}t)$ of exact solutions. If ψ is to approach infinity as $\lambda^{-1}(t)$, then in order that the dispersion and time derivative terms can balance cubic nonlinearity, $\vec{x}$ must scale as λ^{-1} and t as λ^{-2}. Thus a singular solution in which dispersion can balance nonlinearity (spatially independent solutions, some of which can be singular, are unstable) demands scale symmetry. If one inserts $\psi = \lambda^{-1}\varphi(\vec{X} = \lambda^{-1}\vec{x}, T = \int\lambda^{-2}dt)$ into the NLS as the leading term in an asymptotic expansion and if one makes the further ansatz that $\varphi = f(\vec{x})\exp i\theta$, where $\theta = \int\lambda^{-2}dt+$ lower order terms, then the demand that the coefficient of λ^{-3} be zero gives a nonlinear eigenvalue problem for $f(\vec{x})$ for which there is a unique isotropic ground state solution, namely $R(\eta)$. However, the separation ansatz is not forced at this level. One might conjecture that if one attempts to construct a uniformly valid expansion for ψ, then both this ansatz and the behavior of $\lambda(t)$ might result from solvability conditions. This is the point of view taken by Zakharov [3]. Despite the absence of a rigorous argument, it would appear, nevertheless, that symmetry constraints have much to do with the low dimensionality of the singular structures.

Geometry of Phase Space

The dominance of filaments in the dissipation process suggests that the attractor A contains two saddle-like unstable sets M and S and heteroclinic orbits between them. M contains saddle points representing modulationally or nucleationally unstable (we discuss these shortly) solutions of (1), (3) and (4). The stable manifold of S at infinity is low dimensional and corresponds to the idealized collapsing filaments of the unperturbed equation. The unstable manifold of M intersects the stable manifold of S. The unstable manifold of S (the burnout due to Landau damping) intersects the stable manifold of M. The speed of attraction and repulsion at S are governed by two entirely different processes and are not related. The former depends on the faster than exponential collapse while the latter depends on dissipation and, for the Zakharov equation, the slow relaxation of the ion hole. Based on this picture A can be roughly subdivided into two sets A_C and A_H. When the system is in A_H, it is dominated by what we all the hash modes consisting of the background field and radiation modes left over from the formation and collapse of the coherent structures. This set will generally be large dimensional but contributes little to the dissipation rate. On the other hand, when the system is in A_C, it is dominated by the coherent structures, and in particular as the saddle point S at infinity is approached, the trajectories asymptotically tend to the special orbit which we have earlier called the HCI. In other words, the part of the turbulent solution which provides the principal contribution to the dissipation rate is low dimensional. After the energy is removed by Landau damping (or in general by whatever dissipation process is relevant) the phase point returns to the turbulent soup A_H where it again comes under the influence of the saddle points in M and the cycle repeats.

We now turn to a discussion of the structure of the phase space, the nature of the saddle point M and its unstable manifold. Whereas the perturbations of forcing and damping modify the phase space structure, it is the topology of the phase space of the unperturbed system which sets the stage for the large homoclinic excursions. Tw . properties of the unperturbed system, which is Hamiltonian, are crucial. One is the fact that its phase space contains many fixed points and periodic orbits of saddle type and separatrices joining these. The second crucial property is the non-compactness of the constant energy surfaces and the existence of heteroclinic connections (HCI's) which join certain of the saddle points to infinity. Whereas Hamiltonian perturbations of this system can destroy certain tori through resonances and create new chains of elliptic centers and hyperbolic saddles and non-Hamiltonian perturbations can turn the centers into attracting sinks or destroy them altogether, the important point to make is that the hyperbolic nature of the original saddles and the attracting nature of their HCI's remain intact and play a dominant role in the dynamics of the perturbed system. The instabilities which give rise to collapsing filaments in (1) are closely related to the naturally occurring instabilities of the unperturbed NLS equation, an infinite dimensional, Hamiltonian system with Hamiltonian H and the additional motion constants n_ψ

and $\vec{J} = i \int (\psi \bigtriangledown \psi^* - \psi^* \bigtriangledown \psi) d\vec{x}$. There are two types of unstable critical points. The first are nonlocal solutions which are constant or purely periodic in space with a time behavior depending on amplitude (so they are really unstable periodic orbits). These states are unstable to sideband disturbances (fluctuations with a spatial period close to that of the unstable solutions), an instability known as the *modulational instability*. The second type are called cavitons and are analogous to the solitons of the one dimensional equation. Like the collapsing filament, they have zero H value and any perturbation which decreases H will render them unstable. Because of the existence of unstable solutions, the phase space of the unperturbed Hamiltonian system contains many saddle points. Increasing the size of the domain or the amplitude of the ψ field (the important parameter is the L_2 norm) will create saddle-center bifurcations and increase the number of saddles. Hamiltonian perturbations such as the addition of a term $V(x)|\psi|^2$ to H can create additional island chains of hyperbolic saddles and elliptic centers and in particular, if $V(x)$ is a localized potential well, these new critical points can correspond to the just mentioned localized caviton states [7]. The presence of a small amount of dissipation will destroy centers, turning some into sinks, but the saddles will persist. Other non-Hamiltonian perturbations, such as forcing, can destroy the stable sinks and destabilize the weakly stable cavitons which are localized in potential wells. In practice, this scenario often arises [8], particularly for the Zakharov equations and in some instances for the nonlinear Schrödinger equation. If ion damping is large, the hole in the ion acoustic density field remains after the burnout of the electric field. The hole acts as a slowly relaxing potential which can serve to focus electric field energy into a metastable caviton [7]. When the hole amplitude is sufficiently small, the caviton destabilizes and the field intensity and ion acoustic field again form collapsing filaments (see Figure 5). We call this the *nucleational instability*. The phenomenon was discovered in numerical simulations by Doolen, Russell, Rose and DuBois [8] and has also been confirmed in experiments by Cheung and Wong [9]. It is from a combination of modulational and nucleational instabilities that the collapsing filaments are born. The cycle time of the homoclinic excursion in each case depends on (a) the time taken for the phase point to come under the influence of a saddle instability and (b) the growth rate of the instability. In the NLS case it is difficult to estimate the former. In the Zakharov case, however, this time, during which the phase point returns from S back to A_H, can be estimated by calculating how long it takes for the hole to relax [10].

Simple Example of a HCI

The existence of HCI's depends on two crucial properties of the underlying unperturbed (undamped, unforced) equations; the presence of saddle points in the finite part of phase space and the non-compactness of the energy surface on which they lie (or the intersection of the level surfaces of the constants of the motion of there is more than one). The existence of saddle points and the noncompactness

9

of the energy surface means that there are many unstable solutions whose unstable manifolds are unbounded. We do not yet understand why, in infinite dimensional systems, the HCI is attracting and low dimensional although we can illustrate the former property with a simple finite dimensional example. Consider the perturbed Duffing's oscillator $x^{..} + x - 2x^3 = F(t) - (xx_0^{-1})^n x^{.}$, where $F(t)$ is small and the additional factor $(xx_0^{-1})^n$ has been added to the damping term in order to arrange for it to turn on only when x is large. The unperturbed, exactly integrable Hamiltonian system represents a particle in a quartic potential $V(x) = \frac{1}{2}(x^2 - x^4)$ with critical points $x^{.} = x = 0$ (a center) and $x^{.} = 0, x = \pm \frac{1}{\sqrt{2}}$ (saddle points). The unstable and stable manifolds emanating from $x = \pm \frac{1}{\sqrt{2}}$ are the non-compact energy level surfaces $E = \frac{1}{8} = \frac{1}{2}x^{.2} + \frac{1}{2}x^2 - \frac{1}{2}x^4$ which join the saddles to infinity through the HCI's $x^{.} = (x^2 - \frac{1}{2})$ for $x^{.} > 0, x > \frac{1}{\sqrt{2}}$ and $x^{.} = -(x^2 - \frac{1}{2})$ for $x^{.} < 0, x < -\frac{1}{\sqrt{2}}$. The other branches, the stable manifolds of $x^{.}$ and $x = \pm \frac{1}{\sqrt{2}}$, are repellers for increasing time. All energy level surfaces $E > \frac{1}{c}$ and those for $E < \frac{1}{8}$ for which $x^2 > \frac{1}{2}$ escape to infinity in finite time t_0 and it is easy to show that all escaping orbits are asymptotically equal at infinity. By this we mean that the distance between all escaping orbits tends to zero as they approach infinity. To see this easily, consider the Laurent series about the finite blow-up time t_0 in the unperturbed Duffing equation;

$x(t) = (t-t_0)^{-1} + 6(t-t_0) + \sum_{j=1}^{\infty} c_{2j+1}(E)(t-t_0)^{2j+1}$. Observe that the information as to which escaping orbit one is on is contained in the terms cubic and higher in $(t-t_0)$. The singular part of all escaping orbits are the same. One can also introduce a canonical change of coordinates, $u = -x^{-1}, v = x^2(x^{.} - x^2 + \frac{1}{2})$, in which one can see that the orbit $x^{.} = x^2 - \frac{1}{2}, x > \frac{1}{\sqrt{2}}$, corresponding to $E = \frac{1}{8}$, attracts all other orbits escaping to infinity. The fact that Hamiltonian systems can have attracting orbits (the point at infinity itself is not even a fixed point) at infinity does not seem to be generally known although it is apparent in the work of Bogoyavlenskii [11] who examines the neighborhood of infinity for several Hamiltonian systems.

Nonlinear Schrödinger HCI's

This simple example illustrates how the topology of the phase space of the unperturbed system is important in controlling the dynamics of the perturbed system. Likewise in the weakly perturbed nonlinear Schrödinger equation, in which forcing is applied at small wavenumbers and the damping at large, it is the topology of the phase space structure of the unperturbed problem which dominates the dynamics of the perturbed problem. The unperturbed problem is again Hamiltonian although, in this case, it is infinite dimensional with motion constants $n_\psi = \int \psi\psi^* d\vec{x}, J = i\int \psi \nabla \psi^* - \psi^* \nabla \psi)d\vec{x}$ and $H = \frac{1}{2}\int(\nabla\psi \cdot \nabla\psi^* - \frac{1}{2}\psi^2\psi^{*2})d\vec{x}$. In particular, the intersection of the level surfaces and in particular the energy is non compact and there are orbits (HCI's) in the surface $n_\psi \geq n_c = p$ which join the saddle points representing modulational and nucleational instabilities to infinity.

Our picture of the phase space then is as follows. For low levels of forcing (either F is small or the domain area is small), the modulus of the electric field grows till $n_\psi > n_c$ at which stage the phase point eventually comes close to an unstable saddle point which is joined to infinity via a collapsing filament. The instability sets in, the filament is formed, it collapses, a certain portion of its energy is dissipated (depending on the damping structure) and a remnant of high k waves is left over. For the Zakharov system, we expect a more complete burnout. The system returns close to its original state and the process is approximately repeated with the initialization of the collapsing filament being due to either modulational or nucleational instabilities. In particular, either the remnant or the ion acoustic field can provide a cavity for the nucleation of metastable cavitons which collapse once the support disperses away. For larger values of the applied stress (either larger forcing or larger boxes), the value n_ψ of the mean turbulence level is much larger and can be many times n_c. In this case, spatial correlations decay rapidly and many collapsing filaments can occur at different spatial locations although, since each event is so rapid, they will rarely occur in the same time intervals. For these large turbulence levels, the saddle point M represents a collection of saddle points in the turbulent soup part of the attractor A_H, some of which correspond to analogues of the modulational instability of more complicated periodic shapes and others of which are best understood as nucleational instabilities.

Other turbulent situations

We mention here that a similar situation obtains in the Euler equations. For low values of the applied stress, laminar states can be destabilized by identifiable instability mechanisms, centrifugal instabilities, mean flow profiles with inflexional points and so on. These instabilities do not go away when the fluid is more highly stressed and becomes fully turbulent. Indeed saddle points representing local inflexional and centrifugal instabilities remain very much part of the strange attractor of the high Reynolds number Navier Stokes equations and play a large role in transferring energy to high wavenumbers where dissipation acts. In highly turbulent flows, the inflexional profile of the mean flow is not sustained for all time uniformly in space, but if it is sustained long enough in a local region, then rapidly growing packets of three dimensional inflexional instabilities can erupt and carry energy off to the dissipation cemetaries. In addition, the level surfaces in the phase space are noncompact. Moreover, it is not unreasonable to argue that the dissipation rate of shear flow turbulence arises not from the wave-wave interaction familiar from Fourier space cumulant descriptions, but instead to suggest it is dominated by the formation and destruction of thin vortex sheets or surfaces containing vortex tubes (the state S) in which almost all of the vorticity is concentrated. One might conjecture that the initial formation of surfaces of vorticity concentration follows singular solutions (either finite or infinite time) of the Euler equations driven principally by inflexional instabilities. Once formed (the system is close to S), these sheets would

11

be notoriously unstable, to Kelvin-Helmholz instabilities of the tangential velocity discontinuities and to Taylor-Gortler centrifugal instabilities of the helical flows induced by vortex lines embedded in the curved sheets. These secondary instabilities quickly transfer the energy to the viscous cemetaries where energy is dissipated and the system is returned close to a state where approximately the same cycle can repeat.

Finally, we suggest that these ideas are not restricted to the approximation of dissipation rates. Other transport properties such as the momentum exchange from the plate to the outer flow in a turbulent boundary layer also seem to be dominated by "organized events," namely the burst-sweep cycle. It is interesting that Aubry, Holmes, Lumley and Stone [12] have found a type of homoclinic excursion in their analysis of the "long wave" structure of a turbulent boundary layer suggesting the beginning of a burst sweep cycle, although their excursion does not lead to any kind of singular behavior. One might conjecture that the latter could result if one were to add a short scale inflexional wave component which can result from such a wavepacket being phase locked to and growing on the local distortion of the turbulent mean profile. Further, we suggest it may be also valuable to apply these ideas to heat transport at high Rayleigh numbers (where thermal plumes would play the role of singular structures) and Rayleigh-Taylor instabilities.

Acknowledgements

References

[1.] D. Ruelle, Commun. Math. Phys. 87, 287-302 (1982). Commun. Math. Phys. 93, 285-300 (1984).

C. Foias, O. P. Manley, R. Teman and Y. M. Treve, Physica 9D, 157-188 (1983).

C. Doering, J. D. Gibbon, D. D. Holm and B. Nicolaenko, to be published in Nonlinearity (1987).

J. M. Hyman and B. Nicolaenko, Los Alamos Report LA-UR-85-1556.

[2.] A good review article is *"Collapse versus Cavitons"* by A. M. Rubenchik, R. Z. Sagdeev and V. E. Zakharov. Comments on Plasma Physics and Control Fusion 9, 183-206 (1985)

M. V. Goldman, *Reviews of Modern Physics 56, 709 (1984).*

[3.] B. LeMesurier, G. Papanicolaou, P. Sulem and C. Sulem, Private Communication (1988).

V. E. Zakharov, Private Communication (1988).

[4.] M. J. Weinstein. Comm. Partial Differential Equations 11, 545-565 (1986).

[5.] A.C. Newell, D.A. Rand, D. Russell to appear Physica D Special Volume in honor of Joseph Ford (1988).

[6.] A. Majda, R. DiPerna, Private Communication.

[7.] H. A. Rose and M. I. Weinstein, Physica 30D, 207-218 (1988).

[8.] G. D. Doolen, D. DuBois, H. A. Rose, Phys. Rev. Lett. 54, 804 (1985).

D. Russell, D. Dubois, H. A. Rose. Phys. Rev. Lett. 56, 838 (1986).

D. Russell, D. DuBois, H. A. Rose. Phys. Rev. Lett. 60, 581 (1988).

[9.] A. Y. Wong, P. Y. Cheung, Phys. Rev. Lett. 52 1222 (1984).

P. Y. Cheung, A. Y. Wong, Phys. Rev. Lett. 55 1880 (1985).

[10.] H. A. Rose, Private Communication.

[11.] O. I. Bogoyavlenskii, *Methods of the Qualitative Theory of Dynamical Systems in Astrophysics and Gas Dynamics*, Springer-Verlag, Berlin (1981).

[12.] N. Aubry, P. Holmes, J. Lumley, E. Stone, Cornell University Preprint (1988).

13

Figure Captions

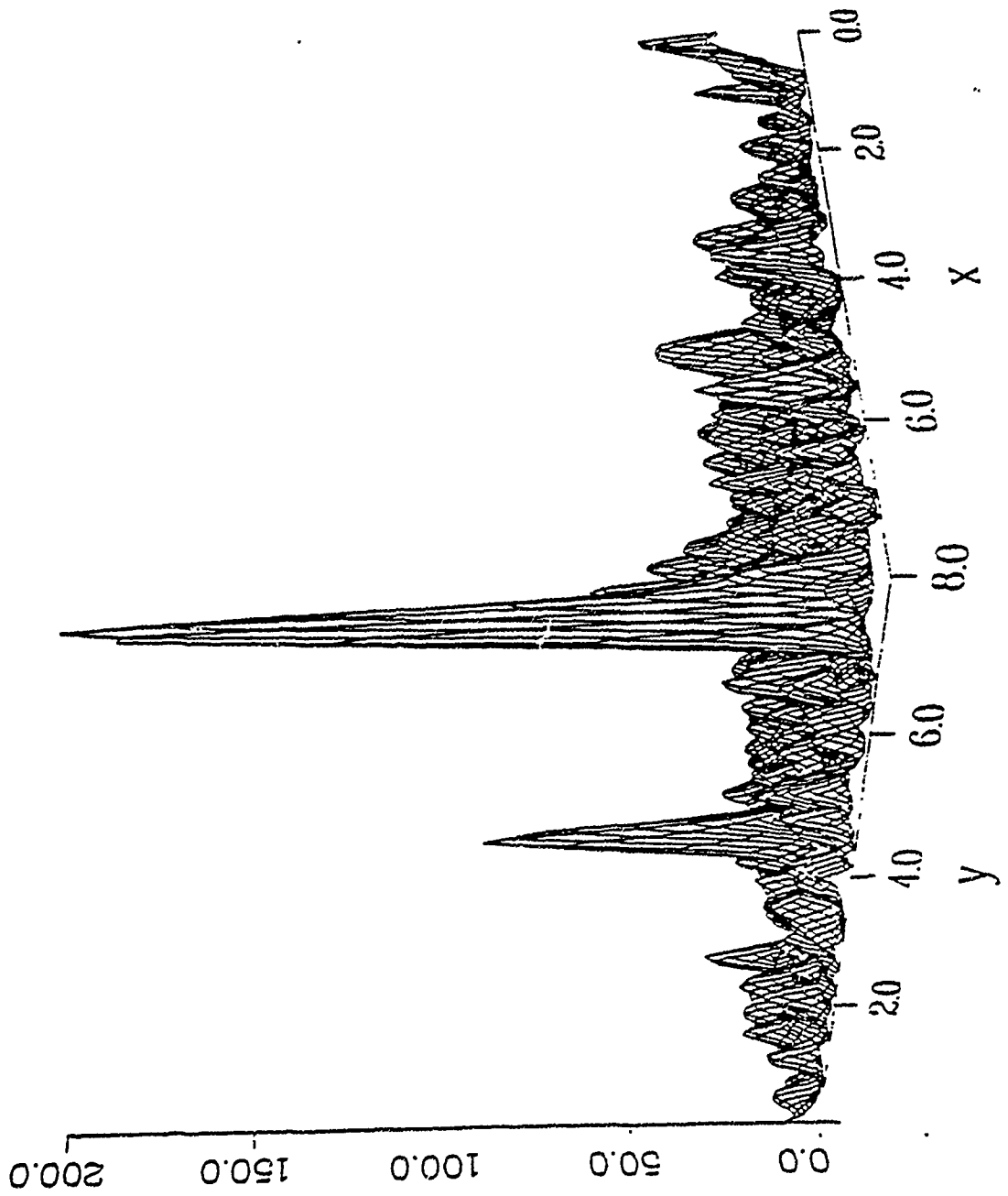Figure 1. Snapshots of $|\psi^2(\vec{x}, t)|$ at times (a) beginning of (b, during and (c) after collapse.

Figure 2. A record over a short period of time of the instantaneous rate of dissipation $\gamma(t) \equiv 2\Sigma_{\vec{k}}\gamma_e(k)|\hat{\psi(\vec{k})}|^2$, its integral $\Gamma(t) \equiv -\int^t \gamma(t')dt'$, and the global spatial maximum of $|\psi(\vec{k})|^2$ as functions of time in the strong turbulent regime with $\gamma_b = 2\delta(k-1)$.

Figure 3. Concentric shells which are the remnants of two simultaneous collapses. Note: simultaneous collapses are rare and these were initiated by a symmetric initial state.

Figure 4. The distribution of r for two-dimensional NLS.

Figure 5. The (a) nucleation, (b) collapse and (c) burnout of a filament of the Zakharov equation. The overshoot of the cavity during burnout encourages tetal dissipation of the filament.
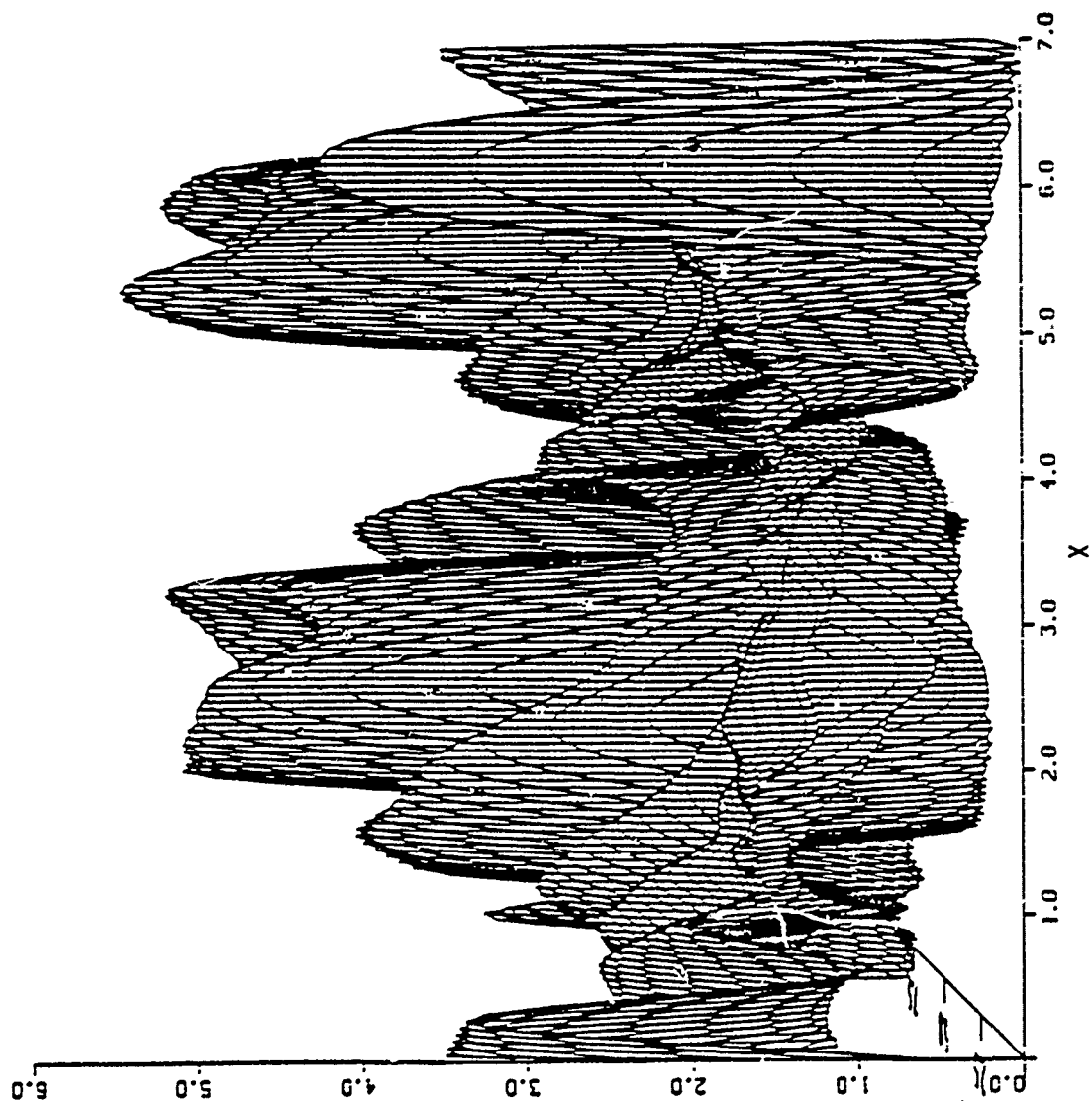
14
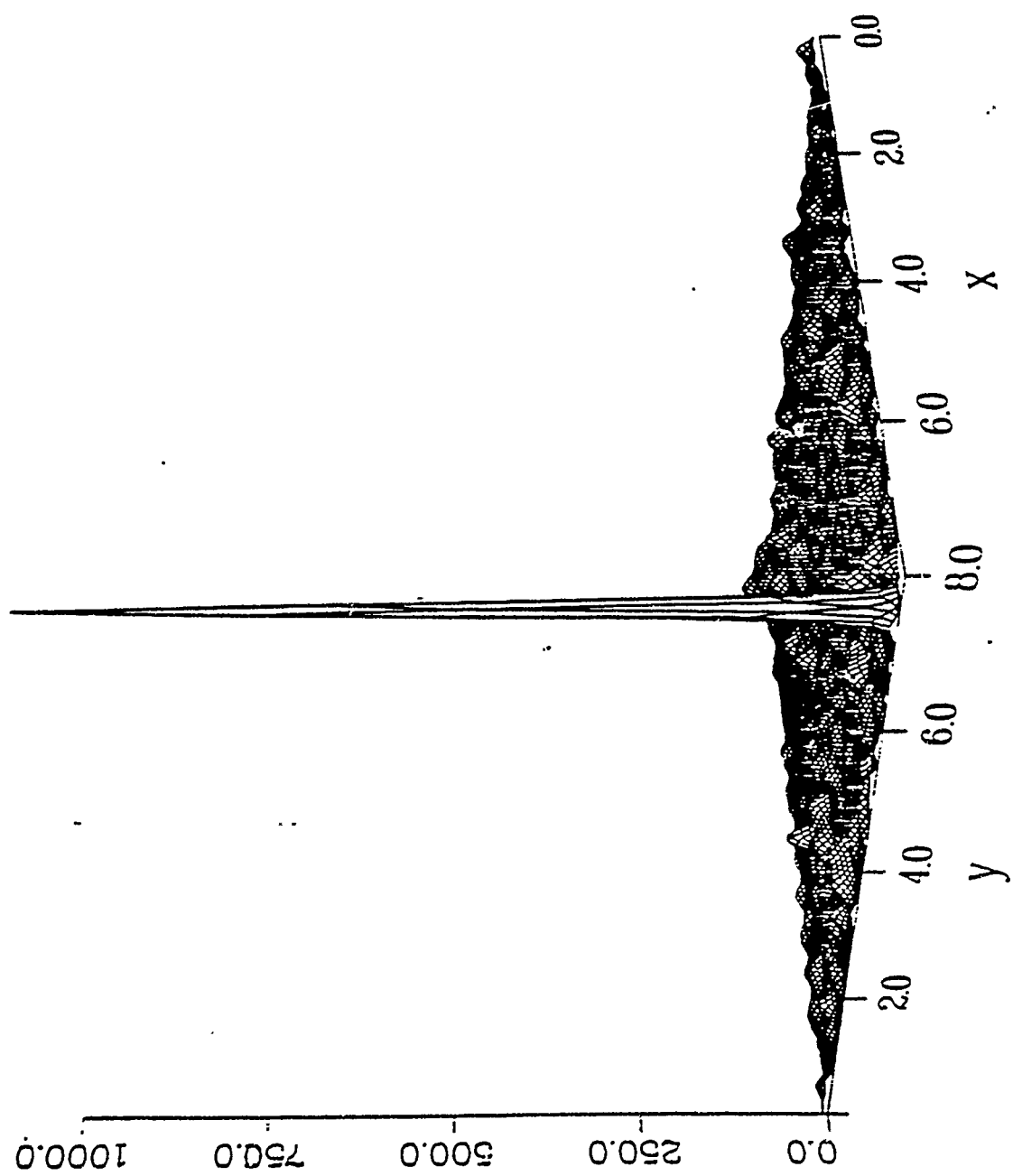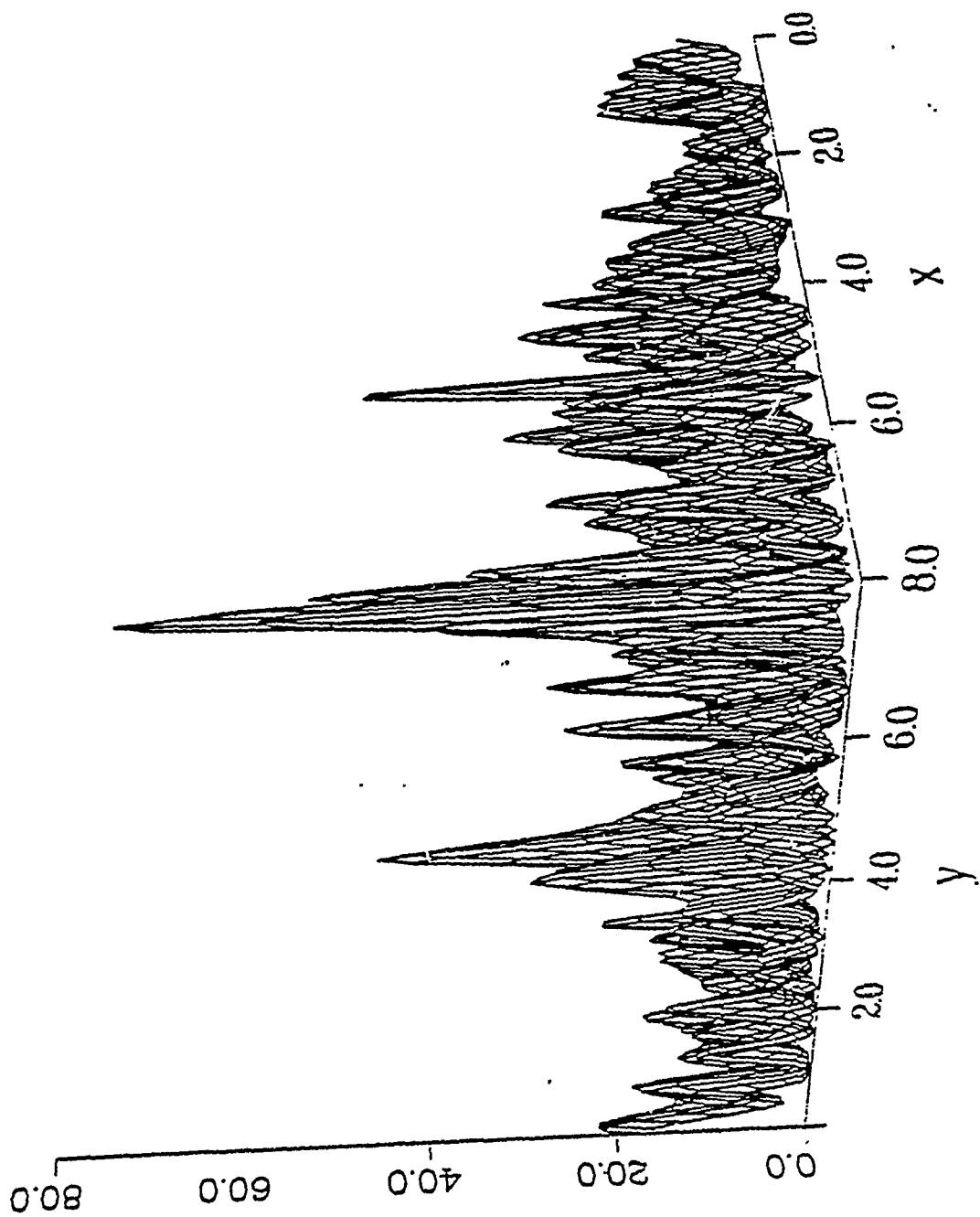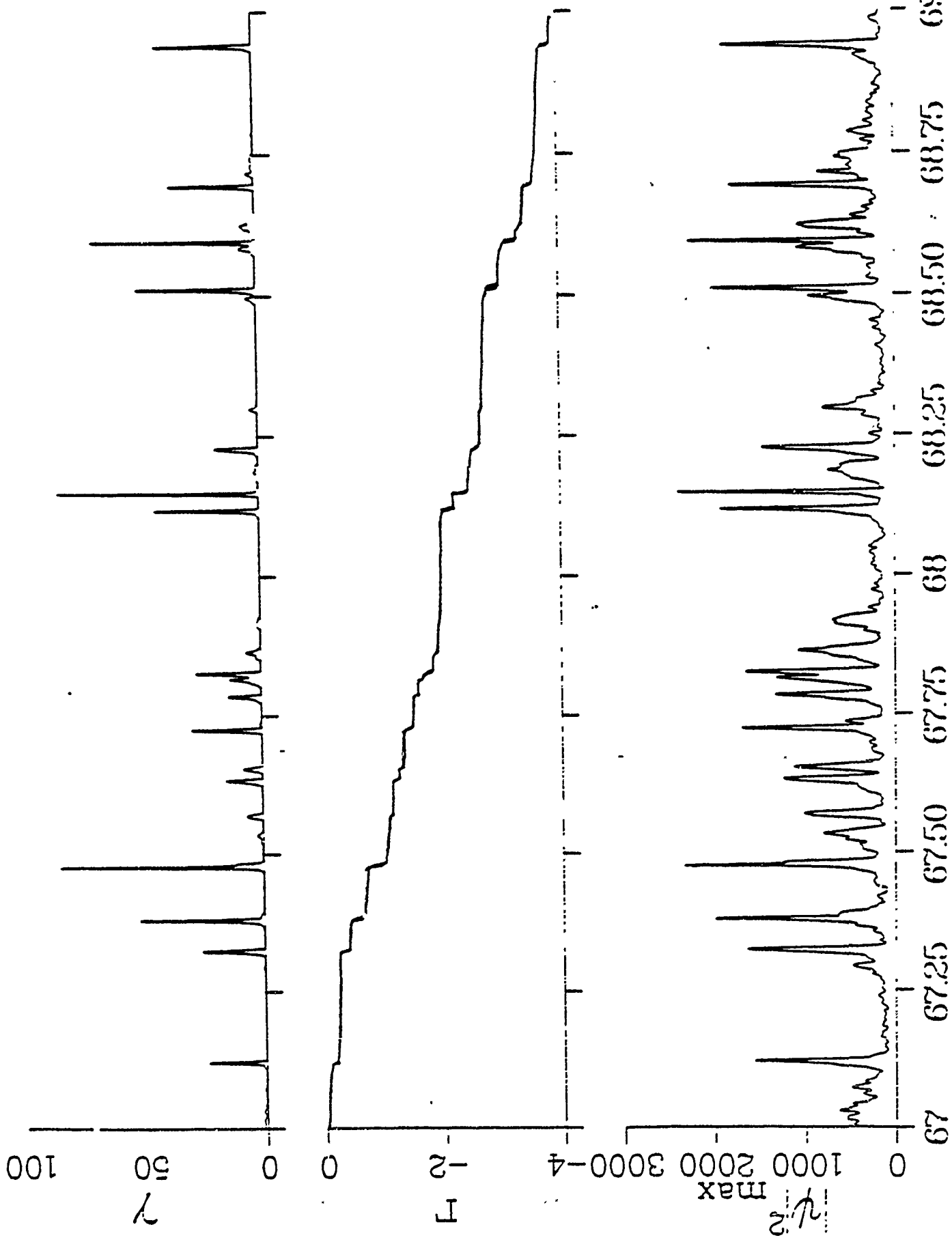
t = 116.016

FIG.

Fig.

$t = 16.036$

t = 176.078

Fig. 5

CLAMP - 1.0000 0.0000

P - 2.00 GO - 0.000E+00 HI - 1036

T - 5.760

Y(0.0)

X

distribution of energies dumped

288 dumps

$p(\delta n)$

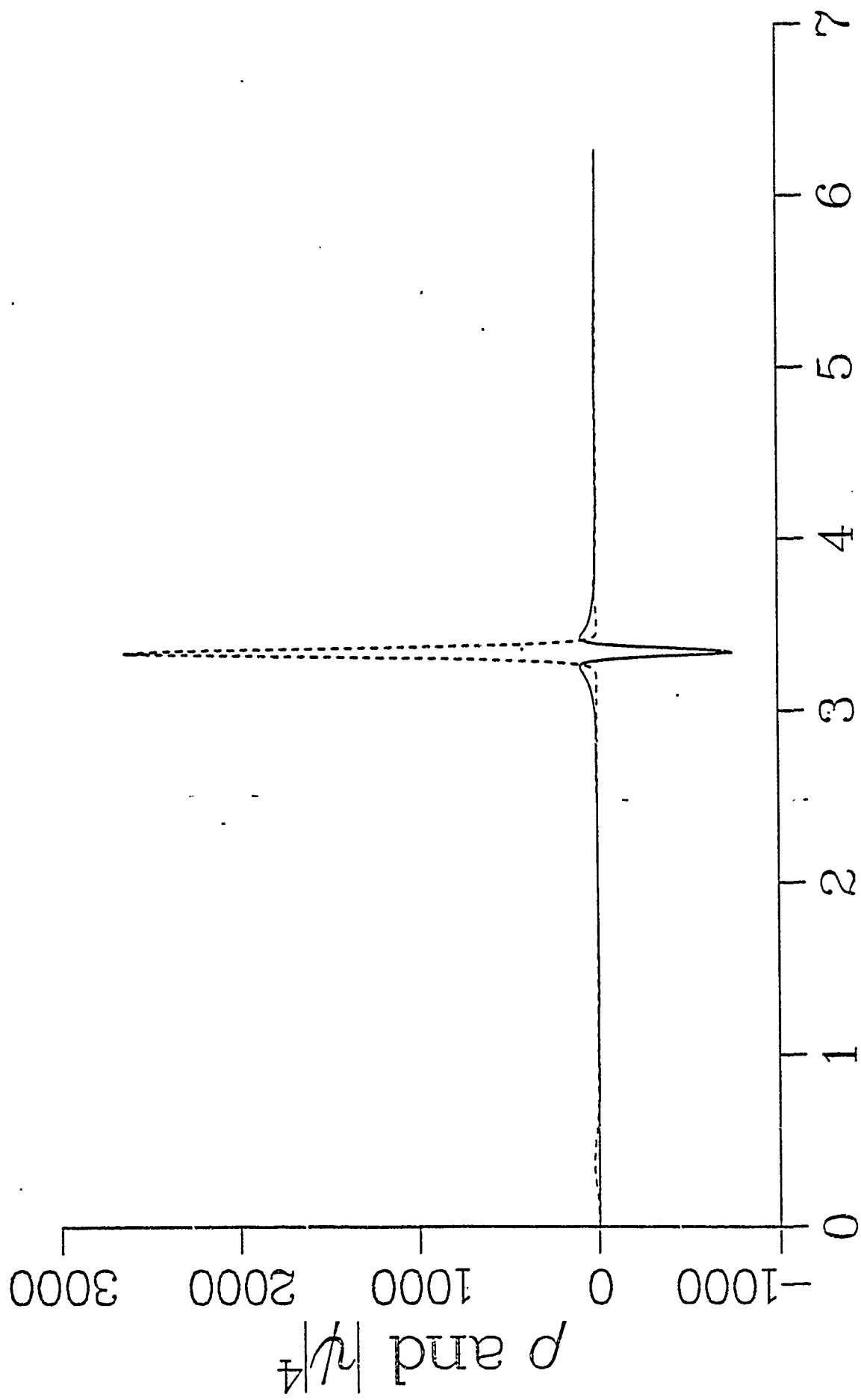δn

Fig 4
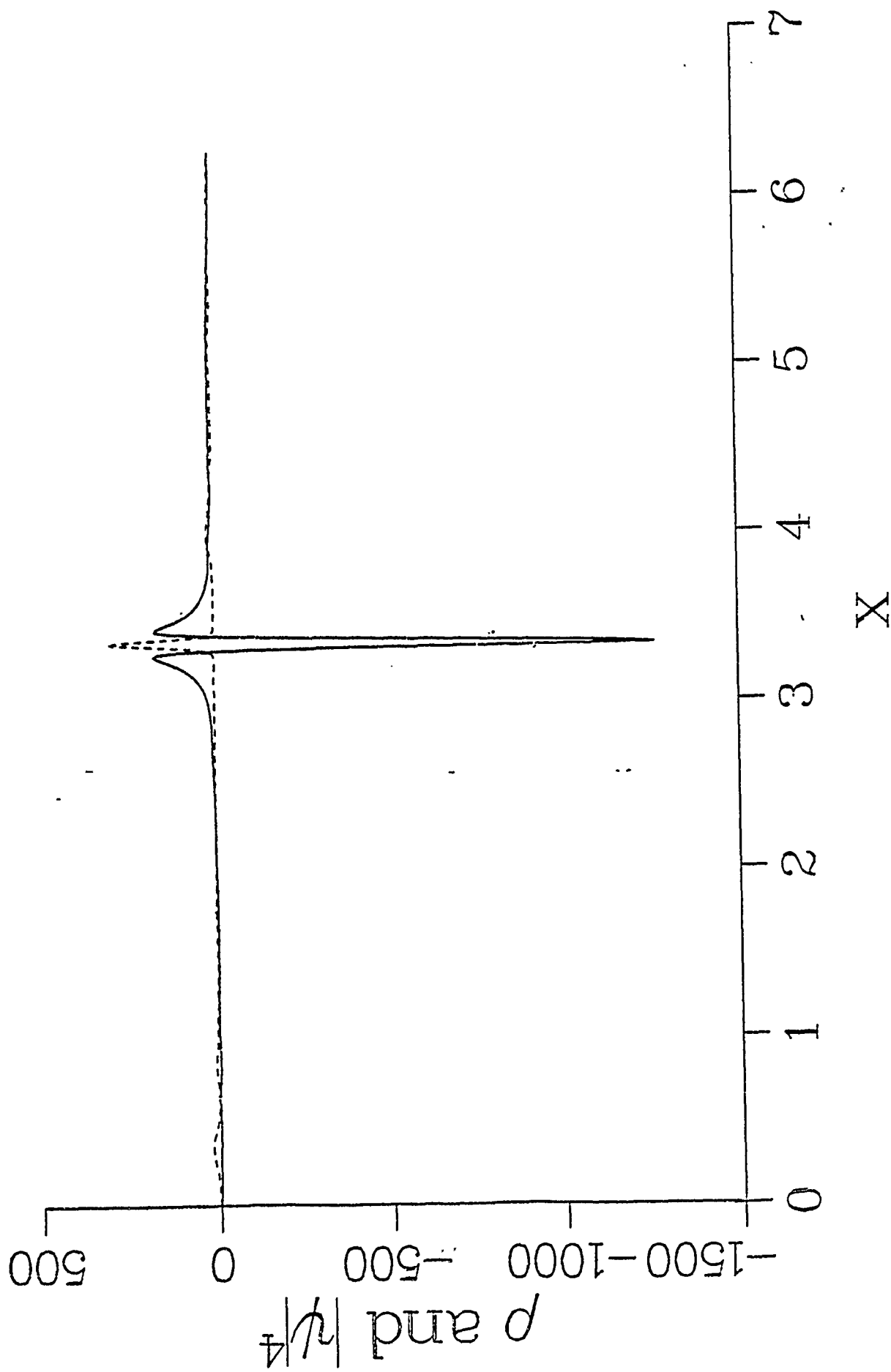
$t = 10.99$

ρ and $|\psi|^4$

X

$t = 11.03$

ρ and $|\psi|^4$

X
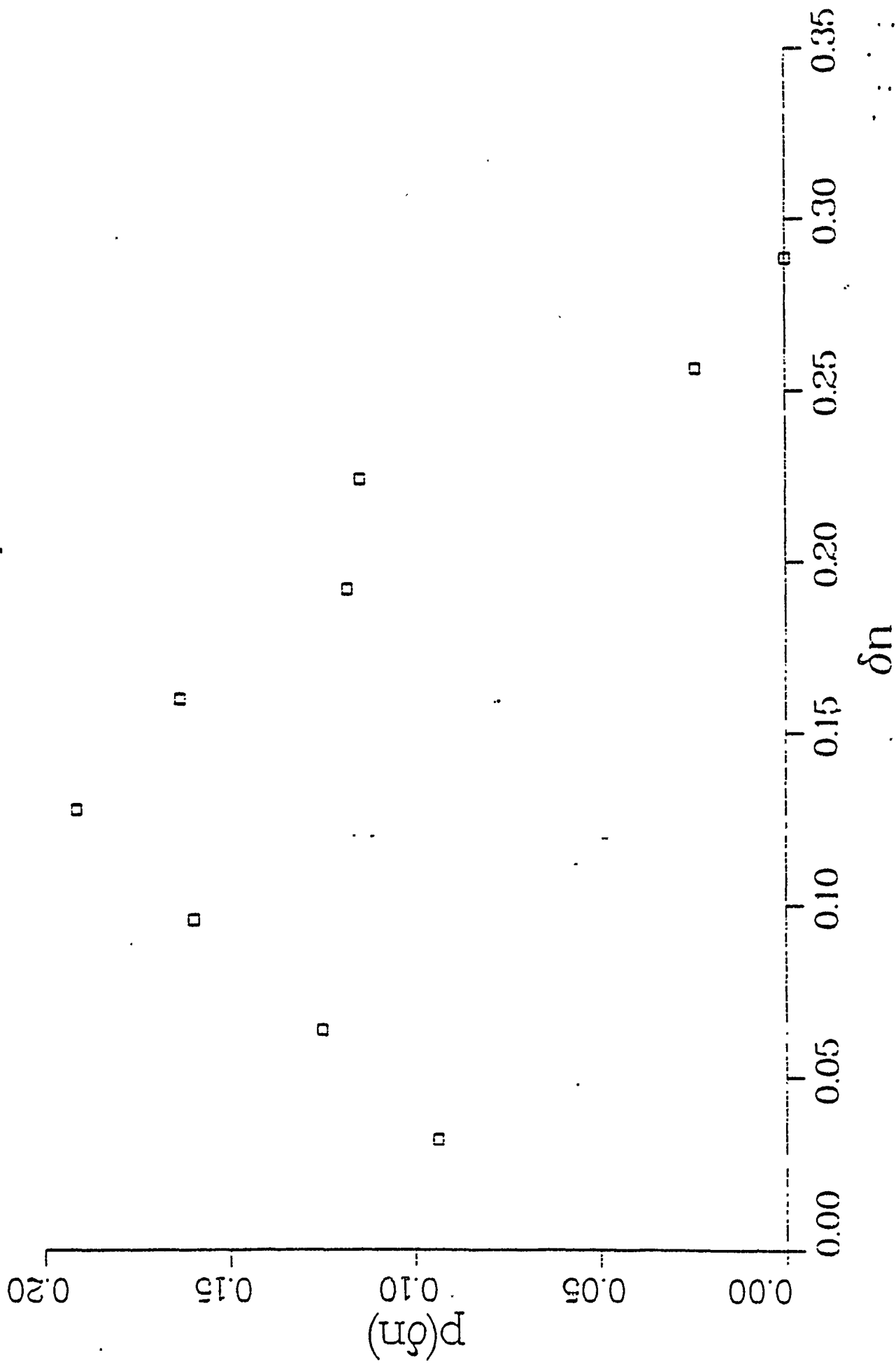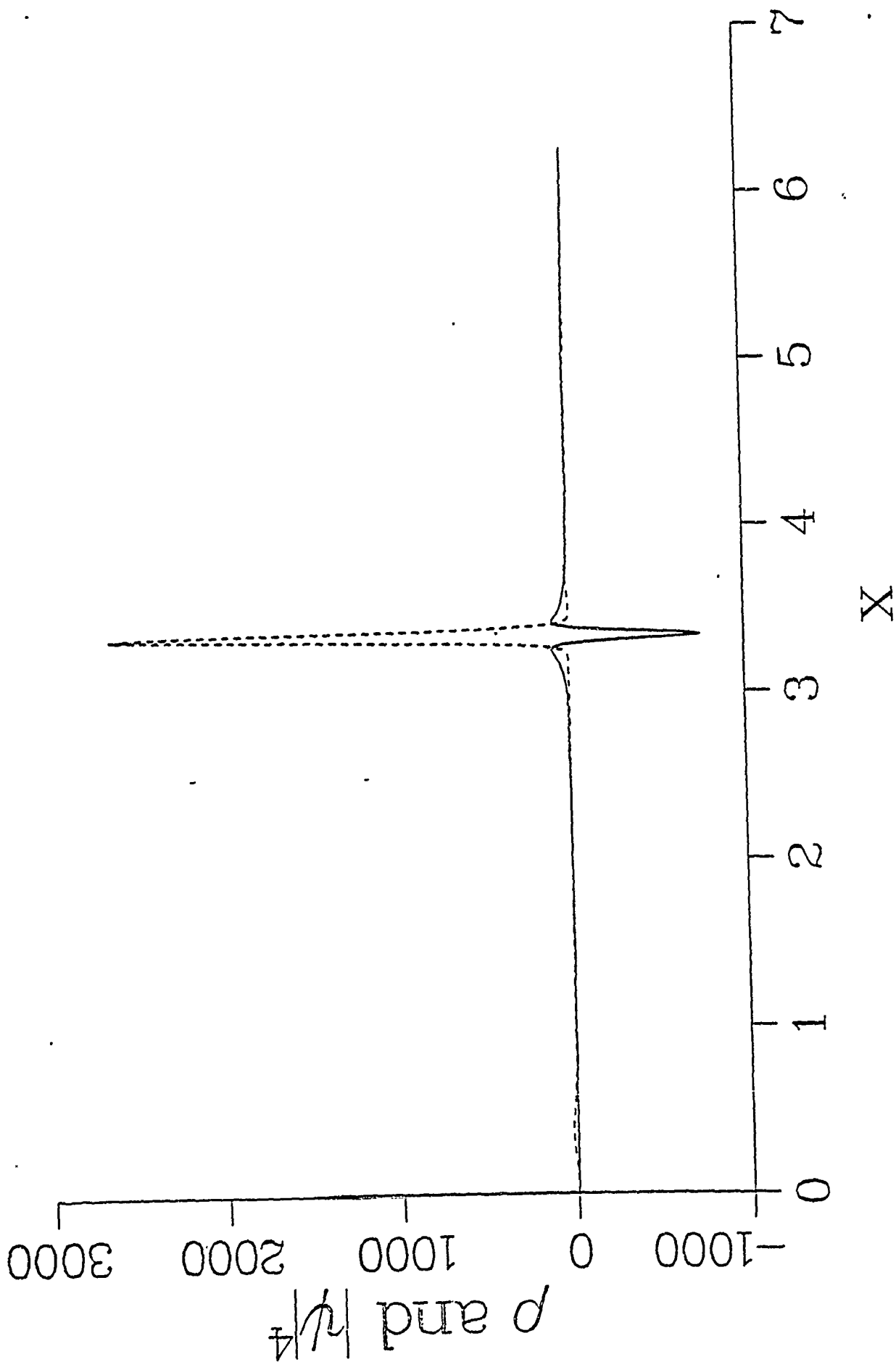
Turbulent Transport
and the Random Occurrence of Coherent Events

Alan C. Newell
Department of Mathematics
University of Arizona
Tucson, AZ 85721

David A. Rand
Mathematics Institute
Warwick University
Coventry CV4 7AL, England

David Russell
Center for Nonlinear Studies
Los Alamos, NM 87545

Abstract

We suggest that the transport properties and dissipation rates of a wide class of turbulent flows are determined by the random occurrence of coherent events which correspond to certain orbits which we call homoclinic excursions in the high dimensional strange attractor. Homoclinic excursions are trajectories in the non-compact phase space that are attracted to special orbits which connect saddle points in the finite region of phase space to infinity and represent coherer* structures in the flow field. This picture also suggests that one can compute fluxeꞁ using a relatively low dimensional description of the flow. A method for extracting the organized structures from a time-series is given and provides a local analogue of the notion of Lyapunov exponents.

Introduction

It is generally accepted that turbulence in shear flows at Reynolds numbers of 10^3 and higher has a large number of active degrees of freedom. Although estimates of Lyapunov and Hausdorff dimensions [1] are strictly upper bounds, the rapid loss of spatial correlations over distances of the Taylor microscale $R^{-\frac{1}{2}}$ and the broadband wavenumber spectrum suggest that many modes are playing an active role in the dynamics. The $R^{\frac{9}{4}}$ estimate, which is consistent with the intuitive idea of Landau that it is necessary to resolve a turbulent flow field in a box of volume V down to the Kolmogoroff inner scale of $(\nu^3/\varepsilon)^{\frac{1}{4}}$ (ν is kinematic viscosity, $\varepsilon = \nu \int_V | \nabla u|^2 d\tilde{x}$ is the energy dissipation rate and is independent of ν for a large range of large Reynolds numbers), means that if R is 10^4, $R^{\frac{9}{4}}$ is a billion! It is unlikely that replacing the Navier-Stokes equations by a system of a billion o.d.e.s. will either bring much insight into the nature of turbulence or make it possible to calculate the invariant measure on the attractor needed to compute averages. Therefore, whereas the concept of a strange attractor on which the flow is everywhere unstable and ergodic is a valuable and necessary one, a new idea is needed if one is to be able to compute in a practical way average flow quantities and in particular those averages which represent transport properties, the flux of heat across a convection layer, momentum across a boundary layer, angular momentum between cylinders rotating at different velocities, mass flux down a pipe or the amount of heavier fluid which falls through a lighter one. It is also important to calculate the dissipation rate which, in systems where energy is fed in at low wavenumbers and removed at high ones, is equivalent to computing the flux or cascade of energy across any middle wavenumber. One of the main goals of a turbulence theory is to predict the transport and the dissipation rate as a function of the applied stress. The purpose of this paper is to suggest one new avenue of approach to these problems of transport in physical and wave space.

The basic idea is fairly simple. There is some evidence that, in a variety of situations, transport is associated with organized flow structures. If this is the case, one would like to identify and isolate those parts of the attractor and those orbits in phase space which are the principal contributors to a particular flux. Our claim is that they are homoclinic excursions analogous to homoclinic orbits which occur at random intervals on the attractor and connect that large dimensional part of the attractor, consisting of states of the system which contribute little to the flux, to itself. The homoclinic excursions are arranged by orbits connecting the main part of the attractor to an organizing structure which is represented in phase space by a generalized saddle. Of particular interest to us is the case where this structure is at infinity and corresponds to a singular solution. We give the orbits connecting saddles in the attractor to the singular structure at infinity the name *heteroclinic connections to infinity* (HCI's). There are also orbits from the singular structure back to the main part of the attractor. The HCI's are important because we shall show that there is a sense in which they are attracting even when the system is

2

conservative. The existence of HCI's depends upon two crucial properties of the unperturbed (undamped, unforced) equations: the presence of saddle points in the phase space of the unperturbed system and the non-compactness of the energy surface on which they lie (or the intersection of the level surfaces of the constants of motion if there is more than one). The existence of saddle points in the phase space of the unperturbed system and the non-compactness of the energy surface means that there are many unstable solutions whose unstable manifolds are unbounded. The HCI, which lives in the unstable manifold, corresponds in physical space to a coherent structure which is usually localized in space, has a finite lifetime and is connected with a family of exact, albeit singular, solutions of the field equations. At infinity, where a large portion of the energy of these solutions is in small scales, the structure becomes unstable to dissipative processes which drain its energy and relax the system back to the neighborhood of its initial state, thus completing the cycle. Towards the end of this paper, we will discuss a prescription for identifying and finding these structures using time series data.

Our picture, then, is that in a wide variety of situations, turbulent transport is achieved and the dissipation rate is governed by *the random occurrence of coherent events*. In order to compute a good approximation of the dissipation rate or flux in question, one need only know the following information, (i) the nature of the homoclinic excursion (equivalently the spatial and temporal shape of the coherent structure) and the energy lost in this cycle, and (ii) the average frequency of occurrence. Although finding approximations to these quantities will not in general be an easy task, it should be considerably simpler than accurately following the full dynamics. Obtaining these estimates by largely deterministic means is not intended to disregard the fact that turbulence is a stochastic process in which statistical fluctuations are important. What it does suggest, however, is that the most natural decomposition of the turbulent field is one in which the field is divided into organized motions represented by dominant orbits in the phase space and statistical fluctuations about these orbits. The method, discussed later, by which we identify the organized structures and their dynamics is a variation of Karhunen-Loeve expansions (later used by Lumley [2] in the context of turbulence) which extract from statistical data dominant shapes and forms. Our method is novel in that it is a weighted local version of the Lumley method and is therefore able to pick out selectively relatively rare coherent events which long time averages would lose. As we have mentioned, we believe that in many cases these dominant shapes will be closely related to exact, singular solutions of the governing equations which act as asymptotic attractors in a sense to be described below. Further, with this decomposition, it may even be possible to approximate the full dynamics on the attractor, at least to some degree of accuracy, by a finite and low dimensional system of o.d.e.'s, with stochastic coefficients reflecting the influence of the many, many other active degrees of freedom contained in the fluctuations about the principal orbits. It is our thesis that a good approximation to the transport may be obtained either by ignoring altogether or by simply taking average values of these stochastic coefficients.

In any event, we suggest that using this decomposition, the fluctuations can be described with low order statistics. The principal difference with previous thinking [3] in which one attempts to embed the attractor in a large but finite dimensional Euclidean manifold (the inertial manifold approach) is that we no longer demand that the approximation to the turbulent field keeps the phase point, which represents the state of the system, always in the attractor. Rather we simply demand that it moves parallel to the real attractor, respecting the directions associated with large homoclinic excursions which we claim are largely responsible for transport. This requirement, much weaker than the cone condition of inertial manifold theory, means that far fewer coordinates are needed to describe those particular features of the dynamics associated with the homoclinic excursions.

Before attempting to mathematize these notions any further, let us first consider a representative case study in which these ideas take concrete form.

The Zakharov model of Langmuir turbulence.

The Zakharov equations,

$$\nabla^2 (i\varphi_t + i\gamma_e \circ \varphi + \frac{3}{2}\omega_p r_d^2 \nabla^2 \varphi) = \frac{\omega_p}{2\pi} \nabla \cdot p(\nabla\varphi + E_0) + \nabla \cdot F, \qquad (1)$$

$$p_{tt} + 2\nu_i \circ p_t - c_s^2 \nabla^2 p = \frac{1}{16\pi M} \nabla^2 \mid \nabla \phi \mid^2 \qquad (2)$$

couple the density fluctuations $p(\vec{x}, t)$ and the longitudinal component of the electric field $\vec{E} = \frac{1}{2}\nabla(\phi e^{i\omega_p t} + (*)) + \vec{E}_0$ in a plasma and constitute a popular nonlinear fluid model of Langmuir turbulence [4]. Here ω_p is the plasma frequency at which a cold plasma is resonant in the longitudinal mode and the envelope $\phi(\vec{x}, t)$ is assumed to vary slowly in time compared to ω_p^{-1}. The linear, dissipative convolution operators γ_e and γ_i are used to model Landau damping; both increase with increasing wavenumber but γ_e does so abruptly in order to cut off the coherent longitudinal oscillations as the Debye wavenumber $k_d = \frac{2\pi}{r_d}$ is approached; r_d is the distance at which the Coulomb potential of a bare charge is diminished exponentially by the ambient plasma. $\vec{F}$ is a forcing term that injects electric field energy into the plasma and is also modelled by a linear convolution operator $\gamma_b \circ \vec{E}$. Equation (2) is the ion acoustic wave equation in which ion density fluctuations are driven by gradients of the electric field intensity, the so-called pondermotive force. If the ions are quasi-stationary, the dominant term on the left hand side of (2) is the last and, in this case, the ion density fluctuation p is directly slaved to the field intensity $\mid \nabla \phi \mid^2$. In one spatial dimension and with suitable rescalings, the Zakharov equations reduce to the familiar nonlinear Schrödinger equation in dimensionless variables for the electric field envelope $\psi(\vec{x}, t)$

$$\frac{\partial \psi}{\partial t} + i \nabla^2 \psi + i|\psi|^2 \psi = F - D. \qquad (3)$$

4

Our case study will principally focus on the two dimensional version of (3). Although this model is a poor approximation to the real physics on several counts (it ignores finite sound speed effects and the role that sound waves play in energy transfer, it assumes the ion density is slaved to the electric field intensity, it is two dimensional and the premises from which it is derived become suspect as the electric field reaches its singular limit), nevertheless it retains the essential features of the full dynamics in the sense that the dissipation rate is controlled by the filament dynamics. Energy is fed in at low k and removed at high k through F and D whose respective Fourier transforms are $\gamma_b(k)\hat{\psi}(k)$ and $\gamma_e(k)\hat{\psi}(k)$ ($\hat{\psi}(\vec{k}, t)$ is the Fourier transform of $\psi(\vec{x}, t)$) with the support of $\gamma_b(k)$ being near $k = 0$ and the support of $\gamma_e(k)$ being $k > k_d$.

For many years it has been conjectured by Soviet colleagues [4] that the principal mechanism for the transfer of spectral energy, at least in the limit of large ion acoustic damping where free wave effects can be ignored, is not resonant wave-wave interactions, but rather the collapse of filaments which are closely related to exact, localized, singular solutions of the unperturbed equations. In the two-dimensional nonlinear Schrödinger equation, these filament solutions take the form [5]

$$|\psi(\vec{x}, t)| \sim \frac{1}{\lambda(t)}R(\eta), \quad \eta = \frac{|\vec{x}|}{\lambda(t)} \tag{4}$$

where the shape R is the unique solution of $R'' + \eta^{-1}R^1 - R + R^3 = 0, R'(0) = 0, R(\infty) = 0$ without zeros in $(0, \infty)$. The function $\lambda(t)$ approaches $(\ln\ln(t_0 - t))^{-1}(t_0 - t)^{\frac{1}{2}}$ as $t \to t_0$ [6]. The filaments preserve the L_2 norm and so the power $n_\psi = \int |\psi|^2 d\vec{x}$ carried by one of these coherent structures is $p = 2\pi \int_0^\infty R^2 \eta d\eta$ and is a pure number equal to .29 in our units independent of time and initial conditions. The value of H for the filament structure is exactly zero but each of its two components $\int |\nabla \psi|^2 d\vec{x}$ and $\int |\psi|^4 d\vec{x}$ becomes unbounded. The structure of the singular filaments for the Zakharov equations and for the nonlinear Schrödinger equation in three dimensions is somewhat different but in each case the role is the same. These solutions are initiated by instabilities of the unperturbed equations and serve to carry the energy from large to small scales simply by squashing it in collapsing filaments. In reality, the singularity is never reached. Once the filament diameter is of the order of the Debye radius, Landau damping becomes important and the energy is transferred from the wave field to electrons, a process known as *burnout*. This cycle of events is shown in Figure 1.

The instabilities which give rise to collapsing filaments in (3) are closely related to the naturally occurring instabilities of the unperturbed nonlinear Schrödinger equation, an infinite dimensional, Hamiltonian system with Hamiltonian H and the additional motion constants n_ψ and $\vec{J} = i \int (\psi \nabla \psi^* - \psi^* \nabla \psi) d\vec{x}$. Although we will discuss the geometry of phase space in more detail in the next section, it is important to mention at least two types of unstable critical points of the dynamical system. The first are nonlocal solutions which are constant or purely periodic in

5

space with a time behavior depending on amplitude (so they are really unstable periodic orbits). These states are unstable to sideband disturbances (fluctuations with a spatial period close to that of the unstable solutions), an instability known as the *modulational instability*. The second type are called cavitons and are analogous to the solitons of the one dimensional equation. Like the collapsing filament, they have zero H value and any perturbation which decreases H will render them unstable. Because of the existence of unstable solutions, the phase space of the unperturbed Hamiltonian system contains many saddle points. Increasing the size of the domain or the amplitude of the ψ field (the important parameter is the L_2 norm) will create saddle-center bifurcations and increase the number of saddles. Hamiltonian perturbations such as the addition of a term $V(x)|\psi|^2$ to H can create additional island chains of hyperbolic saddles and elliptic centers and in particular, if $V(x)$ is a localized potential well, these new critical points can correspond to the just mentioned localized caviton states [7]. The presence of a small amount of dissipation will turn centers into sinks, but the saddles will persist. Other non-Hamiltonian perturbations, such as forcing, can destroy the stable sinks and destabilize the weakly stable cavitons which are localized in potential wells. In practice, this scenario often arises [8], particularly for the Zakharov equations and in some instances for the nonlinear Schrödinger equation. If ion damping is large, the hole in the ion acoustic density field remains after the burnout of the electric field. This hole can serve to focus electric field energy and nucleate a metastable caviton. However, as the hole slowly collapses, the caviton destabilizes to a collapsing filament. We call this the *nucleational instability*. It is from a combination of modulational and nucleational instabilities that the collapsing filaments are born.

We now turn to the numerical evidence for the dominance of collapse events. Figure 2 displays the instantaneous rate of dissipation $\gamma(t) \equiv 2\sum_{\vec{k}}\gamma_e(k)|\psi_k|^2$, its

integral $\Gamma(t) \equiv -\int^t dt'\gamma(t')$, and the global maximum of $|\psi|^2$ over a time interval including several collapses in a strong-turbulent regime. $-\Gamma$ is just the energy lost due to dissipation as a function of time. Observe that a large fraction of the energy dissipation occurs in sudden jumps and is directly correlated to the collapse events. Energy $n_\psi \equiv \sum_{\vec{k}}|\psi_k|^2$ is considered to be dissipated due to collapse only if $\gamma > \gamma_0$, where γ_0 is a threshold parameter. If this inequality holds over the interval $[t_1, t_2]$, then the energy burnt out is $\Gamma(t_1) - \Gamma(t_2)$, and the total energy lost due to collapse for the entire simulation is the sum of all such differences. Denote this total energy lost due to collapse by δn_c and the total energy dissipated by δn_T. In Figure 3 we have plotted the ratio $\delta n_c/\delta n_T$ as a function of γ_0 for several different turbulent regimes. As γ_0 decreases the ratio increases and is of course one at $\gamma_0 = 0$. $\gamma_0 = 1$ was the smallest value that gave ratios judged to be free from contamination by non-collapse events for all cases studied, so it was chosen as the standard cut-off rate. With this choice of γ_0, as much as 80% of the total energy dissipated is dissipated by collapsing filaments in the most energetic case examined ($< n_\psi > \cong 10$). In

6

the weakest case ($< n_\psi > \cong 5$) more than 70% of the dissipated energy was lost in burned out filaments. Furthermore, these estimates of the energy dissipation are conservative because we have not yet included the more gradual loss due to the decay of the high k remnant left over from the collapse. The reason for this remnant is peculiar to the two dimensional nonlinear Schrödinger equation and occurs because a singular filament of this equation carries the minimum threshold energy p required to sustain collapse. (In contrast, the energy of a collapsing Zakharov filament, again a constant of the motion, can take on a continuous range of values above the critical threshold.) Therefore, when a significant portion of the filament's spectral energy lies in the dissipative range ($k > k_d$), some of its energy is lost, collapse is arrested and only a partial burnout occurs. A histogram showing the distribution of the fraction of the filament energy lost in the burnout is shown in Figure 4. It leaves behind a remnant in the form of broadened concentric cylindrical shells of field energy centered at the collapse site (see Figures 1e, f). In order to follow the energy associated with the remnant, we monitor (Figure 5) the field energy inside a small cell centered at the collapse site. We note in Figure 5b that the burnout ($t \simeq .08$) of the central part of the filament, or core, causes the fastest depletion of energy in the cell, but also that it is immediately followed by a slower depletion (the drop over the time interval $.08 < t < .12$, which we call the "shoulder"). The slower loss is primarily due to the fluxing of the remnant through the cell boundary. If we add the energy loss $rp, 0 < r \leq 1$, due to the burnout of the core to that carried out of the cell by the remnant, we obtain a total loss of energy in the cell very close to the total amount p carried by the collapsing filament.

The remnant plays two roles in the dissipation process. First, it provides a nucleating center for new collapses, a fact we have verified by examining the spatial distribution of collapse sites. As a consequence the frequency of collapses increases. In Figure 6, we plot a histogram of the times between successive events w for the case $\gamma_b = 2$. The distribution is nearly Poisson with a mean time between events of $\omega_c^{-1} =< 2 > \simeq .08$. Second, the gradual damping of the remnant enhances the ambient dissipation rate $< \gamma_A >$ (i.e., the dissipation rate averaged over time intervals free from collapse) over that amount we would expect from other dissipative mechanisms. In order to verify this, we carried out the following relaxation experiment. By changing the sign of the nonlinearity in equation (3) from plus to minus, we obtain a system with the same linear dispersion as the plus system and therefore presumably the same resonant wave interaction character but without the unstable modulational and nucleational instabilities and collapsing solutions. Initializing the two systems identical, we ran them with the forcing turned off ($\gamma_b = 0$) and compared their dissipation rates between collapses of the (+) system, before their energies had separated by more than 10% of the common initial value. The ambient dissipation rate of the (+) system was typically 50% greater than that of the non-collapsing (-) system while the collapse remnants were dissipated. Including collapse events in the tally, the (+) system lost energy three times as fast as the (-) system. We conclude, therefore, that the amount of energy dissipated by

7

non-collapse mechanisms is at most one quarter of the total energy dissipated.

Therefore, the energy dissipation budget is as follows. The average total dissipation rate $< \gamma >$ is given by

$$< \gamma >= \omega_c < r > p+ < \gamma_A > . \qquad (5)$$

The ambient dissipation rate can be eliminated in terms of $\frac{\delta n_c}{\delta n_T}$ since $\frac{\omega_c <r>p}{<\gamma>} = \frac{\delta n_c}{\delta n_T}$ and we obtain

$$< \gamma >= \omega_c p < r > \frac{\delta n_T}{\delta n_c} \qquad (6)$$

In (5) and (6), $< \gamma >$ depends only on the mean turbulence level $< n_\psi >$ but, as we have pointed out, $< \gamma_A >$ and ω_c depend both on $< n_\psi >$ and the nature of the dissipation $< r >$ depends only on the latter. In Figure 7, we plot both $< \gamma >$ and ω_c as a fraction of $< n_\psi >$ and, consistant with (6), these curves are parallel over a large range of $< n_\psi >$. Indeed, we checked the product $< \gamma > \omega_c^{-1}$ for a range of values of $< n_\psi >$ and found it to be almost independent of the mean turbulence energy level and equal to 13 and equal to the product $< r > \frac{(\delta n)_T}{(\delta n)_c}$ taken from Figures 3 and 4 ($< r > \simeq \cdot 3, \frac{(\delta n)_c}{(\delta n)_T} \simeq .75$). We expect that as the dissipation mechanism is postponed to higher k, the fraction of energy lost in burnout will increase and the histogram in Figure 4 will accumulate at $p = .29$. We also expect that ω_c will decrease proportionately and that in this limit the product $\omega_c < r >$ can in principal be activated theoretically by arguing that in a homoclinic excursion the phase point spends the longest time in its cycle near the saddles in the finite part of phase space. If this were the case $\omega_c < r >$ would be given by a product of σ, the growth rate of the modulational or nucleational instabilities, and k^2, the mean density of collapses. Both these quantities should depend mainly on $< n_\psi >$. Verification of these suggestions requires extensive computation which is presently underway but not yet complete.

In summary, then, we have demonstrated that the turbulent transport of field energy to dissipative spatial scales in the two dimensional nonlinear Schrödinger equation is overwhelmingly dominated by the explosive collapse of localized states or filaments, just as it is dominated by caviton collapse in the Zakharov equations. To help visualize these events as fluctuations about a basic homoclinic excursion(s) we have plotted flow trajectories projected onto the global observables n_ψ, H and $|\psi|^2_{max}$ to produce a curve in three dimensions shown in Figure 8a. In Figure 8b, we have projected this curve onto the three coordinate planes to aid visualization. Those trajectories which are fluctuations about homoclinic excursions are the sparse loops passing through the largest values of $|\psi|^2_{max}$. The denser, more jittery part of the curve lies in what we call (in the next section) the hash part of the attractor.

Whereas these results confirm the thesis that coherent collapse events dominate dissipation, the expense involved in two dimensional experiments did not allow us

to run a sufficient number of simulations in order to determine in what limit, if any, $\frac{\delta n_c}{\delta n_t}$ approaches unity. In connection with this question, and in parallel with the ideas of DiPerna and Majda [9], one would also like to develop the notion of a weak solution in which solutions of the undamped equations could be continued beyond the collapse time by simply deleting the collapsed filament and lowering the L_2 norm of the solution by a fixed amount. In order to examine these questions, we simulated the one dimensional nonlinear Schrödinger and Zakharov models with quintic nonlinearities on a grid of 1024 points. Aliasing errors were removed by smoothly interpolating ψ onto a grid of 8×1024 points before forming the nonlinear frequency $|\psi|^4$. The results for NLS showed that, for the same turbulence levels, the percentage of the dissipation rate accounted for by collapses rose from 59% at $k_d = 128$ (where, because the dissipation effects are clearly felt in the early stages, there are many failed attempts to form collapsing filaments), to 72% for $k_d = 256$, to 82% for $k_d = 512$. The average loss of energy per collapse decreases with k_d (the amount of energy greater than k_d in the Fourier transform of the collapsing filament decreases with increasing k_d) but the frequency of events increases proportionately so that the average dissipation rate remains the same. The evidence clearly suggests that in the large k_d limit, all the energy dissipated is dissipated by collapse events which occur infinitely often with infinitisemal losses of energy per event.

A much more striking result was obtained when we ran the very same experiment on the Zakharov model

$$\psi_t - i\psi_{xx} + i\rho\psi = F - \varepsilon D \tag{7}$$

$$\rho_{tt} + 2\nu \circ \rho_t - \rho_{xx} = (|\psi|^4)_{xx} \tag{8}$$

where F and D are as before and $2\nu \circ \rho_t$ is a convolution integral modelling ion damping. The ion acoustic field $\rho(x,t)$ is no longer slaved to the electric field intensity (for NLS, ρ in the equation (7) is replaced by $-|\psi|^4$). Therefore, during collapse, in which the fields take on a self-similar form close to (2) but in which the inertial acceleration ρ_{tt} is also important, the cavity formed by the ion field encourages total burnout of the filament. We found that when $\varepsilon = 1, k_d = 32, < n_\psi >= 1.625$, the average energy $< r > p$ lost per event was 1.95. the average time between events was .83 and $\frac{\delta n_c}{\delta n}$ was 92%. (For the Zakharov model, the amount of energy carried in the filament, a constant of the motion for the unperturbed equations, can take on a range of values greater than the threshold value $p = .43$ in this case. Thus $r > 1$). The distribution of r rose sharply after $r = 1$, had a mean of 1.95/.43 and had a relatively long tail. Also, we observed that all the collapses occurred in 9 nonoverlapping sites, were driven by the nucleational instability and the sites drifted about the box. When we increased k_d to 64, $< n_\psi >= 1.8$, the frequency of events increased to $(.66)^{-1}$ (there were 151 events in 100 time units) and the distribution of r came closer to one. The average energy lost per event was 1.55 and $\frac{\delta n_c}{\delta n_t}$ was 95%. (In contrast, at the same parameter values and in the same time interval, the NLS model had 972 events with an average energy loss of .09 and

9

$\frac{\delta n_z}{\delta n_t}$ was 72%.) Further, when we decreased ε to $\frac{1}{4}$ (again $k_d = 64$), the distribution of r came closer to threshold and $\frac{\delta n_z}{\delta n_t}$ was 98%. This leads us to conjecture that as k_d increases and ε decreases, the distribution of r will cluster about one, and that each collapsing event will burn off exactly the threshold energy $p = .43$. In this asymptotic limit, the weak solution of the unforced, undamped equation in which the turbulence eventually decays, is found by simply removing the collapsing filament from the field and reducing the L_2 norm by p. (The weak limit, i.e. $\psi(x, 0)$ is a weak solution if $\int \varphi(x)\psi(x, 0)dx = \lim_{\lambda \to 0} \int \varphi(x)\psi(x, \lambda)dx$ where φ is smooth, of a collapsing filament is zero because it oscillates very fast and its width decays at a faster rate than its amplitude increases). We will report more details elsewhere. We are also currently testing some ideas concerning the estimation of the frequency of events.

In Figure 9, we give the angle-averaged correlation function

$$C_\psi(\vec{\rho}) = \int_0^{2\pi} \frac{d\theta}{2\pi} < \psi(\vec{x} + \vec{\rho})\psi^*(\vec{x}) >$$

$$= \int_0^{2\pi} \frac{d\theta}{2\pi} \sum_{\vec{k}} e^{ik\rho \cos \theta} < |\hat{\psi}(\vec{k})|^2 >$$

$$= \sum_{\vec{k}} J_0(k\rho) < |\hat{\psi}(\vec{k})|^2 >$$

in the turbulent regime $\gamma_b = .2$. Observe that the correlation length $\lambda = 2\pi < k^2 >^{-\frac{1}{2}} \simeq .7$ is much less than the simulation box size (2π) so that the turbulence is independent of the periodic boundary conditions.

We end this section with a few remarks about the two-dimensional numerical scheme. In calculating solutions to (3), we use the following "split-step" numerical algorithm to advance the solution from t to $t + dt$.

$$\psi(\vec{x}, t + dt) = \psi^{(1)}(\vec{x})exp(-i|\psi^{(1)}(\vec{x})|^2 dt)$$

where (^refers to Fourier transform)

$$\hat{\psi}^{(1)}(\vec{k}) = \hat{\psi}(\vec{k}, t)exp(\gamma_b(k) - \gamma_e(k) + ik^2)dt$$

This method exactly conserves $n_\psi(\equiv \int d\vec{x}|\psi|^2)$ in the conservative limit ($\gamma_e \to 0$) and when aliasing errors are absent; errors in the Hamiltonian $\equiv \int(|\nabla\psi|^2 - \frac{1}{2}|\psi|^4)d\vec{x}$ are $0(dt^2)$. Aliasing errors incurred during the nonlinear part of the evolution are minimized by strong dissipation at short scales (see figure 9) that curtails the time-averaged spectrum (see figure 10). Our time step (dt) is 10^{-4}, and is sufficient to

resolve the maximum nonlinear frequencies ($|\psi|^2_{max} \leq 4 \times 10^3$) encountered in the most intense turbulent regime studied. The Landau damping function used is shown in Figure 10. Its asymptotic shape is chosen to be sufficiently steep ($\sim k^{1+\epsilon}, \epsilon > 0$) so that the collapsing filament is eventually arrested but not too steep so as to reflect the collapsing filament in $k-space$. It depends on a single parameter, the ion-to-electron mass ratio M, which in our analysis we take to be 7344 (the mass ratio in a singly-ionized Helium plasma), and increases abruptly at $k \cong .2k_d = .2(\frac{3}{2}\sqrt{M})$. The turbulence energy level is changed by varying the forcing term F. In all cases

$$ F \equiv \gamma_b[\psi(\triangle k_x, \triangle k_y) + \psi(-\triangle k_x, \triangle k_y) + \psi(\triangle k_x, -\triangle k_y) + \psi(-\triangle k_x, -\triangle k_y)], $$

i.e., energy is injected by linearly destabilizing four modes symmetrically in $k-space$, where $\triangle k_x \equiv \frac{2\pi}{L_x}, \triangle k_y \equiv \frac{2\pi}{L_y}$, and $L_x = L_y = 2\pi$. (Our simulations are in a square box 2π long on each side spanned by a regular grid of 128^2 points.) Because this scalar forcing is isotropic, the turbulence is isotropic. (See Figure 10). Notice that as a filament collapses it will decouple from the forcing which is confined to long wavelengths. Thus the dominant transport mechanism (collapse) is independent of the details of injection.

Geometry of phase space

While the full attractor A is large dimensional, the dominance of filaments suggests that A is the fuzzy covering of a skeleton which consists of generalized saddle points M and S and two heteroclinic orbits. In the case study just discussed, M is the set of saddle points which are modulationally or nucleationally unstable and S is the idealized collapsing filament, namely the singular self-similar solution of the two dimensional nonlinear Schrödinger equation. The unstable manifold of M intersects the stable manifold of S and vice versa. Based on this picture, A can be subdivided into two subsets A_H and A_C. When the system is in the turbulent soup A_H, it is dominated by what we call the *hash modes* consisting of the background field and radiation modes left over from the formation of the coherent structures (the filaments of Langmuir turbulence). This set is generally large dimensional and in the case of shear flow turbulence could have dimension $R^{\frac{9}{4}}$. On the other hand, when the system is in A_C, it is dominated by the coherent structures, although large dimensional fluctuations about these orbits are still present. The orbits in A_C are organized by a low dimensional submanifold of solutions B, which is the stable manifold of an unstable saddle point S, possibly at infinity, corresponding to an idealized state. In general, S may be a manifold of idealized states and in many cases will be the orbit of some group action representing the symmetries (translation, scaling) which are properties of the system at hand. In particular, if the spatial dimension is large, coherent structures, each with the same shape, can be localized at several locations, although occurring at different times, with an approximately uniform density reflecting the amount of power (energy density times area or volume) needed to form the structure. (In Langmuir turbulence, each

11

filament requires an area of k^{-2}; k depends on the turbulence intensity level.) In constructing the phase space, one should think of the system as being confined to a box of a sufficient size to contain one coherent structure or to a lattice in which case the idealized solution S consists of an array of discrete translates of the prototype and we consider the system to be in the state S when any one is triggered. The unstable manifold of S (the burnout due to Landau damping) is asymptotic to A_H. The speeds of attraction and repulsion at S are governed by two entirely different processes and are not related. The former is determined by the faster than exponential rate at which the filament becomes singular, the latter is governed governed by dissipation. The picture we have described is drawn schematically in Figure 12, and corresponds closely to an actual orbit of the nonlinear Schrödinger equation shown already in Figure 8.

We now turn to a discussion of the structure of the phase space, the nature of the saddle point M and its unstable manifold. Whereas the perturbations of forcing and damping modify the phase space structure, it is the topology of the phase space of the unperturbed system which sets the stage for the large homoclinic excursions. Two properties of the unperturbed system, which is Hamiltonian, are crucial. One is the fact that its phase space contains many saddle points corresponding to unstable fixed points and periodic orbits and separatrices joining these saddles. The second crucial property is the non-compactness of the constant energy surfaces and the existence of heteroclinic connections (HCI's) which join certain of the saddle points to infinity. Whereas Hamiltonian perturbations of this system can destroy resonant KAM tori and create new chains of elliptic centers and hyperbolic saddles and non-Hamiltonian perturbations can turn the centers into attracting sinks or destroy them altogether, the hyperbolic nature of the original saddles and their HCI's remain intact and play a dominant role in the dynamics of the perturbed system. As an example, consider the perturbed Duffing's oscillator

$$x^{\cdot\cdot} + x - 2x^3 = F(t) - \left(\frac{x}{x_0}\right)^n x^{\cdot} \tag{9}$$

where $F(t)$ is small and the additional factor $\left(\frac{x}{x_0}\right)^n$ has been added to the damping term in order to arrange for it to turn on only when x is large. The unperturbed, exactly integrable Hamiltonian system represents a particle in a quartic potential $V(x) = \frac{1}{2}(x^2 - x^4)$ with critical points $x^{\cdot} = x = 0$ (a center) and $x^{\cdot} = 0$, $x = \pm \frac{1}{\sqrt{2}}$ (saddle points). Its phase plane is shown in Figure 13. The unstable and stable manifolds emanating from $x = \pm \frac{1}{\sqrt{2}}$ are the non-compact energy level surfaces $E = \frac{1}{8} = \frac{1}{2}x^{\cdot 2} + \frac{1}{2}x^2 - \frac{1}{2}x^4$ which join the saddles to infinity through the HCI's $x^{\cdot} = (x^2 - \frac{1}{2})$ for $x^{\cdot} > 0, x > \frac{1}{\sqrt{2}}$ and $x^{\cdot} = -(x^2 - \frac{1}{2})$ for $x^{\cdot} < 0, x < -\frac{1}{\sqrt{2}}$. The other branches, the stable manifolds of $x^{\cdot}$ and $x = \pm \frac{1}{\sqrt{2}}$, are repellers for positive time. In particular, observe that all energy level surfaces $E > \frac{1}{8}$ and those for $E < \frac{1}{8}$ for which $x^2 > \frac{1}{2}$ approach the HCI's at infinity and that any point on these trajectories

will reach infinity in a finite time. This can be seen in several ways. First, notice that the distance $x_1 - x_2$ between two constant energy curves E_1 and E_2 at a given value of $x^{\cdot}$ is given by $(x_1^2 - x_2^2)(x_1^2 + x_2^2 - 1) = 2E_2 - 2E_1$ so that asymptotically $x_1 - x_2 \sim (2E_2 - 2E_1)(x_1 + x_2)^{-1}(x_1^2 + x_2^2)^{-1}$. Second, one can construct a Laurent series for any solution in the neighborhood of infinity,

$$x = \frac{1}{t - t_0} + \frac{1}{6}(t - t_0) + c(t - t_0)^3 + \sum_{n > 3} a_n(c)(t - t_0)^n$$

which, because the system is integrable, has the Painlevé property (the series is Laurent and has the required number of free constants, namely two, t_0 and c; all the other coefficients a_n can be calculated explicitly in terms of c). The free constant c is related to the energy $E = -5c + \frac{7}{72}$. The distance between any two orbits is the minimum over t_1 and t_2 of $x(t_1, c_1) - x(t_2, c_2)$ which goes to zero like $(t - t_1)^3$. *We have thus introduced a new concept into Hamiltonian systems with non-compact energy surfaces, namely the notion that certain orbits (HCI's) can serve as attractors for all other orbits at infinity in the sense that they are asymptotically all the same.* This notion does not violate conservation of volume in phase space. Close to infinity, the stretching of nearby points in a direction parallel to the HCI is faster than exponential (the local stretching exponent in this direction is infinite) and therefore the contraction in the direction perpendicular to the HCI is also faster than exponential. For small forcing, the orbits of the perturbed systems which escape to infinity also follow the HCI very closely until $x > x_0$ at which point dissipation sets in. However, the important point is that for x_0 large, all escaping orbits are approximately parallel to the HCI over large regions of the phase space.

One can look at the nature of the phase plane at the line at infinity by introducing homogeneous projective coordinates given by $x = \frac{X}{Z}, x^{\cdot} = y = \frac{Y}{Z}$ in which coordinates the direction field $(x - 2x^3)dx + ydy = 0$ becomes $(XZ^3 - 2X^3Z)dX + YZ^3dY + (2X^4 - X^2Z^2 - Y^2Z^2)dZ = 0$. Since the critical point at infinity is $X = Z = 0$, it is interesting to look at the direction field in the affine chart given by $Y \neq 0$. The line field in the X, Z coordinates is obtained by setting $Y = 1$ and $dY = 0$. We observe in Figure 12 that invariant manifolds $(Y^2 + X^2)Z^2 - X^4 - 2EZ^4 = 0$ organize the flow field in the neighborhood of the line at infinity and in particular all of them converge from the half plane $X > 0$ to the point $X = Z = 0$ on the line at infinity and then reemerge in the left hand plane. The convergence of these curves at infinity again shows that the HCI is an attractor there.

This simple example illustrates how the topology of the phase space of the unperturbed system is important in controlling the dynamics of the perturbed system. Likewise in the weakly perturbed nonlinear Schrödinger equation, in which forcing is applied at small wavenumbers and the damping at large, it is the topology of the phase space structure of the unperturbed problem which dominates the

dynamics of the perturbed problem. The unperturbed problem is again Hamiltonian although, in this case, it is infinite dimensional with motion constraints $n_\psi = \int \psi \psi^* d\vec{x}$, $J = i \int \psi \nabla \psi^* - \psi^* \nabla \psi) d\vec{x}$ and $H = \frac{1}{2} \int (\nabla \psi \cdot \nabla \psi^* - \frac{1}{2} \psi^2 \psi^{*2}) d\vec{x}$. In particular, as we have mentioned, it is known that the energy surface is non-compact and when $H \leq 0$, there are orbits in any surface $n_\psi \geq n_c = 2\pi \int_0^\infty R^2(\eta) \eta d\eta$ which connect the unstable saddle points to infinity. We remark, however, that in our simlulation H was almost always positive although taken in the neighborhood of a collapse it was zero. The negativity of H is a sufficient but not necessary condition for collapse.

Our picture of the phase space then is as follows. For low levels of forcing (either F is small or the domain area is small), the modulus of the electric field grows till $n_\psi > n_c$ at which stage the phase point eventually comes close to a modulationally unstable saddle point which is joined to infinity via a collapsing filament. The instability sets in, the filament is formed, it collapses, a certain portion of its energy is dissipated (depending on the damping structure) and a remnant of high k waves is left over. The system returns close to its original state and the process is approximately repeated with the initialization of the collapsing filament being due to either modulational or nucleational instabilities. In particular, the remnant can provide a cavity for the nucleation of metastable cavitons which collapse once the support disperses away. For larger values of the applied stress (either larger forcing or larger boxes), the value n of the mean turbulence level is much larger and can be many times n_c. In this case, spatial correlations decay rapidly and many collapsing filaments can occur at different spatial locations although since each event is so rapid, they will rarely occur in the same time intervals. For these large turbulence levels, the saddle point M in Figure 12 represents a collection of saddle points in the turbulent soup part of the attractor A_H, some of which correspond to analogues of the modulational instability of more complicated periodic shapes and others of which are best understood as nucleational instabilities. As we have mentioned, the collapsing filament is often initiated in the remnant of a hole left by a previous event or in holes simply produced by random fluctuations. No matter what the mechanism, the important point is that the attractor contains many saddle points M which are connected to infinity through HCI's and the phase point passes sufficiently close to these points so that the large homoclinic excursion is initiated.

We mention here that a similar situation obtains in the Euler equations. For low values of the applied stress, laminar states can be destabilized by identifiable instability mechanisms, centrifugal instabilities, mean flow profiles with inflexional points and so on. These instabilities do not go away when the fluid becomes fully turbulent. Indeed saddle points representing local inflexional and centrifugal instabilities remain very much part of the strange attractor of the high Reynolds number Navier Stokes equations and play a large role in transferring energy to high wavenumbers where dissipation acts. In highly turbulent flows, the inflexional pro-

14

file of the mean flow is not sustained for all time uniformly in space, but if it is sustained long enough in a local region (see the discussion on turbulent boundary layers in the following section), then rapidly growing packets of three dimensional inflexional instabilities can erupt and carry energy off to the dissipation cemetaries.

Other illustrations of the random occurrence of coherent events

This view of turbulent transport, in which the major contribution comes from a part of the attractor which corresponds to coherent structures whose dynamics can be captured with a finite number of degrees of freedom, while not universal, should have widespread application. We now suggest several other contexts in in which these ideas may be important. We *stress* that in no case do we feel we have presented the complete and final solution, but simply wish to suggest that it may be worthwhile to look at each of these situations from a new viewpoint. The first is the burst-sweep cycle [10] which appears to dominate the production of turbulent energy and momentum transport in turbulent boundary layers. Although no candidate for the coherent structure which models the four step process constituting the burst phase of this cycle has yet been put forward (there have been suggestions [11]), it is not improbable that a singular, finite time collapse solution of the Euler equations plays a significant role. This basic structure could probably be captured by a simpler set of p.d.e.'s, analogous to the Zakharov equations, in which a long scale, three-dimensional Tollmein-Schlichting like disturbance with large downstream vorticity (streaks) is synchronously coupled to a packet of short inflexional waves produced by an inflexional instability of the mean turbulence velocity profile caused by the induced outflow of the streaks [10,11]. The inflexional instability, ever present in shear flows, together with the finite amplitude distortion of the mean profile by the long scale state, plays the role that modulational and nucleational like instabilities do in Langmuir turbulence. It continuously drives the initial stage of the bursting solution.

Convection at large Rayleigh numbers is a second area in which the transport properties are likely to be organized by coherent structures, in this case the slightly tilted plumes observed by Krishnamurti and Howard [12] which dominate the flow for a large range of Prandtl P and Rayleigh numbers R_a. More recent observations by Libchaber [13] in what he calls the soft turbulence regime ($R_c < 10^7$) would seem to lend some credence to the admittedly simplified picture, suggested many years ago by Howard [14], that the plumes would occur at a frequency determined by the time $R_a^{-\frac{2}{3}}$ it takes for a conductive layer to build to a depth $R_a^{-\frac{1}{3}}$ so as to be convectively unstable. A crude picture in which one imagines that the coherent plumes carry off all the heat in the unstable conductive layer would suggest a Nusselt number proportional to $R_a^{\frac{1}{3}}$ which is approximately what is observed. The inferences of the Howard argument are also consistent with a "mixing-length" analysis given in an earlier paper by Kraichnan [15]. To be sure, this picture is greatly oversimplified and it is hard to see how the plumes, which combine into larger and larger ones,

remember the Howard time scale. Nevertheless, Libchaber observes this scale as dominant in the power spectrum of his signal, measured many conductive layer depths from the bottom of the tank, over a large range of Rayleigh numbers up to approximately 10^7. At this stage, local Reynolds numbers, which are proportional to the square root of the Rayleigh number, are in the shear flow instability range and other structures are produced which modify somewhat the Howard picture.

Third [15], we suggest that the self-similar features seen in the Rayleigh-Taylor unstable interface two fluids of different densities are exact, singular solutions of the Euler equations, which if they were known, would help one to calculate an approximation to the mass flux of heavier through lighter fluid. In the absence of a length scale (surface tension is ignored), the set of attracting states S at infinity will be a complicated fractal set reflecting the scale symmetries, but the basic elements of S would represent the spikes (containing the heavier fluid falling through the lighter) and bubbles (the lighter fluid pushing up through the heavier). Fourth [16], it is not unreasonable to argue that the dissipation rate of shear flow turbulence arises not from the wave-wave interaction familiar from Fourier space cumulant descriptions, but instead to suggest it is dominated by the formation and destruction of thin vortex sheets (the state S) in which almost all of the vorticity is concentrated. We conjecture that the initial formation of surfaces of vorticity concentration follows singular solutions of the Euler equations driven principally by inflexional instabilities. Once formed (the system is close to S), these sheets are notoriously unstable, to Kelvin-Helmholz instabilities of the tangential velocity discontinuities and to Taylor-Gortler centrifugal instabilities of the helical flows induced by vortex lines embedded in the curved sheets. These secondary instabilities [17,18] quickly transfer the energy to the viscous cemetaries where energy is dissipated and the system is returned close to a state where approximately the same cycle can repeat.

Our last case study concerns the generation of turbulent spots in a boundary layer. This example is somewhat different in nature to the preceding examples but nevertheless exemplifies the general idea of transport occurring as a result of the random occurrence of coherent events - in this case the formation and convection of the spots - which can be associated with homoclinic excursions. We shall also discuss a simplified model and make some experimental predictions. However, before doing this, let us recall the initial stages of the boundary layer instability without receptivity (undue influence of fluctuations in the outer flow). When the Reynold's number, based on the boundary layer thickness which depends on the distance from the leading edge, reaches a critical value, the unstable two dimensional Tollmein-Schlichting (T.S.) wave concentrated at the critical layer quickly becomes three dimensional thereby creating downstream vorticity. The induced secondary flow causes an outward flow near the crests (the most downstream part of the distorted " vortex" lines) and an inward flow near the troughs. The three dimensional distortion is enhanced by the mean shear, the downstream vorticity increases and the initially sinusoidal three dimensional deformation of the vortex

line becomes strongly distorted into the form of an elongated hairpin vortex. The induced outward flow carries slow moving fluid to the outer part of the boundary layer and causes the mean turbulent profile to develop inflexion points localized in both time and the spanwise direction. At these points, short wavelength packets of an inflexionally unstable nature can grow and be absolutely (rather than convectively) unstable if they can phase lock with the travelling three dimensional disturbance which gives rise to their formation in the first place. Along these trajectories turbulent spots are formed which spread spatially into surrounding regions by destabilizing the neighboring laminar flow. Our picture of the spots is that they are essentially localized wavepackets in which the waves are breaking. Suppose one monitors the velocity field $v(t)$ at a point just before the area in which the spots tend to form. A reconstruction of the attractor from this time-series should show an attractor $\tilde{A}$ with a well-defined phase corresponding to the phase of the incoming T.S. waves and we propose using the methods of the following section to check this conjecture. However, monitoring the velocity field in the full region one will find an attractor A which will have an A_H somewhat similar to $\tilde{A}$, but also with a part A_C consisting of the homoclinic excursions which occur when a spot forms and is convected downstream. When the spot reaches the region where they have coalesced or left the channel, the system has returned to A_H.

The phase space associated with this dynamics is somewhat different from that proposed previously for collapsing filaments. Nevertheless, while the homoclinic excursion will not go to infinity, it will have several features in common with the previous picture. We consider here a very simple mathematical model to illustrate what we have in mind. Consider a locally unstable attracting periodic orbit γ in phase space. This is an orbit which is attracting in the usual sense that all its Floquet multipliers have modules less than one, but which at some points x in γ is actually repulsive. An example of such as orbit would be given by the periodic solution $x = 0$ for the time-dependent system.

$$X(x,s): \frac{dx}{dt} = a(s)x + \mathcal{O}(x^2), \frac{ds}{dt} = 1, (s,s) \in R \times T^1 \qquad (10)$$

where a(s) is a smooth function which is -1 for $0 < s < 1/2$, 1 for $5/8 < s < 3/4$ and nearly linear in between. Another more natural example is given by the following flow in the plane (See Figure 14). If the periodic orbit γ is close to the saddle M then γ will be unstable near M even though γ is attracting in the usual sense. Now returning to the general picture, suppose that such a system is subject to some periodic or almost-periodic forcing or perturbation. If the perturbation is large when the state is near the unstable part of γ then one will see a relatively large excursion of γ, otherwise the perturbation will be quickly damped out. This picture is a useful oversimplification of the dynamical phase-space structure associated with spots. The attractor A_H like γ is unstable in some parts so that the incoming waves perturb the state sufficiently to send it on an excursion in A_C. Of course, we are not

17

suggesting that A_C and A_H are uncoupled as in the simple example: indeed, they are part of a single strange attractor. But these can be thought of as coming from a common picture as we now indicate. Consider again the situation shown in Figure . If this system is periodically forced then the total system is described by a Poincare map corresponding to advancing one period of the forcing and the above picture can be regarded as being associated with the vector field $X(x, s)$ given in Equation (10) for s frozen. Suppose that the way in which this frozen vector field changes during one cycle of the forcing is such that a limit cycle gets pushed through the stable manifold of the saddle M. Then homoclinic orbits are formed in the complete system and this will have an attractor consisting of a set A_H of orbits close to the cycle γ and horseshoes near M, and homoclinic excursions going from a region close to M back to A_H. If this is a reasonable approximation of the phase space then we can make a prediction. There should be a correlation between the creation of spots and the phase on A_H. Experimentally this can be checked by reconstructing A using the usual time-series methods and recording when spots occur in the region just downstream from the monitoring point.

Identification of coherent structures

As the final part of this paper, we want to propose a method of time series analysis which can identify those modes which contribute most to transport. These ideas are based on and are a modification of the singular value decomposition (SVD) methods of Broomhead and King [19] to improve phase-space constriction techniques and Lumley's method for identifying coherent structures in turbulent flows. We will elaborate on these ideas in more depth in a future publication with David Broomhead but here we will sketch the main points. The principal goal of the method is to extract organized structures which may come and go from what appears to be a sea of disorganized and statistical fluctuations.

Firstly, let us recall the basic ideas from the perspective of dynamical systems. We suppose that we have a dynamical system acting as a Hilbert space H with an attractor A which has a natural measure ν. Let the mean $\bar{v} = \int v \nu(dv)$ be subtracted from each of the vectors v so that they then have zero mean. We define an orthogonal basis $e_1, e_2, \ldots$ of H by maximizing

$$F = \int (e \cdot v)^2 \nu(dv) + \lambda(|e|^2 - 1) \tag{11}$$

to get e_1, and then, given $e_1, \ldots, e_i$, taking for e_{i+1} the maximum of F in the orthogonal complement of $e_1, \ldots, e_i$. We ignore for the moment the non-generic situation where F does not have such maxima and where A is contained in a finite-dimensional linear subspace. For the maximal basis, we find

$$F = \sigma_i^2 = \int (e_i \cdot v)^2 \nu(dv) \tag{12}$$

18

Then the σ_i can be regarded as the moments of inertia of A if A is regarded as a body the mass of whose points is given by ν. The e_i are the corresponding axes of inertia and these can be easily calculated by constructing the inertia tensor by differentiating (11) and solving for its eigenvectors. In this case the inertia tension is the $n \times n$ matrix $X^t X$ where X is the $n \times N$ matrix whose i^{th} row is the vector $\vec{v}_i$. This is completely practical procedure which we have carried out on a number of (finite dimensional realizations of) p.d.e.'s. In practice, the vectors $\vec{v}_i$, $i = 1 \cdots N$, could be the $n-$ vector $V(\vec{r}_j, t_i)$, when $\vec{r}_j$ is an array of n points distributed in space and V is some flow component which is measured at the sequence of times $t_i, i = 1, \cdots N$. The (i, j) element in the inertia tensor is then the correlation function $< V(\vec{r}_i, t) V(\vec{r}_j, t) >$. A major reason for the importance of this basis is that if $v(t)$ is a generic solution in A and $\phi_1, \phi_2, \ldots$ is any orthogonal basis for H, then the r.m.s. error of a k-th order truncation

$$\lim_{T \to \infty} T^{-1} \int_0^T \| v(t) - \sum_{j=0}^k (v(t) \cdot \phi_j) \phi_j \|^2 \, dt \qquad (13)$$

is minimal for all $k \geq 0$ precisely when $\phi_j = e_j$ for all $j \geq 1$.

The *local version* of this procedure is equally important, because of the intermittency and fluctuation of the organized structures. Like the filaments of Langmuir turbulence, they will often have a transient character and averages taken over all time or over the global attractor will miss them. Accordingly, we define the notion of a local SVD as follows. Given $x \in A$, let $B_\epsilon(x)$ denote the ball of radius ϵ about x. Instead of taking the whole of A, we regard the points in $B_\epsilon(x)$ as making up the mass with their weights again given by ν, but suitably normalized. Just as in the global case, we can then obtain an orthogonal decomposition of H and the associated moments. We assume that, as $\epsilon \to 0$, the axes converge to the axes

$$e(x) : \qquad e_1(x), e_2(x), e_3(x), \ldots$$

and have the spectrum

$$\sigma(x) : \sigma_1(x) > \sigma_2(x) > \sigma_3(x) > \cdots$$

If the flow field is locally dominated by a d-dimensional structure, then the spectrum of moments $\sigma(x)$ has the property that the $\sigma_j(x)$ decay exponentially in j for $j > d$. This feature is very important as it allows us to contruct a local analogue of the Lyapunov spectrum, which is defined as the set of growth rates of successively larger sub volumes of the tangent space of a trajectory in the phase space. Under fairly weak assumptions (sufficient hyperbolicity on the attractor to ensure that any trajectory eventually covers the attractor), the Lyapunov spectrum exists as

19

a global quantity. It would be tempting to suggest (hope!) that this is a natural decomposition of the Lyapunov spectrum into a small set of a d order one exponents and a much larger set D whose magnitudes cluster around zero. In general, this will not be true, because the homoclinic excursions are dramatic local events which, although responsible for transport, may be relatively rare and therefore a global average using the usual density of points invariant measure on the attractor will smear local large values of the growth rate over the whole trajectory. Therefore it is unlikely that the Lyapunov spectrum will decompose as one might optimistically hope. Neither can the Lyapunov exponent be defined locally. However the local SVD decomposition is well defined and does discriminate between various directions in the local tangent space. For example, if we take a ball on the attractor at a point x from which a the homoclinic excursion begins, the d directions associated with the dominant moments inertia $\sigma_j(x)$ do span what we have called the order one unstable manifold of A_H at x.

Moreover, we can adapt these further in order to look for correlations between organized structures and the transport properties of the flow. To do this we have to bring in the ideas of Broomhead and King on time-series analysis. Suppose that besides measuring a representation of the state $v(t)$ at time t, we also record a measure $n(t)$ of the transported quantity. For simplicity of notation and compatibility with real data we assume that the time t is discrete. For each t consider the vectors

$$w(t) = (v(t), n(t-a), \ldots, n(t-b)).$$

Let $\tilde{A}$ denote the set $\cap_{T>0} \cup_{t=T}^{\infty} \{w(t)\}$ and construct the axes $\tilde{e}_i$ and moments of inertia $\tilde{\sigma}_i$ for $\tilde{A}$ as for the attractor A in the global procedure above. In practice $\tilde{A}$ will be finite so for ν one takes the measure on $\tilde{A}$ which give the points equal weight. For small i the axes

$$\tilde{e}_i = (e_i, n_{-a}, \ldots, n_b)$$

will then give the dominant structures, each being an important spatial structure e_i together with the transport time-series $n_{-a}, \ldots n_b$ correlated with this. It thus gives us the relationship between spatial structures and transport. The problem is that the spatial structures which transport the most may not correspond to the dominant moments because of their infrequent occurrence (and hence low weight with respect to ν), or because they may get mixed (as linear combinations) with modes transporting less. To overcome this problem we propose that the vectors $v(t)$ should be weighted by $\lambda n(t+c)$ for some suitable c and $\lambda > 0$. Provided λ is large enough, the dominant moments should then correspond to those which transport most. For example, λ might be chosen to be the transport itself or some suitable power thereof. As well as obtaining the relationship between spatial modes and transport properties, this procedure singles out those modes which transport most.

20

Finally, we note that one can perform a local version of the global axes of inertia. This may be especially useful when there are problems with phase fluctuations or variations [20].

Acknowledgements

References and Footnotes

[1.] There have been several papers on the estimation of the Hausdorff dimension of the attractor for Navier-Stokes and other simpler p.d.e.'s such as Kuramoto-Sivashinsky(KS) and complex Ginzburg-Landau (CGL). Before listing them, we want to make several remarks. (i) The $R^{\frac{9}{4}}$ estimate for the Navier Stokes equations is an upper bound which assumes the global existence of solutions and the existence of certain integrals, neither of which has been established. (ii) The nature of the power spectrum, the rapid loss of spatial conditions on the Taylor microscale of $R^{-\frac{1}{2}}$, the apparent importance of the Kolmogoroff inner scale all suggest that for large Reynolds numbers the upper bound is not unexpected or a gross overestimate. (iii) Even if one knows the Hausdorff dimension of the attractor is $R^{\frac{9}{4}}$, this does not mean that there is an inertial manifold (global center manifold); namely there is a subdivision of the Hilbert space in which the flow lives into active and passive subspaces P and Q, P finite dimensional, and the inertial manifold is the graph of the mapping from P to Q with the property that it attracts all trajectories exponentially. The existence of an inertial manifold which can be proven for the simpler p.d.e.'s like KS and CGL means that the dynamics on the attractor can be replaced by a dynamics on P governed by a finite, albeit large dimensional system of equations.

[2.] J.L. Lumley *Coherent structures in Turbulence*. Transition and Turbulence. Ed. R.E. Meyer. Academic Press. 1981 pp. 215-242.

[3.] D. Ruelle, *Large volume limit of the distribution of characteristics exponents in turbulence*, Commun. Math. Phys. 87, 287-302 (1982). *Characteristic exponents for a viscous fluid subjected to time dependent forces*, Commun. Math. Phys. 93, 285-300 (1984).

C. Foias, O. P. Manley, R. Teman and Y. M. Treve, *Asymptotic analysis of the Navier-Strokes equation*, Physica 9D, 157-188 (1983).

C. Doering, J. D. Gibbon, D. D. Holm and B. Nicolaenko, *Low dimensional behavior in the complex Ginzburg-Landau equation*, to be published in Nonlinearity (1987).

J. M. Hyman and B. Nicolaenko, *The Kuramoto-Sivashinsky equation: a bridge between PDE's and dynamical systems*, Los Alamos Report LA-UR-85-1556.

[4.] A good review article is *"Collapse versus Cavitons"* by A. M. Rubenchik, R. Z. Sagdeev and V. E. Zakharov. Comments on Plasma Physics and Control Fusion 9, 183-206 (1985)

22

In this article, the authors argue that the prevailing evidence supports the assertion that, as a rule, Langmuir turbulence is a set of collapsing cavitons rather than quasi-stationary cavitons although they are aware that a convincing proof that this is the case will require more evidence.

M. V. Goldman, *Reviews of Modern Physics* 56, *709 (1984)*.

[5.] M. J. Weinstein. *"On the Structure and Formation of Singularities in Solutions to Nonlinear Partial Differential Equations*. Comm. Partial Differential Equations 11, 545-565 (1986).

[6] B. LeMesurier, G. Papanicolaou, Sulem, Sulem, Private Communication (1988).

V. E. Zakharov, Private Communication (1988).

[7.] H. Rose and M. Weinstein. *On the Bound States of the Nonlinear Schrödinger Equation with a Linear Potential.* Preprint 1987.

[8.] D. Russell, D. Dubois, H. Rose. *Collapsing Caviton Turbulence in One Dimension.* Physics Review Letters 56, 838 (1986).

D. Russell, D. DuBois, H. Rose. *Nucleation in Two Dimensional Langmuir Turbulence.* Submitted Physics Review Letters, 1987.

[9.] A. Majda, R. DiPerna, Private Communication

[10.] Kline, S. J., Reynolds, W. C., Schraub, F. A. and Runstadler, D. W. 1967. *The Structure of Turbulent Boundary Layers.* J. Fluid Mech. 30, 741-773.

[11.] M. T. Landahl, *Wave Breakdown and Turbulence.* Siam J. Appl. Math. 28, 735-756 (1975)

M. T. Landahl. *Ordered and Disordered Structures in Shear Flows.* Woods Hole GFD Physics 1986. Report number WHOI-86-45. pgs. 2-74 3,

N Aubry, P. Holmes, J. L. Lumley and E. Stone. *The Dynamics of Coherent Structures in the Wall Region of a Turbulent Boundary Layer.*

M. T. Landahl, *Coherent structures in turbulence and Prandtl's mixing length theory,* Z. Flugwiss. Weltraumforsch. 8 Vol. 4, 233-242, (1984).

A. C. Newell *Chaos and Turbulence,* Wood's Hole GFD Program 1986 Report number WHOI-86-65. pgs. 90-102.

[12.] R. Krishnamurti and L. N. Howard, *Large Scale Flow Generation in Turbulent Convection. Proc. Natl. Acad. Sci.* 78, 1981-1985 (1981)

[13.] A. Libchaber. Private Communication (1987)

23

[14.] L.N. Howard. *Convection at high Rayleigh number.* Proc 11th Int. Cong. Appl. Mech. Munich 1964. Springer-Verlag 1969. pp. 1109-1115.

[15.] R.H. Kraichnan. *Turbulent thermal convection at arbitrary Prandtl number,* Phys. Fluids S, 1374-1389 (1962).

[16.] D. H. Sharp. *An Overview of Rayleigh-Taylor Instability.* Physica 12D 3-18 (1984)

[17.] P.G. Saffman *"Lectures on Homogeneous Turbulence",* International School of Nonlinear Physics and Mathematics. Munich, 1966. Published as a Caltech Report.

A.A. Townsend *On the Fine Scale Structure of Turbulence.* Proc. Roy. Soc. A208 534. (1951).

[18.] S.A. Orszag and A. Patera. *Secondary Instability of wall bounded shear flows.* J. Fluid Mech. 128 347-385 (1982).

[19.] D. Broomhead and G. King. *Extracting Qualitative Dynamics from Experimental Data.* Physica 20D 217-236 (1986).

[20.] D. Broomhead, A.C. Newell and D.A. Rand. *Identification of Galerkin Bases by local Singular Valued Decomposition.* To appear.

Figure Captions

(1) Snapshots of $|\psi(\underline{x})|^2$ at times before (a) during (b) and after (c) the collapse of a filament in the turbulent ensemble sustained by driving with $\nu_b = 0.2$. The nearly simultaneous collapse of two filaments (d) and their remnants (e and f) shortly after collapse. Note the outward propagation and diminution of the concentric cylindrical shells that comprise the remnants.

(2) (a) The instantaneous rate of dissipation $\gamma(t) \equiv 2\sum_{\underline{k}} \gamma_e(k)|\hat{\psi}(\underline{k})|^2$, its integral $\Gamma(t) \equiv -\int^t \gamma(t\prime)dt\prime$, and the global spatial maximum of $|\psi(\underline{x})|^2$ as functions of time in the strong turbulent regime sustained with $\nu_b = 2$.

    (b) As in (a) but for a longer time. Notice that strong, sudden dissipation is exactly correlated with collapse and that the loss of energy $(-\Gamma)$ is approximately linear over long times.

(3) The total energy dissipated by collapsed filaments (δn_c) divided by the total energy dissipated (δn_T) for three different turbulent ensembles differing in mean intensity, $< n_\psi >$, as a function of the cut-off rate γ_0 used to define filament collapse. (See text for discussion.) Note that this ratio necessarily approaches one as $\gamma_0 \to 0$.

(4) A histogram of energies (δn) dissipated in the strong turbulent regime maintained by driving with $\delta_b = 2$. The cut off delta $\gamma_0 = 10$. Note that the distribution shifts towards the critical value $p = .29$ as $\gamma_0 \to 0$ (see texty for discussion).

(5) (a) As in Fig. 2(a) but confined to a small domain or "box" centered at a single collapse site in the case $\gamma_b = .2$. (The time origin has been redefined for convenience.)

    (b) The total energy in the box $(n_{box} \equiv \int_{box} d \to x|\psi(\to x)|^2$ and the conservative flux through the boundary of the box

$$(flux \equiv \int^t dt' 2Im \int_{\partial box} d\ell\hat{n} \cdot (\psi \nabla \psi^*))$$

as functions of time. Note the "shoulder" in the n_{box} graph, corresponding to the fluxing of the collapse remnant out of the box immediately following the sudden burnout of the core of the filament. Adding the energy lost in burnout $(t \cong .08)$ to that carried away by the remnant $(.08 < t < .12$, i.e., the shoulder) we obtain very nearly the critical value $p = .29$.

(6) A histogram of times passed between successive collapse events in the case $\nu_b = 2$. Note that the distribution is nearly Poisson, with a mean time between events of $< \tau > \cong .08$. Fluctuations are still affecting the tail.

(7) Mean dissipation rate $< \gamma > \equiv \sum_{\underline{k}} 2\gamma_e(k) < |\hat{\psi}(\underline{k})|^2 >$ and mean time between collapse as a function of the level of turbulence ($< n_\psi >$ for several different cases.

(8) Flow trajectories in the turbulent regime with $\nu_b = .85$ covering about 10 collapse events. The trajectories are projected onto the global observables $(n_\psi, H, |4|^2_m ax)$ to produce a curve in 3 dimensions displayed in (a). In (b) we have projected this curve onto the three coordinate planes to aid visualization. Those trajectories that are fluctutions about homoclinic excursions are the smooth sparse loops passing through the larger values of $|\psi|^2 max$. The denser, more jittery part of the curve lies in A_H.

(9) Angle-averaged correlation function.

(10) The damping function, $\gamma_e(k)$. Note the rapid turn-on of damping at $k_0 \cong 30 \cong .2k_d$, where $k_d = \frac{3}{2}\sqrt{M}$ and in all cases studied $M = 7344$.

(11) A contour plot of the long-time averaged spectral energy density $< |\hat{\psi}(\underline{k})|^2 >$. The scale is logarithmic: energy densities on adjacent solid contours differ by a factor or 100. Note that the turbulence is isotropic and that the damping (Fig. 3) confines the (time-averaged) energy to long and intermediate scales.

(12) A schematic drawing of the attractor and the homoclinic excursion.

(13) Phase plane for $x^{\cdot\cdot} = -x + 2x^3$.

(14) A scenario for the homoclinic excursion associated with turbulent spots.

Figure 1a

$t = 146.016$

Figure 1b

t = 146.036

Figure 1c

$\tau = 146.048$

Figure 1d
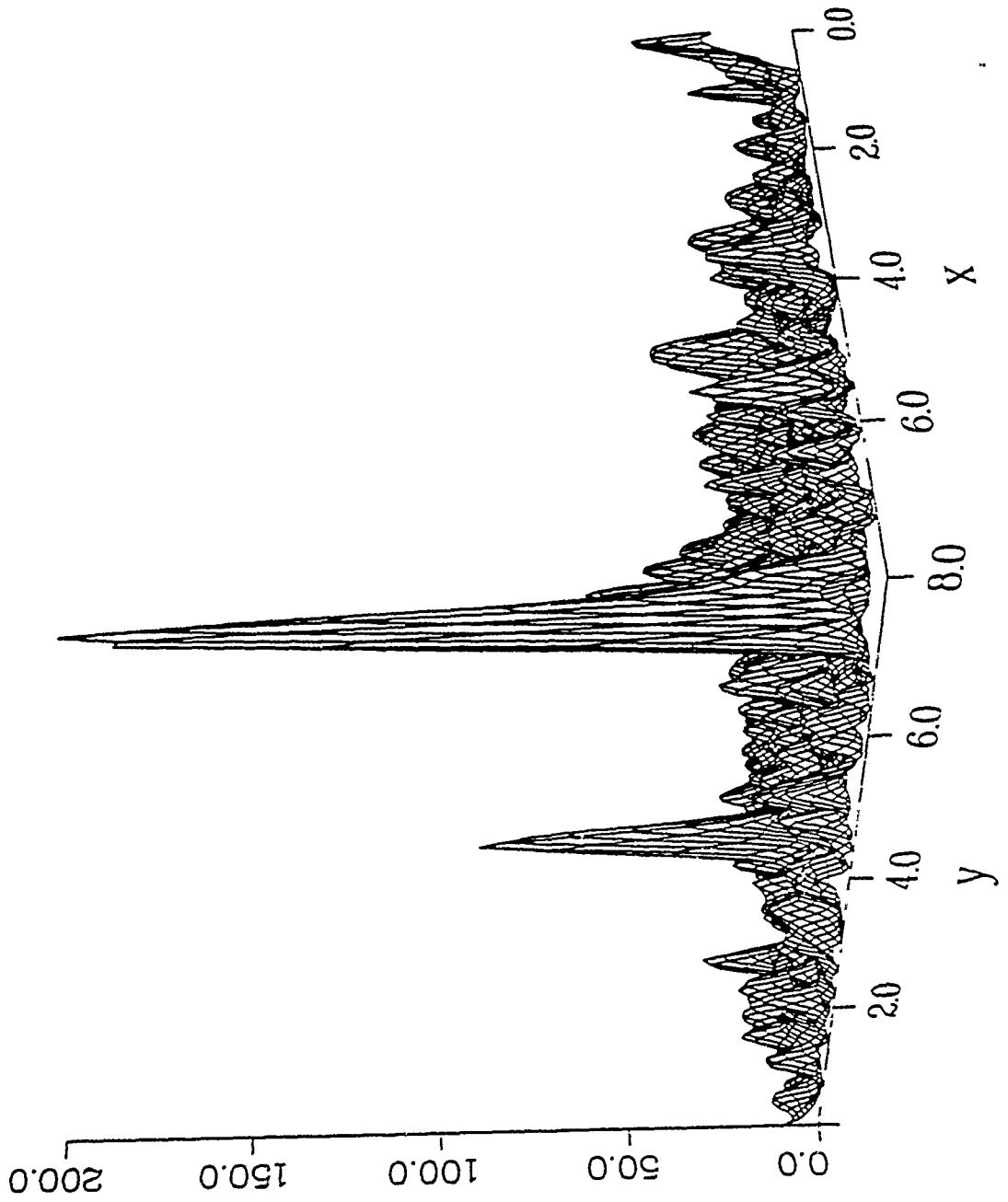
P = 2.00 GO = 0.000E+00 MI = 1836
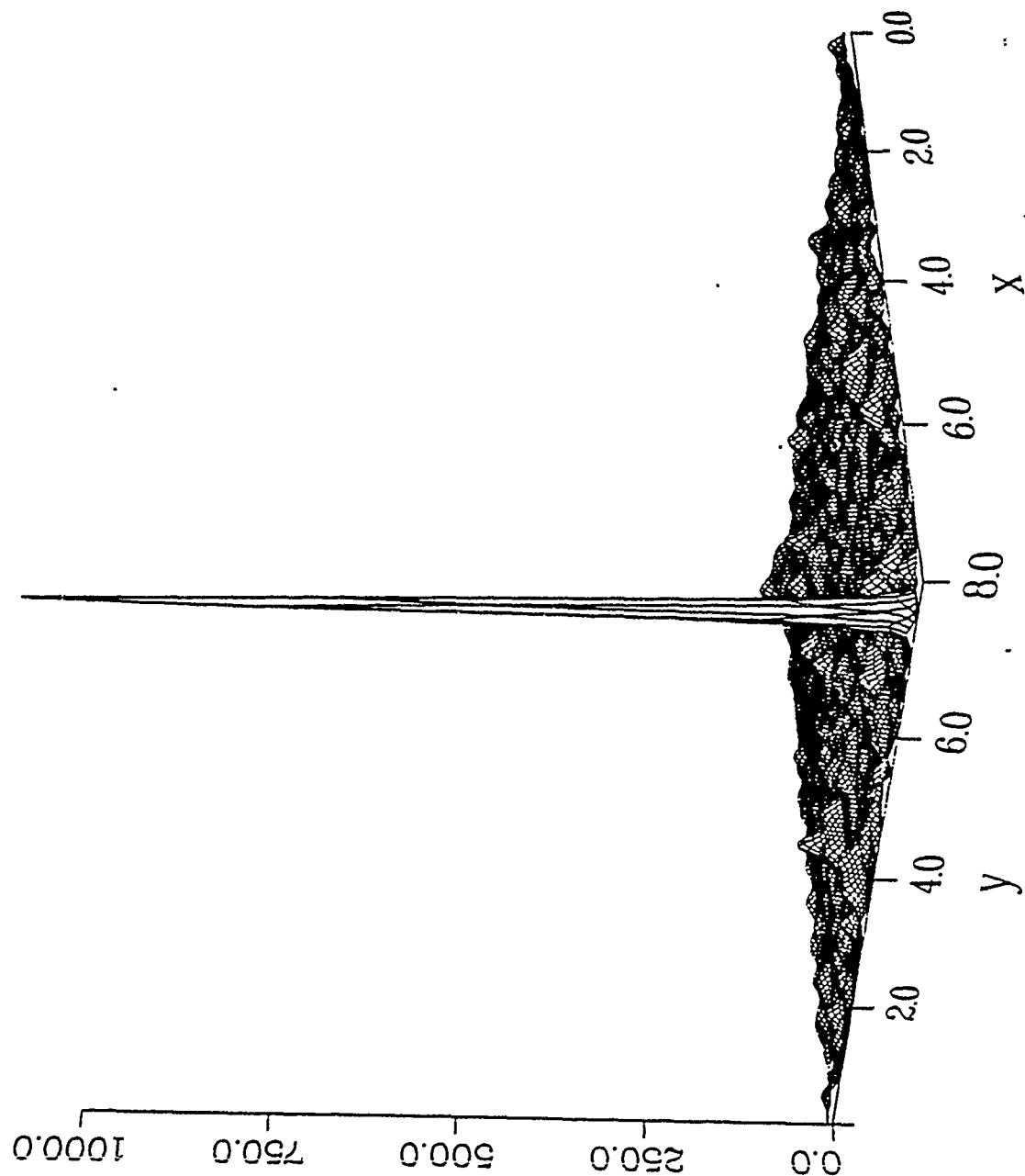
CLAMP 1.0000 0.0000
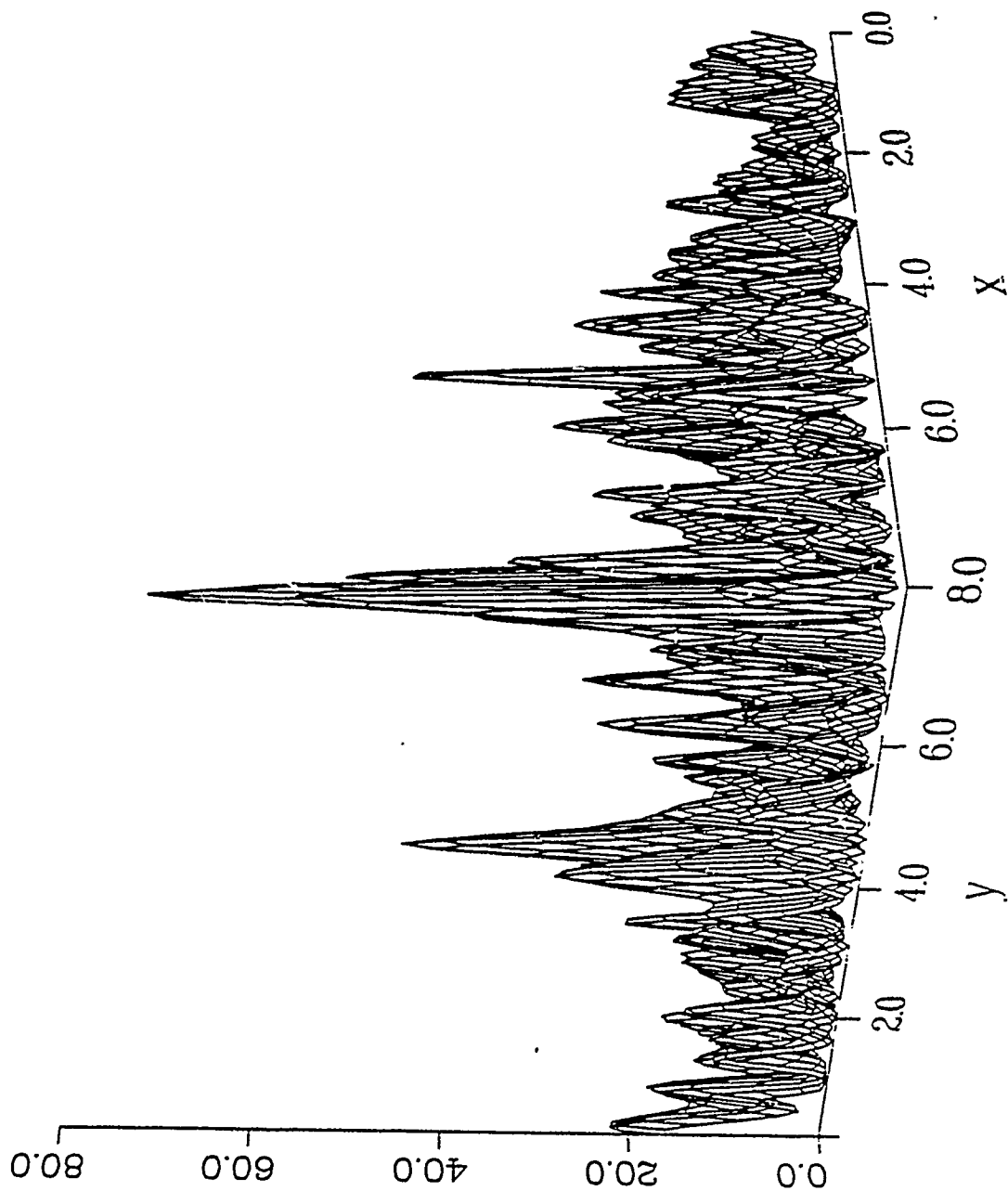
T = 5.680
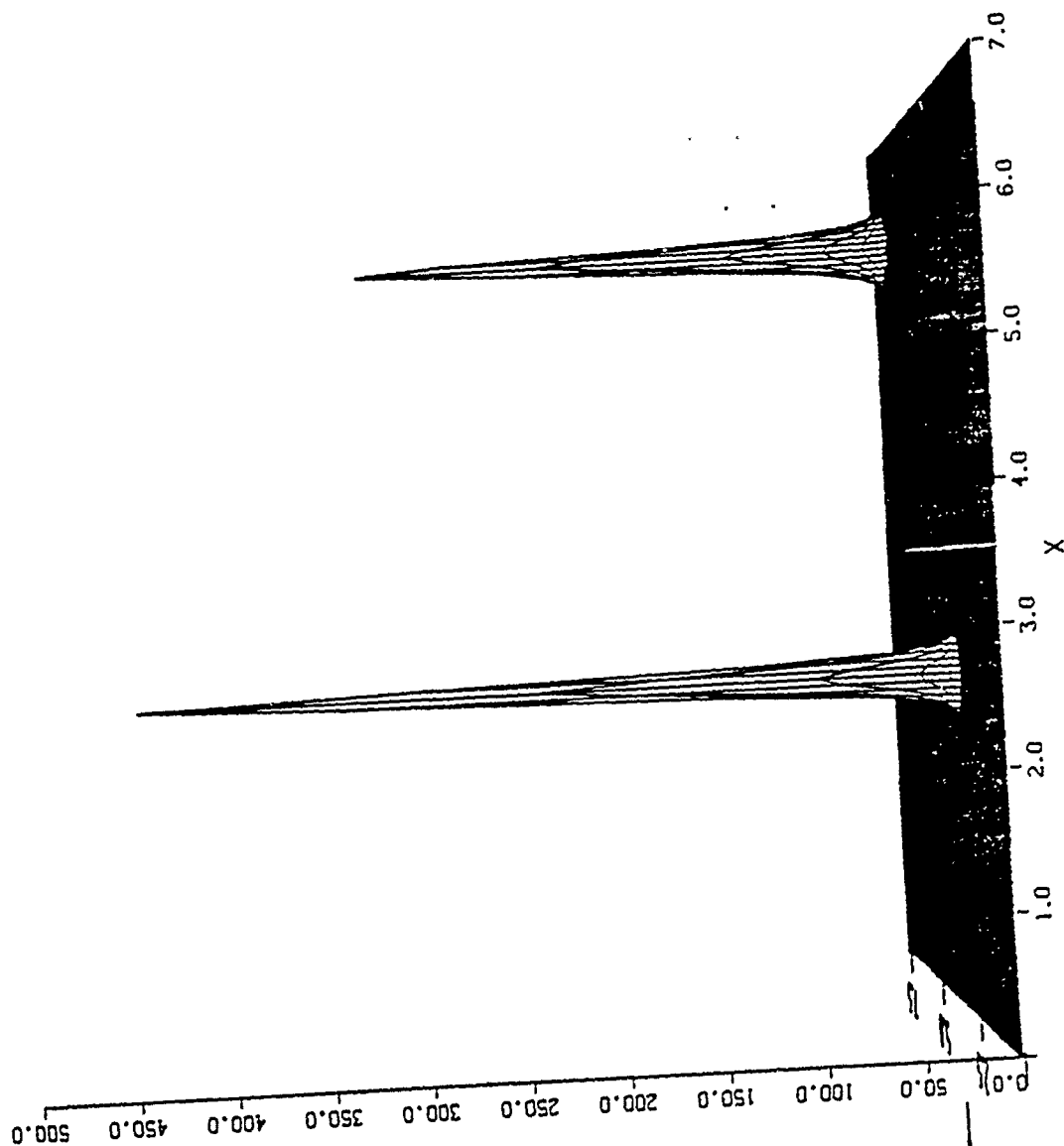
Figure 1e

CLAMP = 1.0000   0.0000

P = 2.00 GO = 0.000E+00 MI = 1836

T = 5.740.
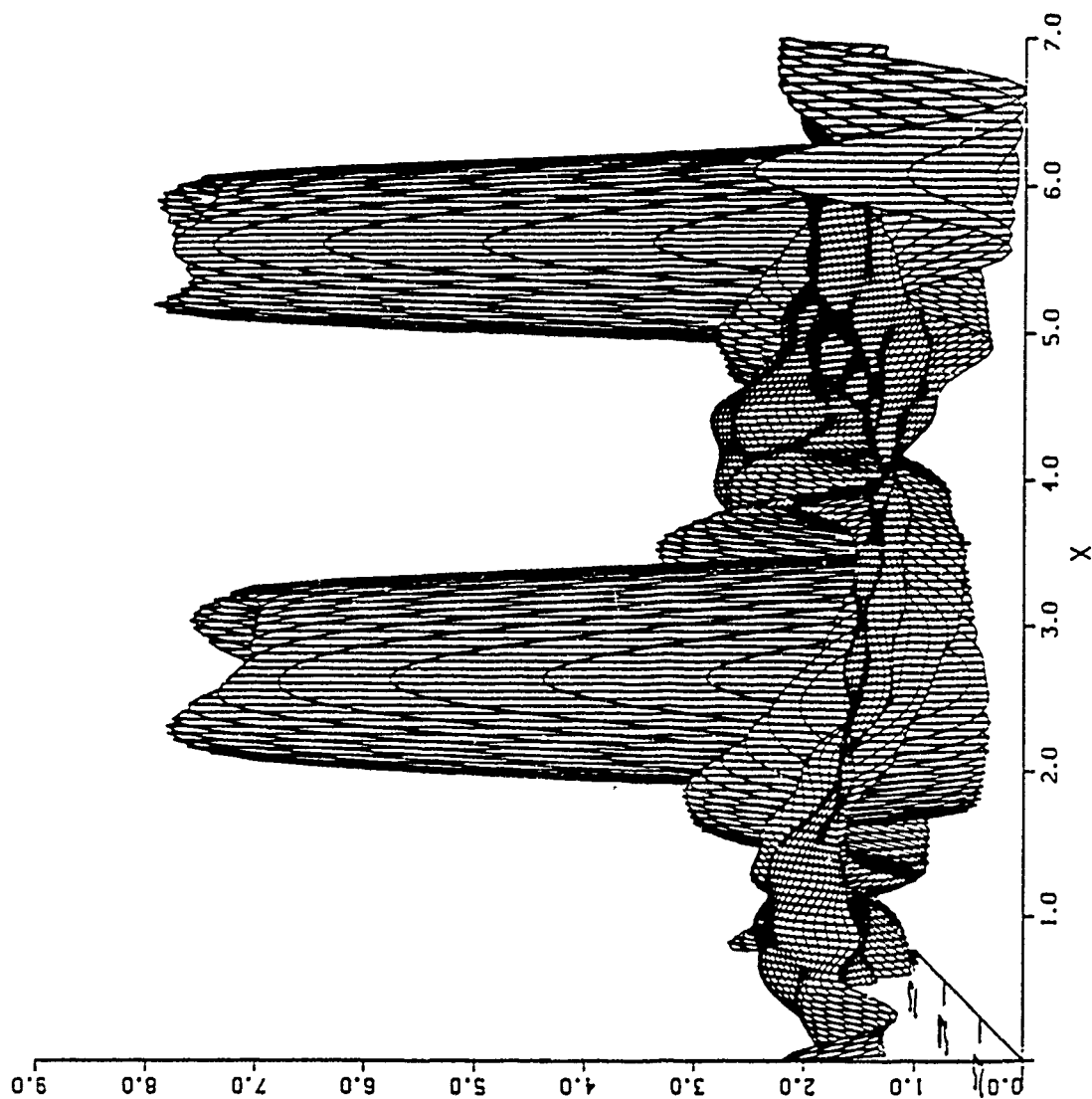
Figure 1f

CLAMP   1.0000   0.0000

P - 2.00 G0 - 0.000E+00 MI - 1836

T - 5.760
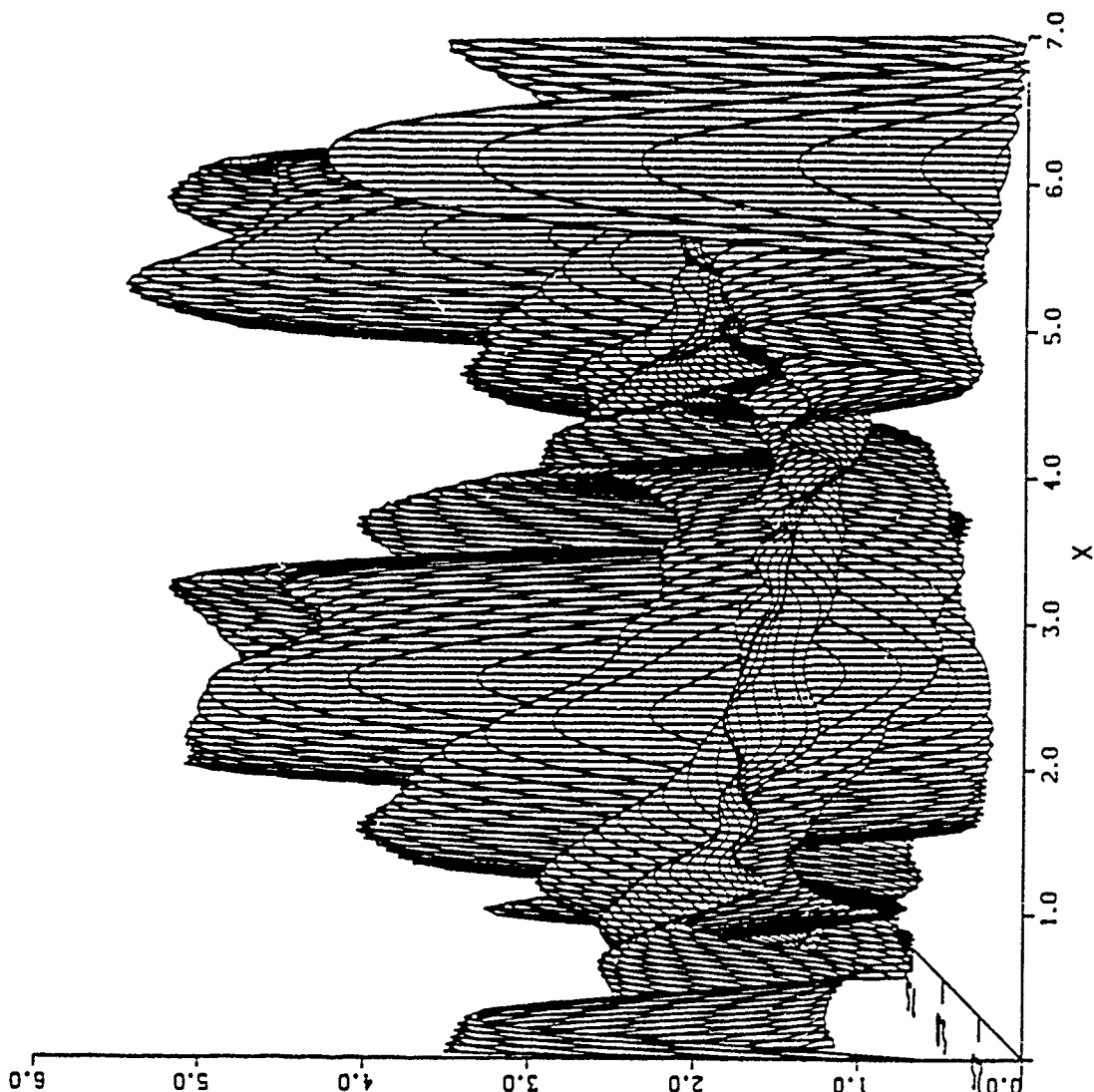
Figure 2a
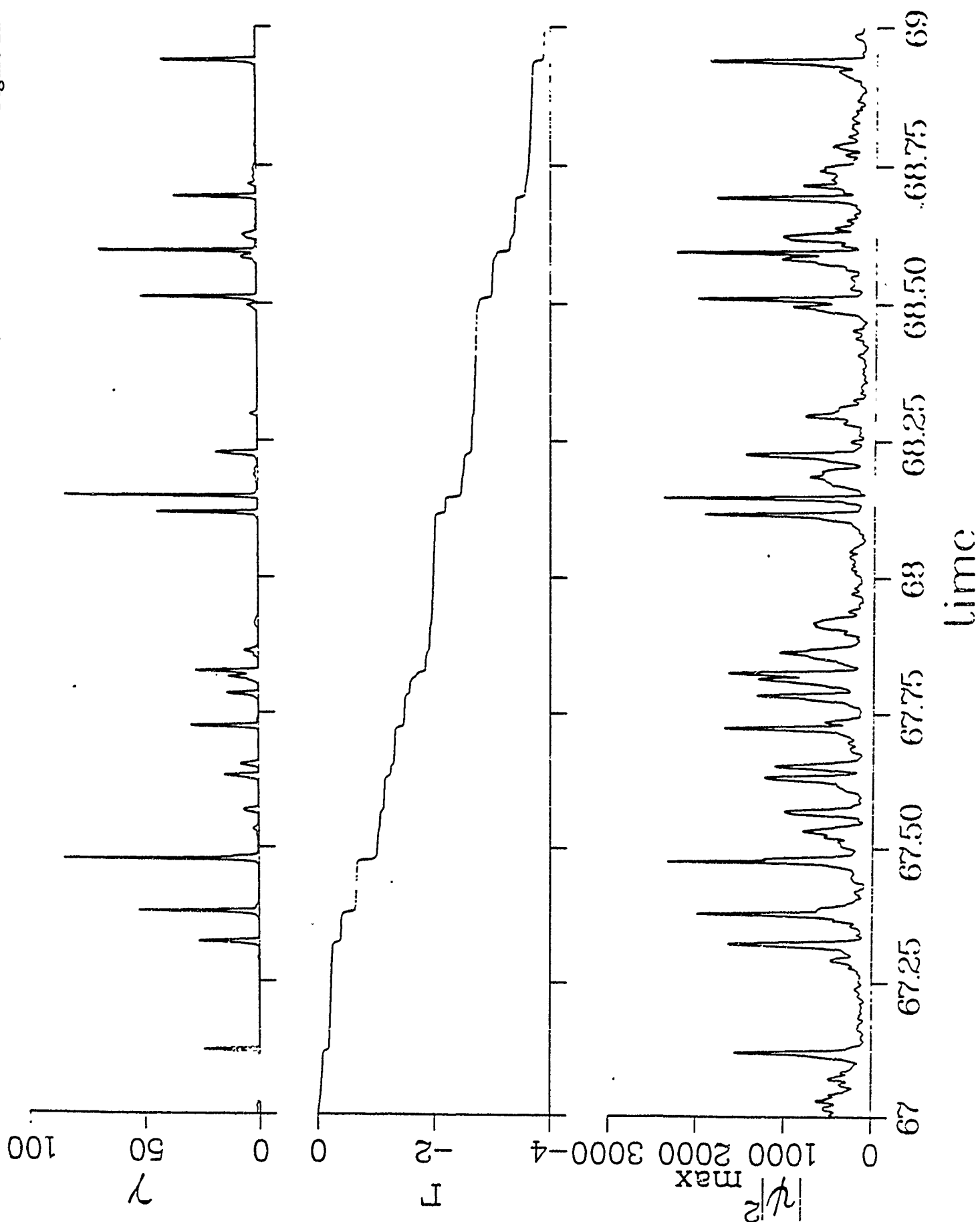
Figure 20
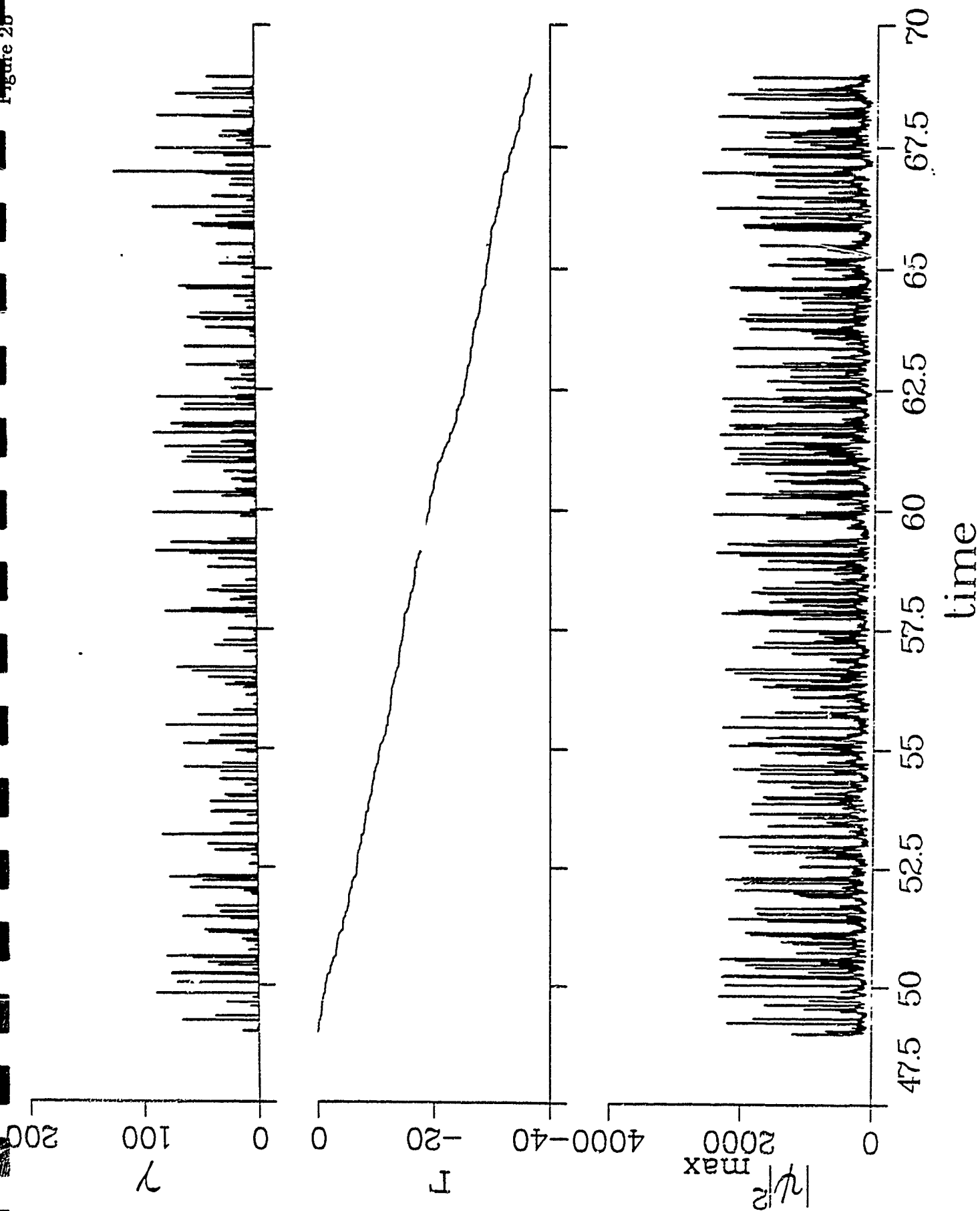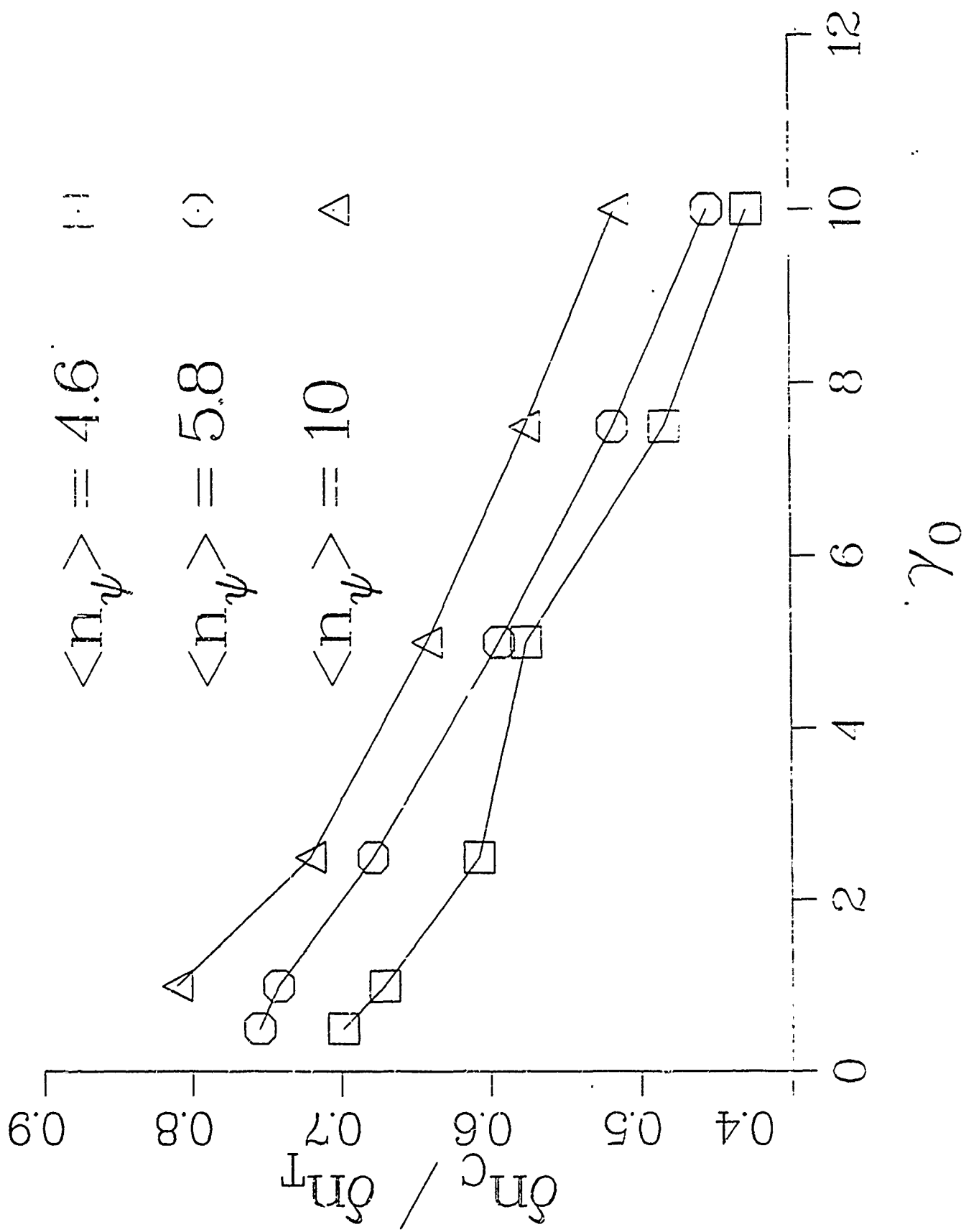
Figure 3

Figure 4

distribution of energies dumped

288 dumps

$p(\delta n)$ vs δn
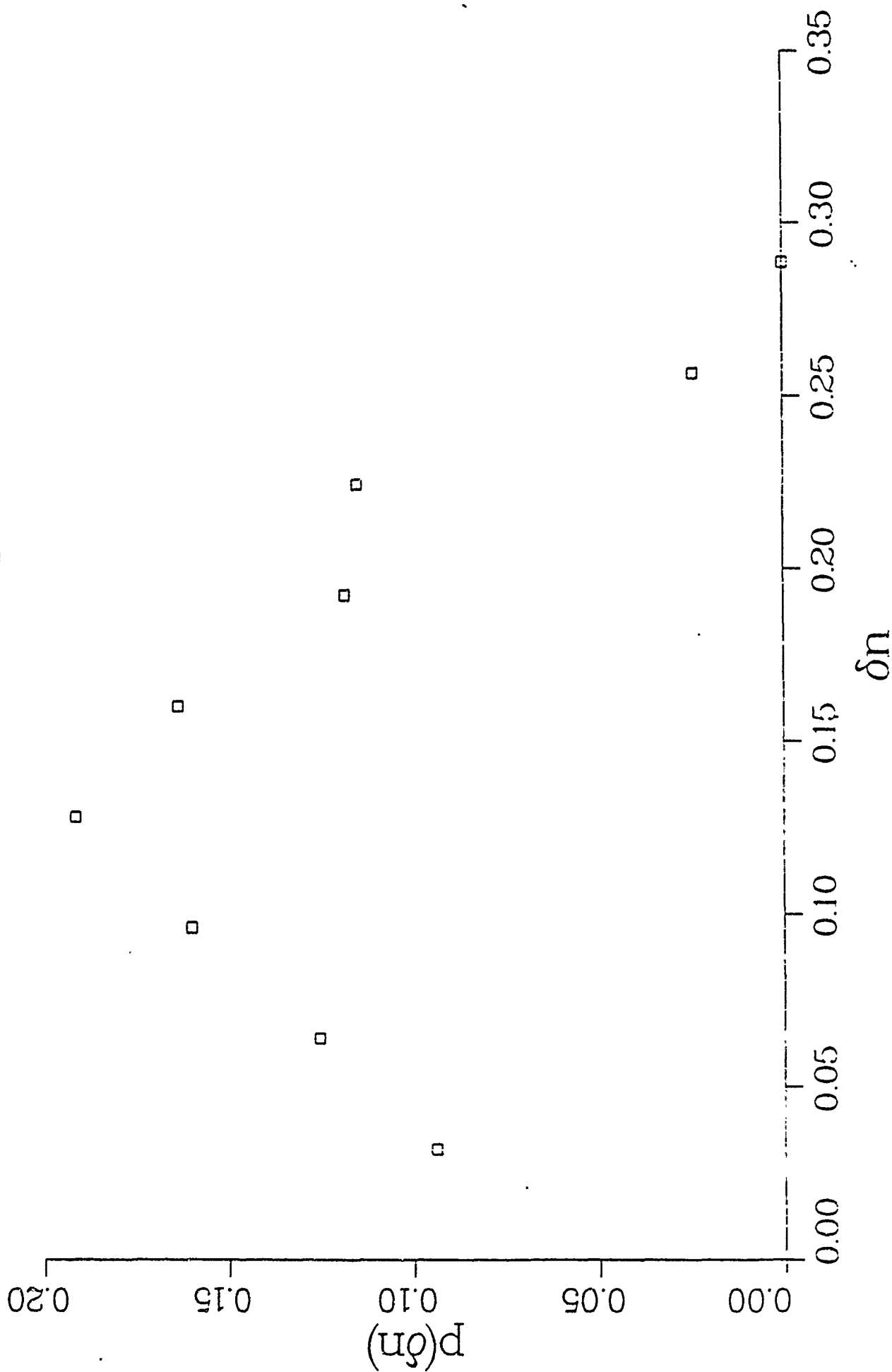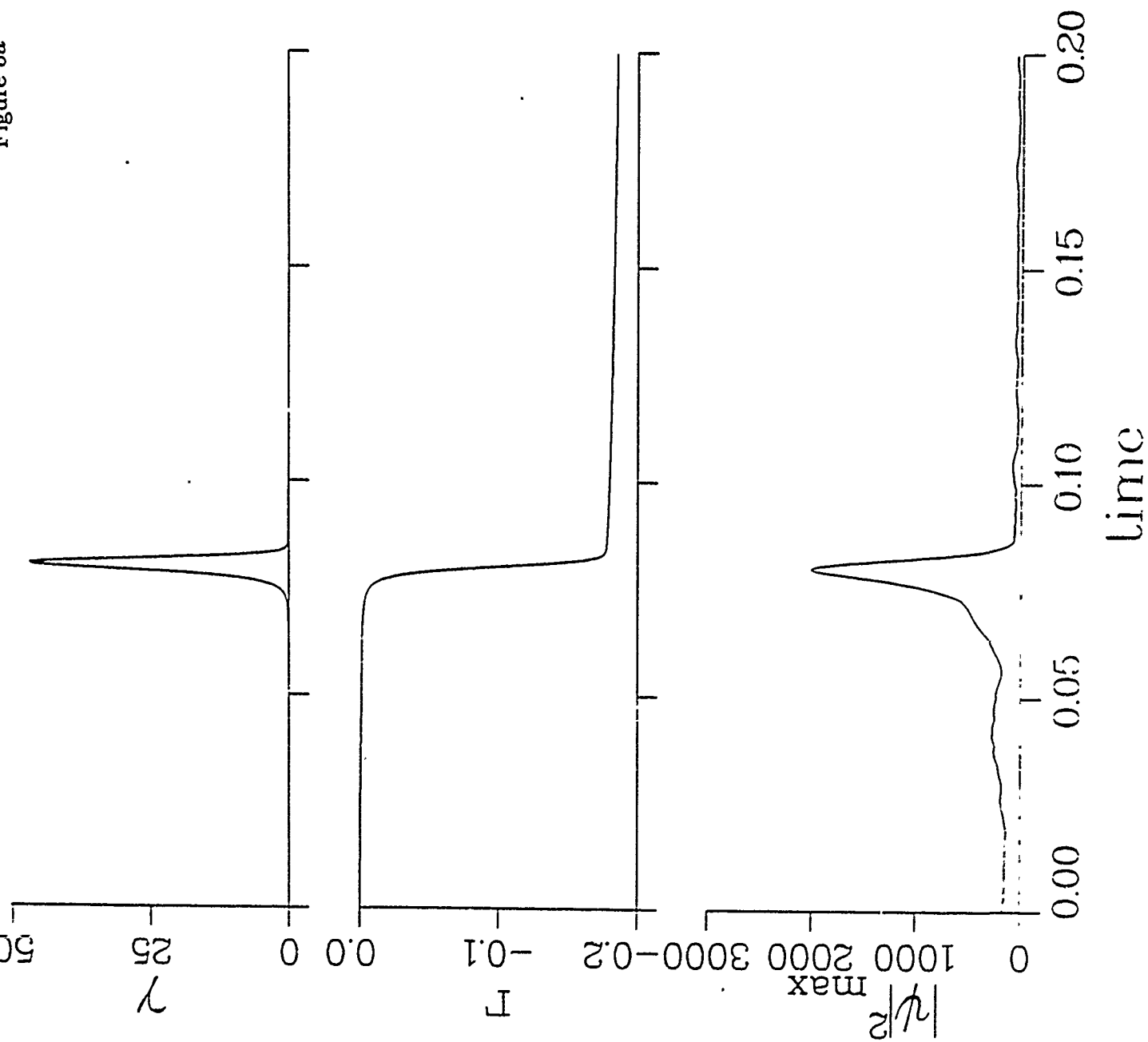
Figure 5a

Figure 5b
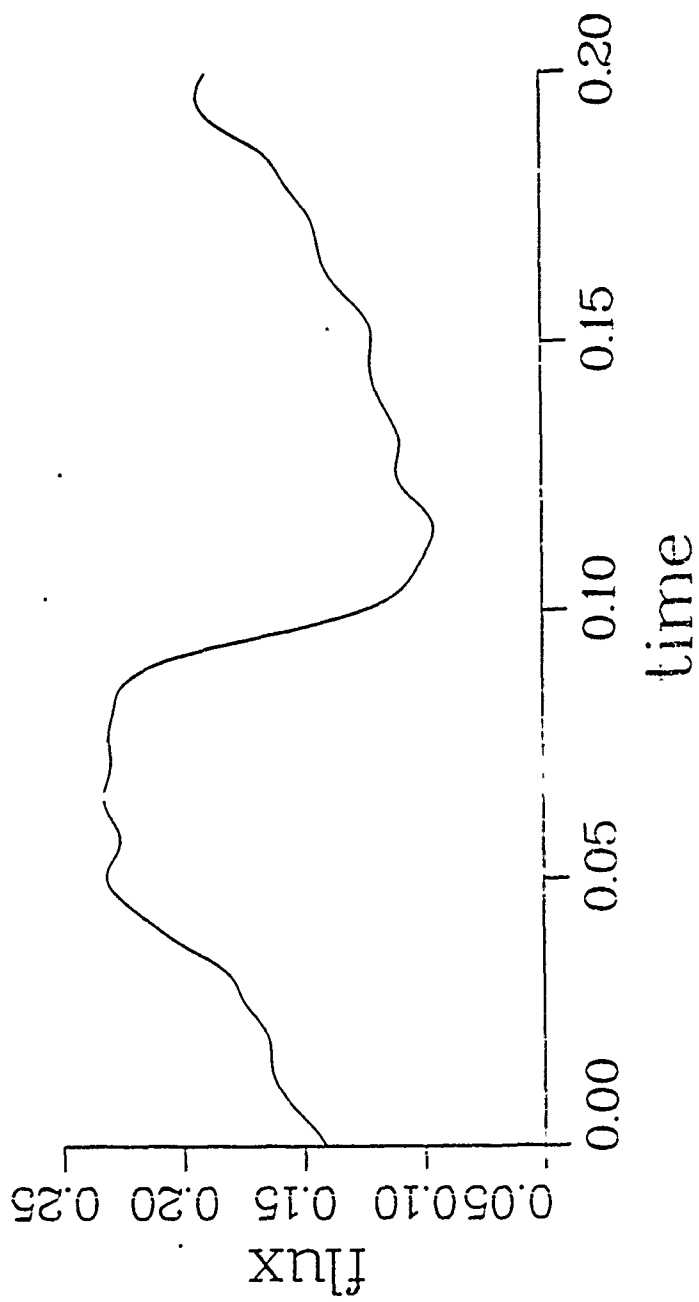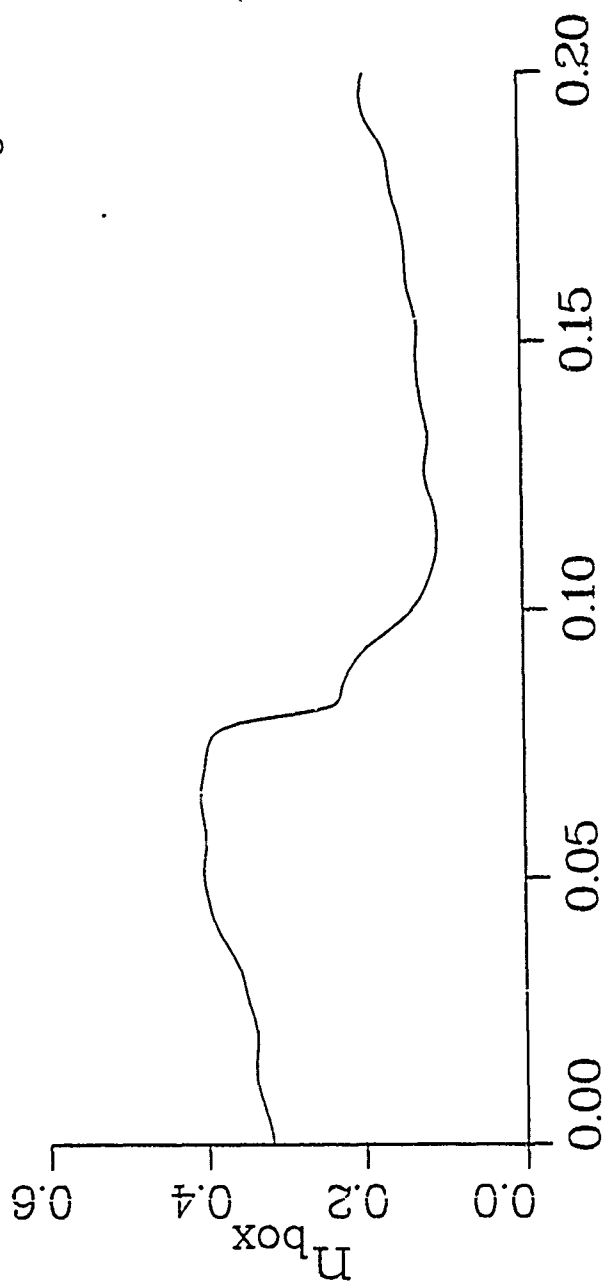
Figure 6
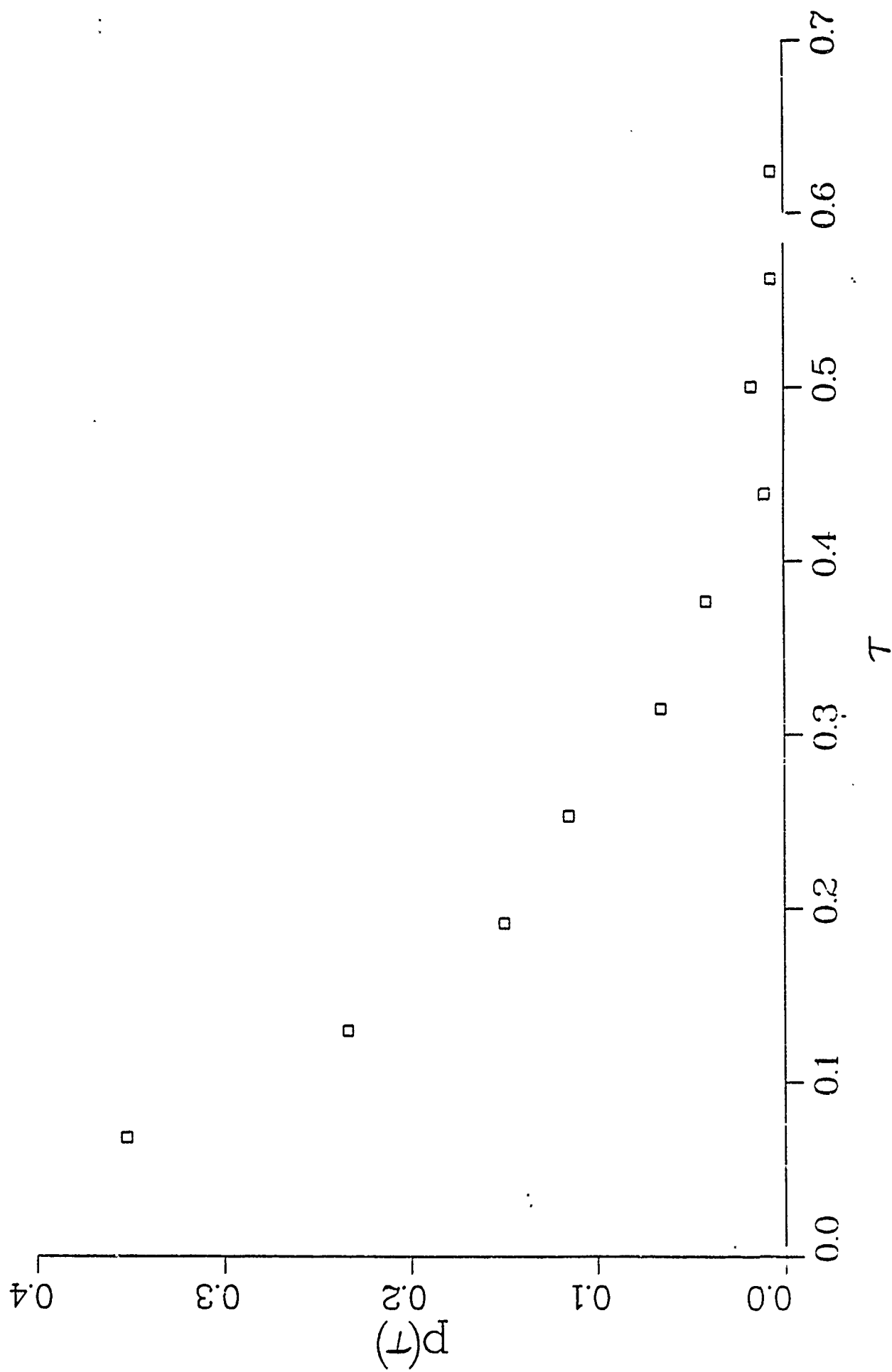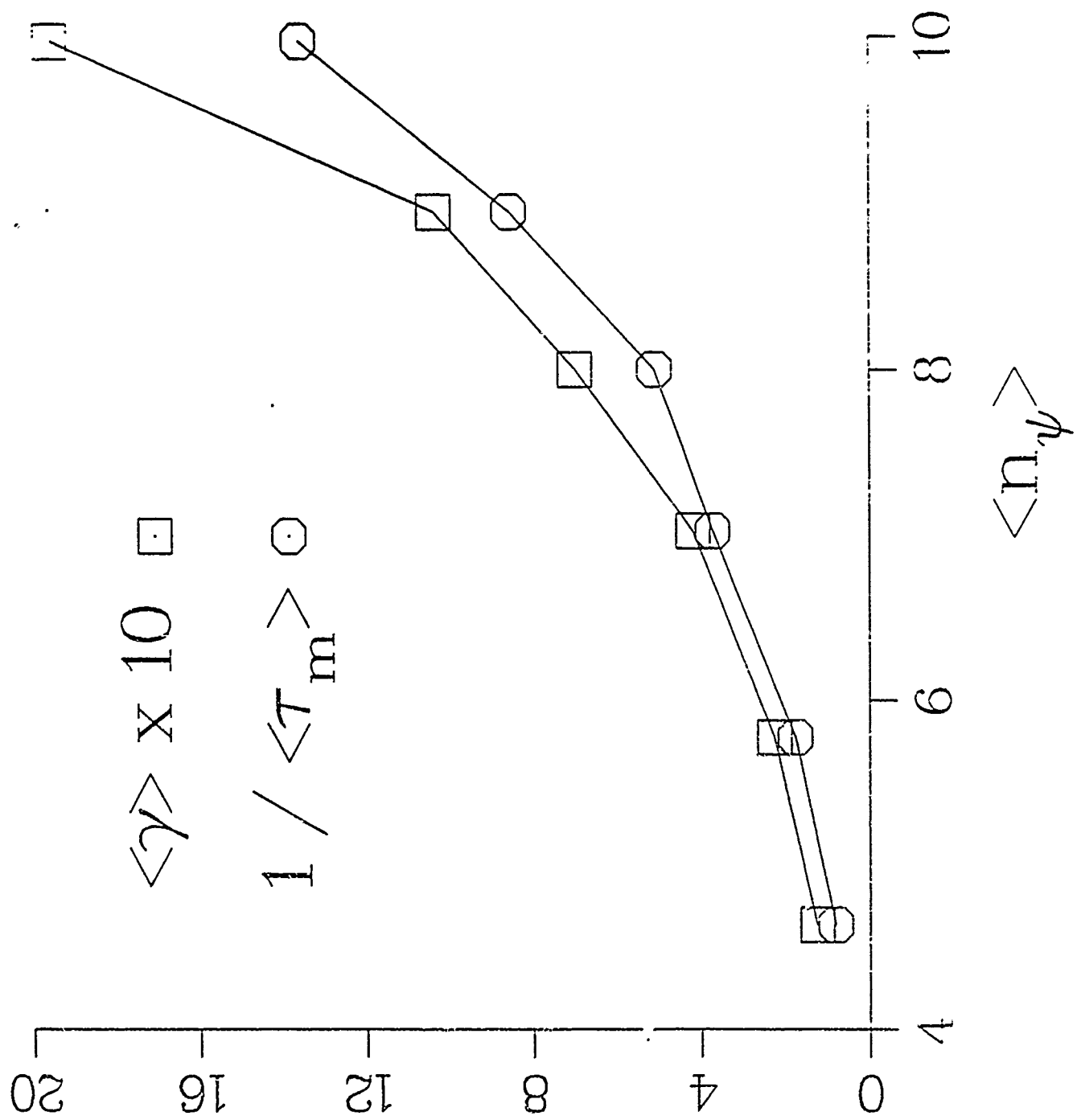
Figure 8a
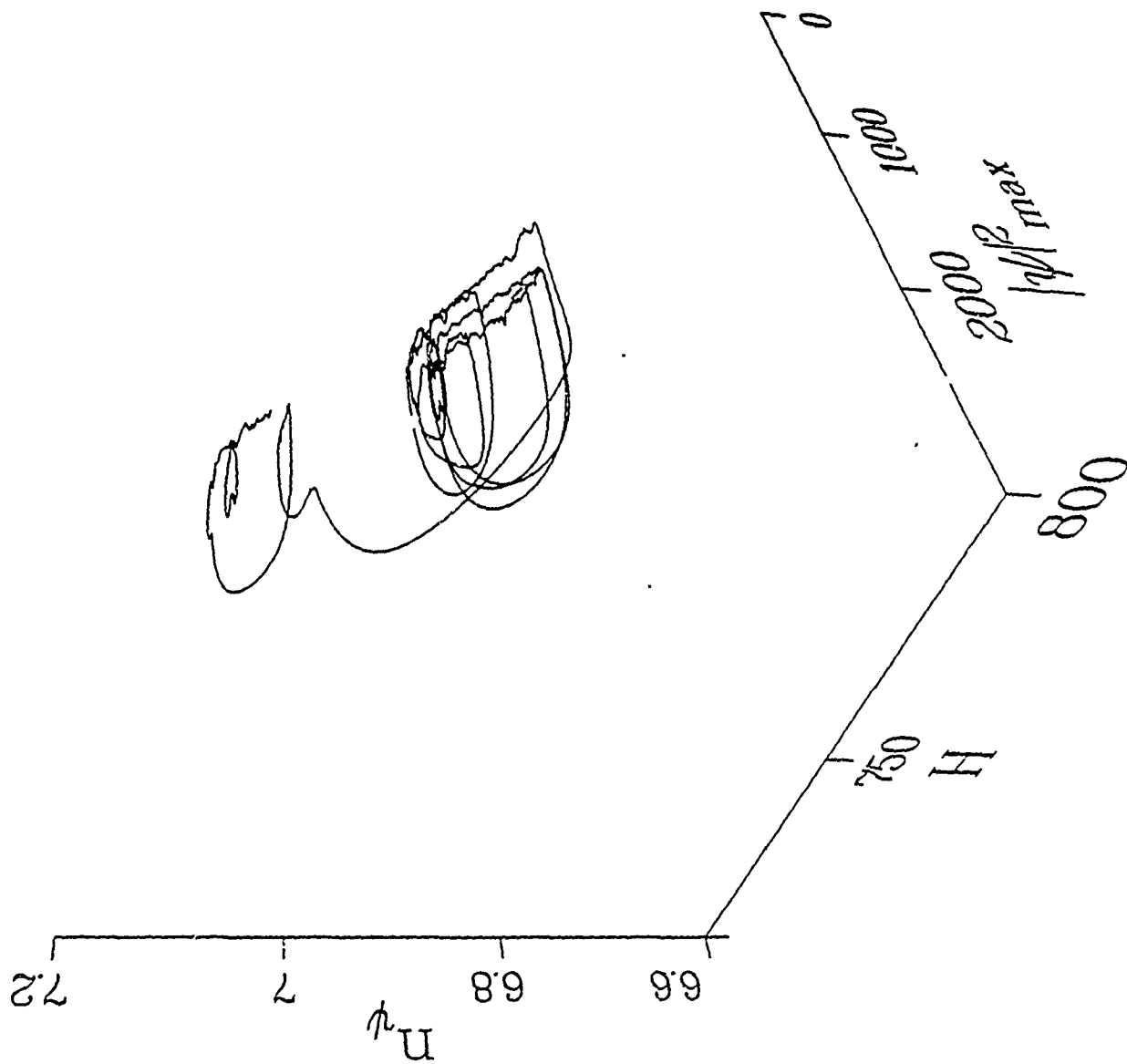
Figure 8b
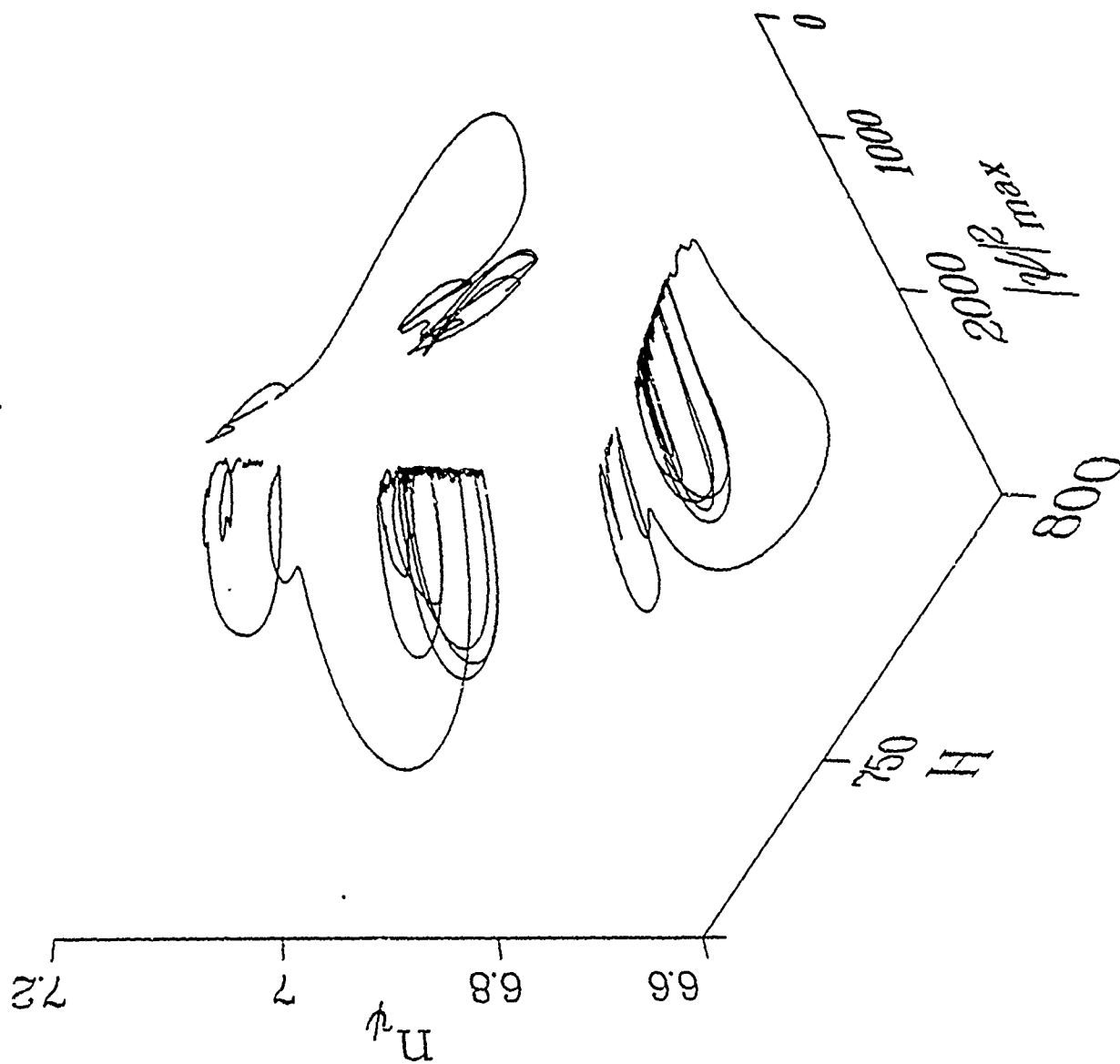
Figure 9

rms k = 9.126
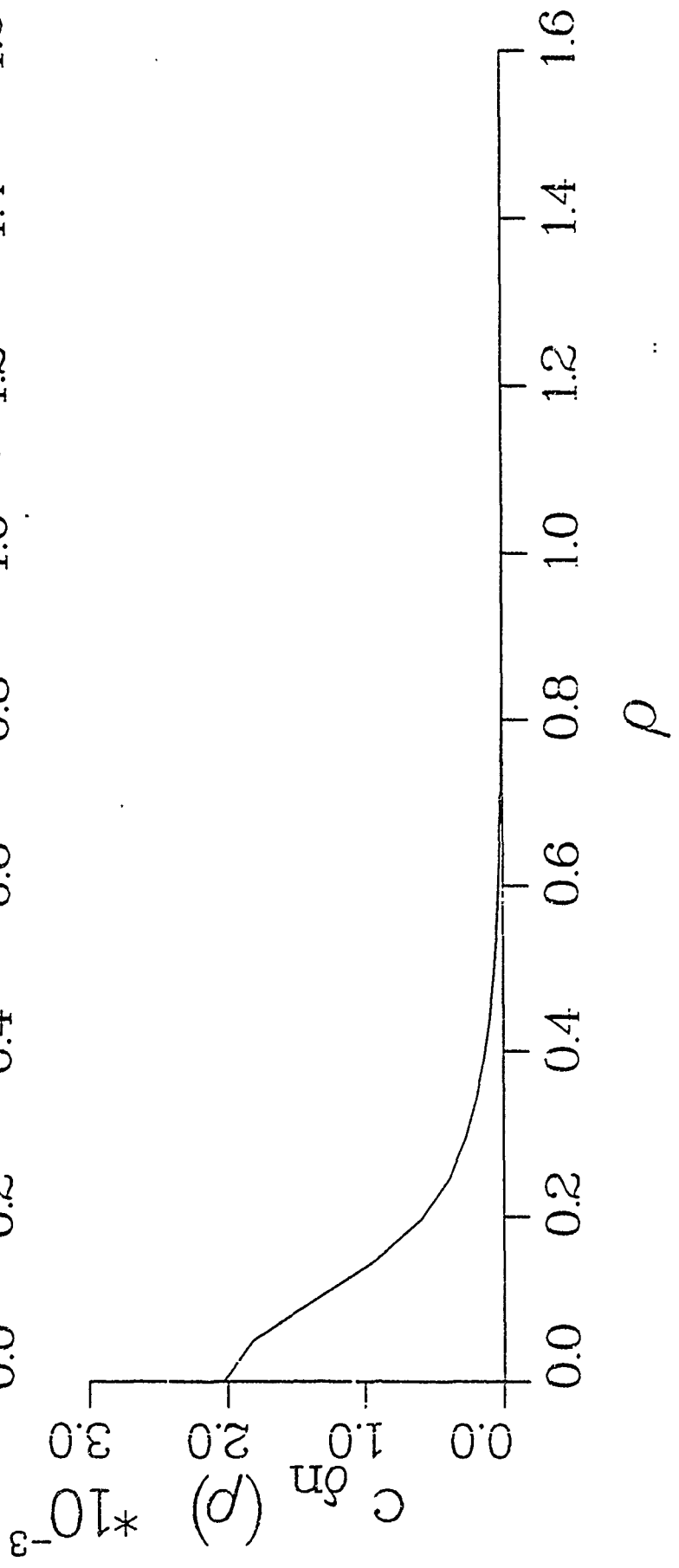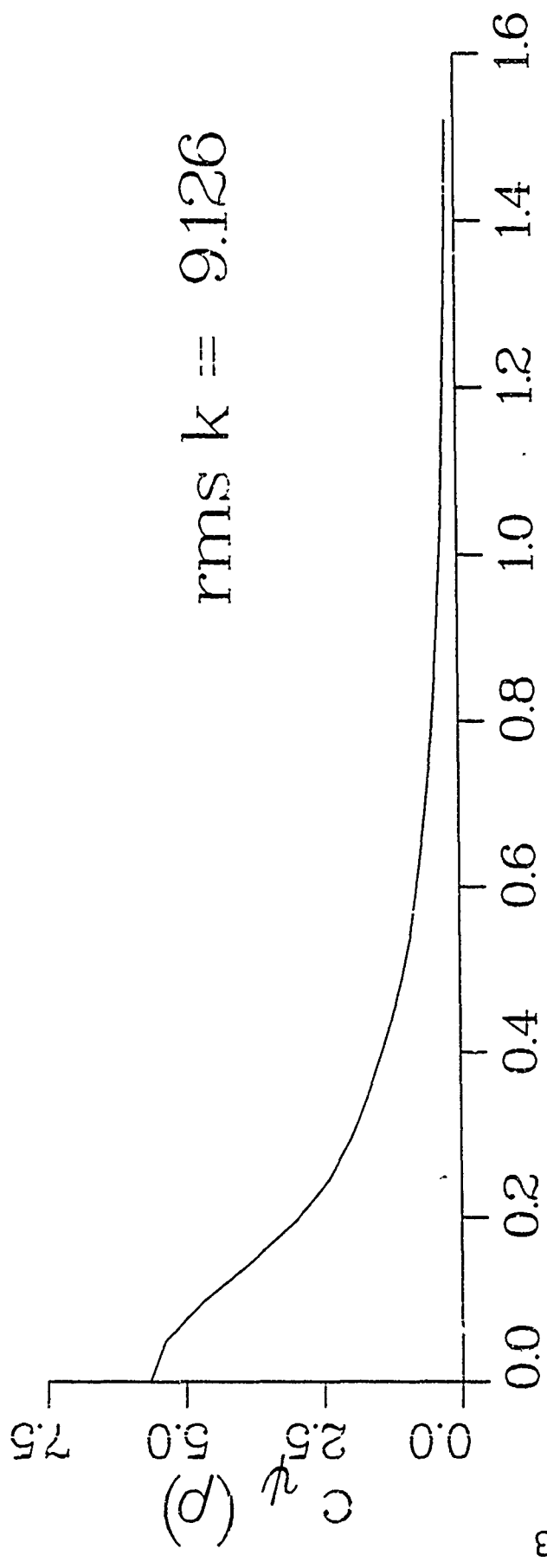
Figure 10

time averaged psi spectrum

Figure 11

damping function

$\gamma_e(k)$
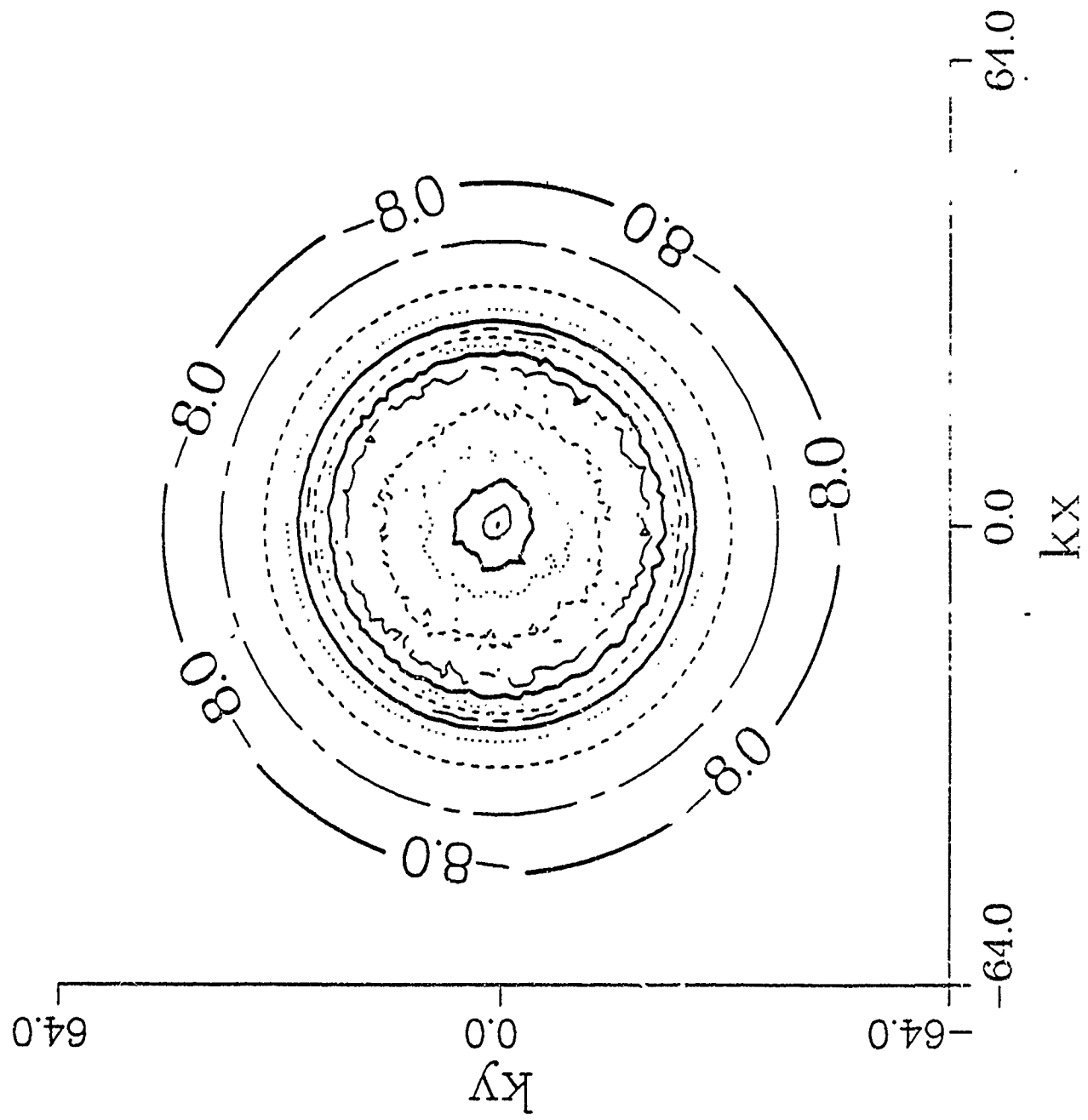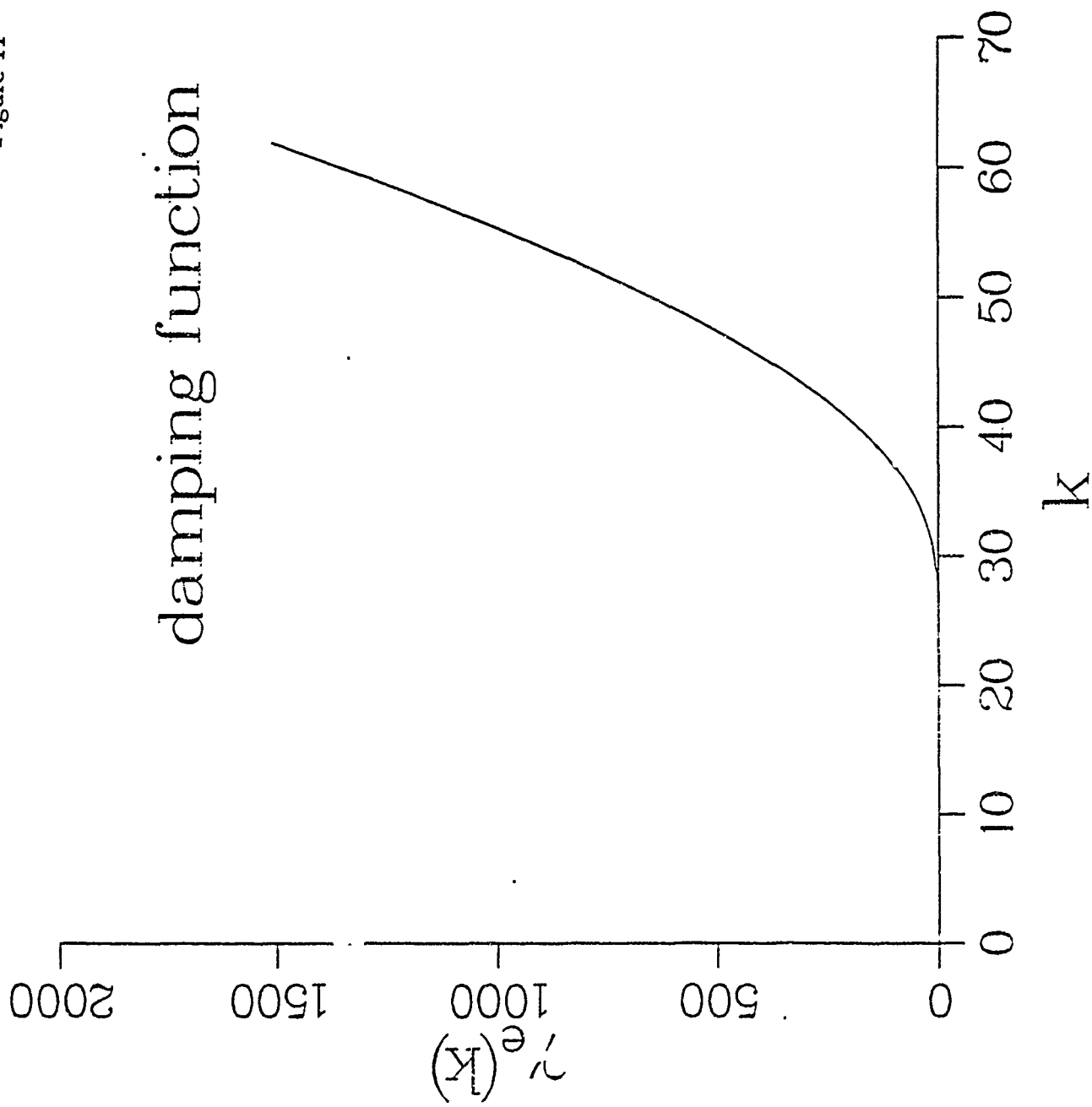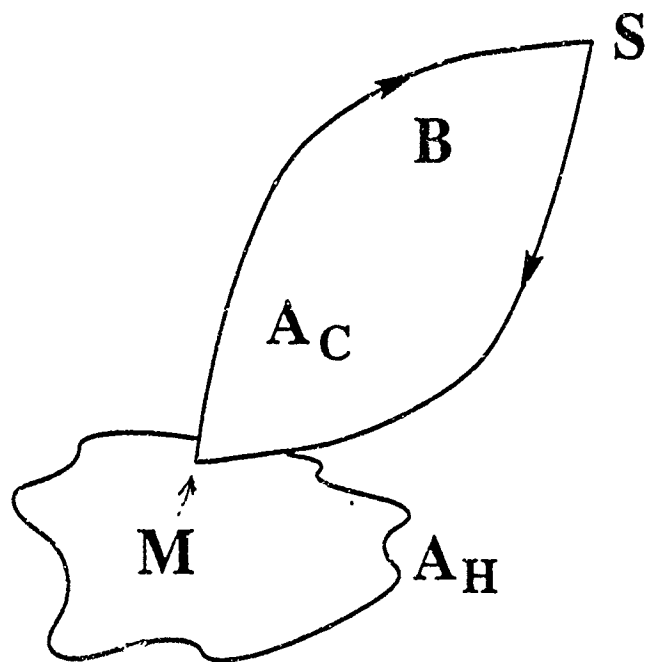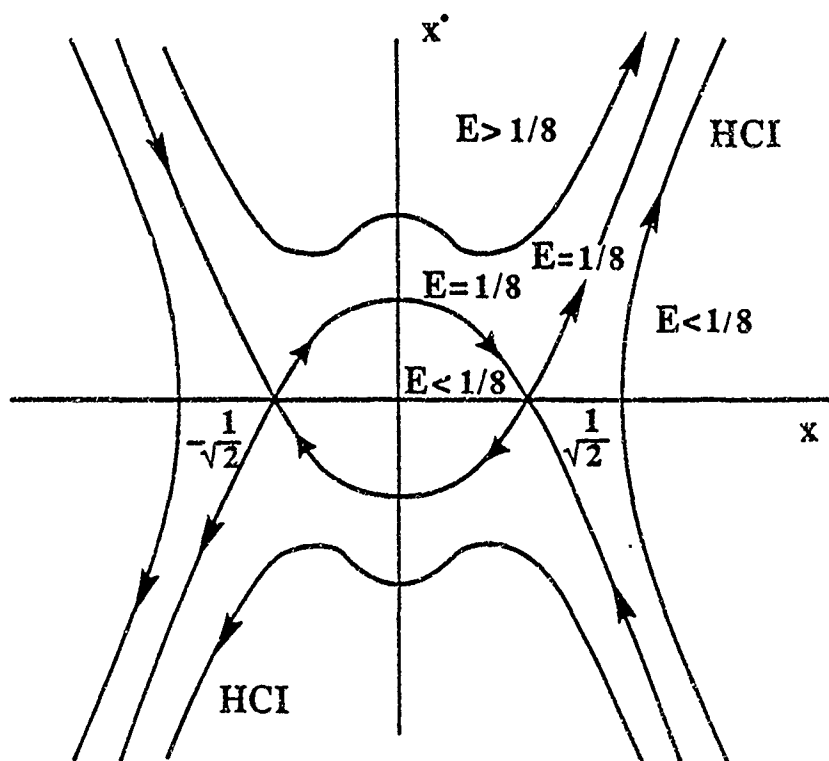
Figure 12

Figure 13a.
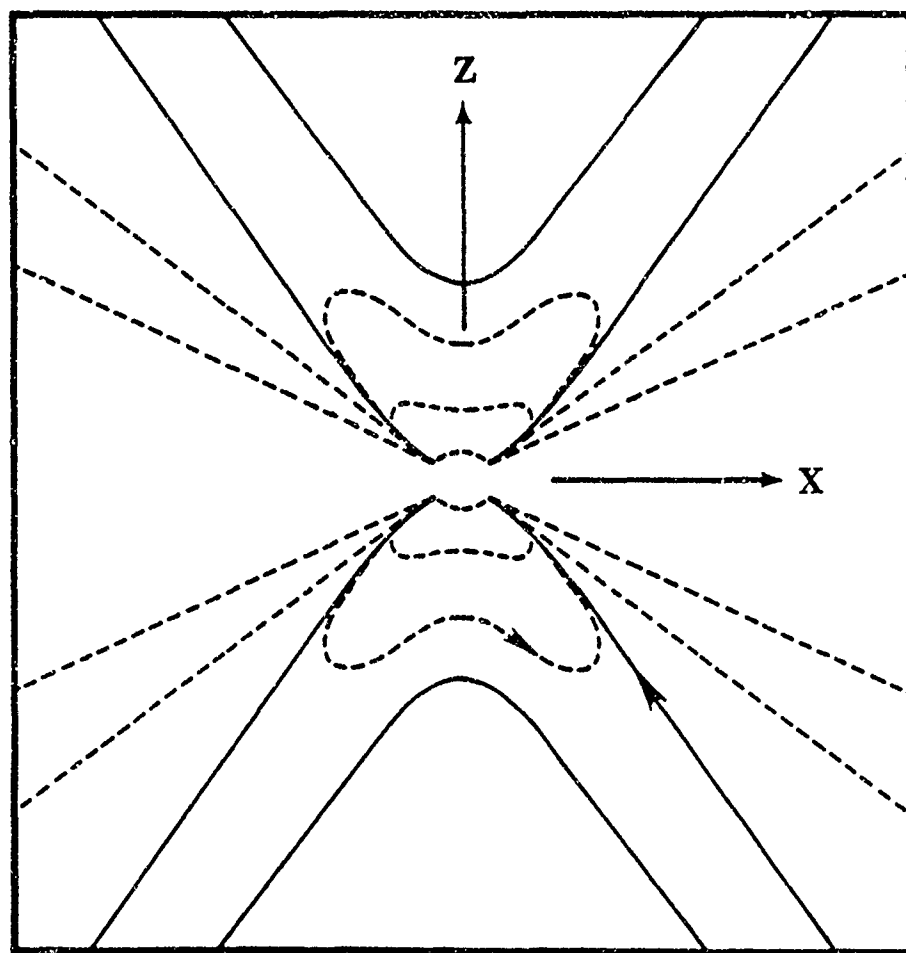
Figure 13b
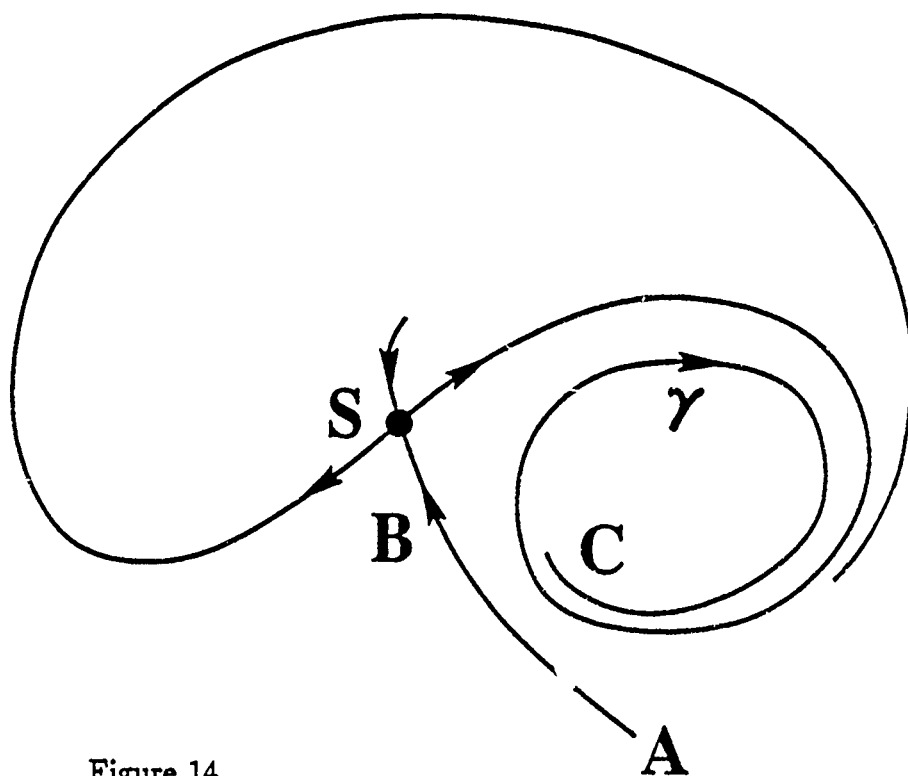
Figure 14

Streamwise Evolution of Naturally Occurring Instabilities

R. A. Petersen

Power spectral densities of streamwise component u' measured at r/D = 0.5 and at various streamwise positions within the laminar/turbulent transition region of axisymmetric jet at U_j = 16 m/s. The initial instability frequency is near 1200 Hz. Successive parings result in spectral peaks at 600 Hz and 300 Hz. The inertial subrange ($f^{-5/3}$*) emerges near x/D = 0.8.

Fourier Decomposition

Since the velocity field is statistically homogeneous and periodic in the aximuthal direction, it is appropriate to decompose the field into Fourier modes. Measurements at [x/D,r/D] = [0.2,0.5], jet speed = 16 m/s.

TOP: Sample time series from eight hot wire sensors. Sample: 1024 points digitized at 50 Hz.

BOTTOM: Decomposed time series. Naturally occurring instabilities are predominantly axisymmetric.

Phase Portrait

Stereoscopic representation phase portrait embedded in three dimensions. Modes: $a_0(t)$, $b_1(t)$, $a_2(t)$; jet speed = 16 m/s; measurement location [x/D,r/D] = [0.2,0.5]; 1024 points @ 50 kHz.

Even though the time series exhibits temporal and spatial coherence, the phase portrait appears high dimensional. Consequently, an attempt is made to develop a statistical model from the phase portrait.

$\Phi_{uu}(f)$

x/D = 0.2

0.3

0.4

0.5

0.6

0.7

0.8

0.9

1.0

10 10^2 10^3 10^4

Frequency, f, Hz

2.

3
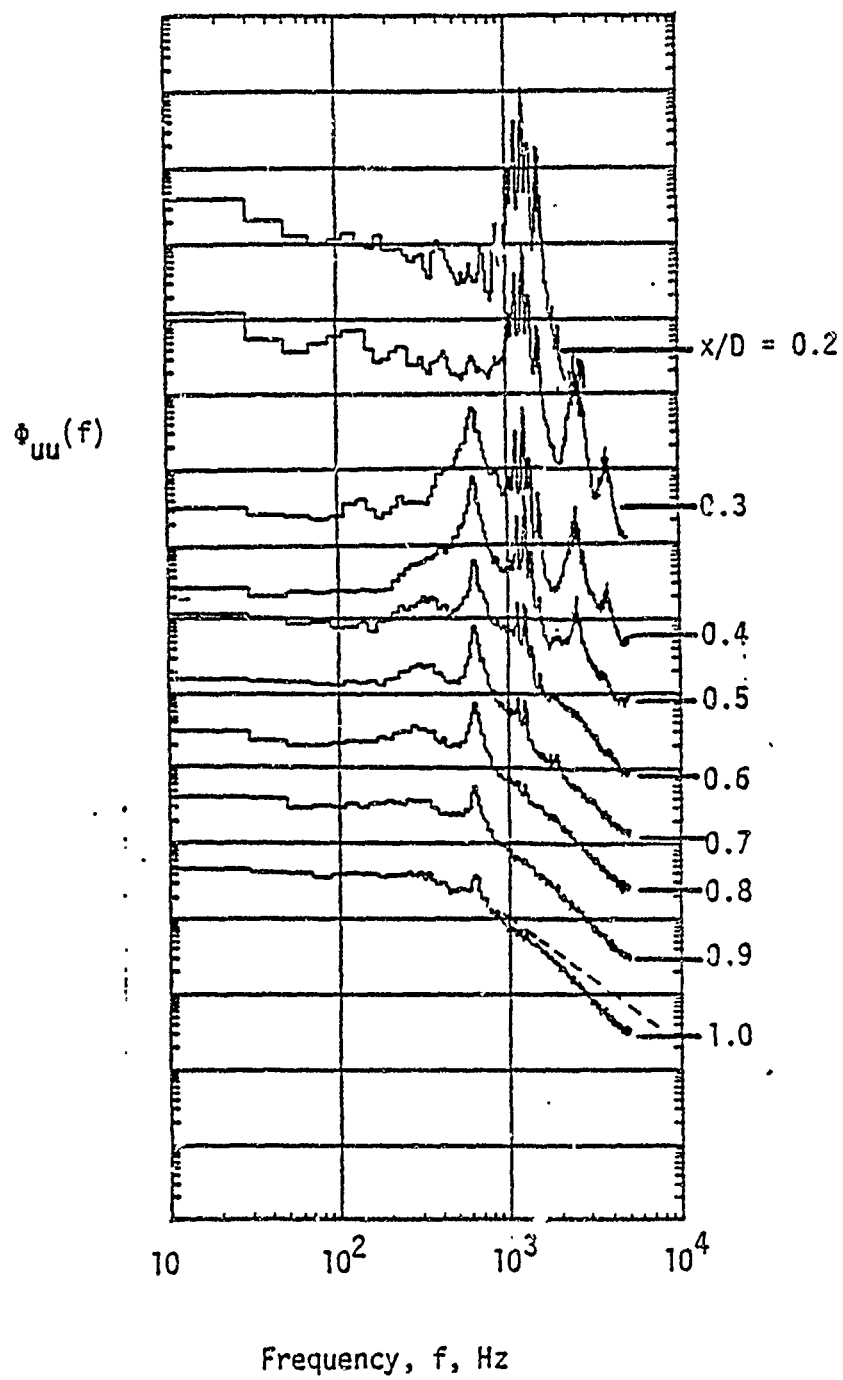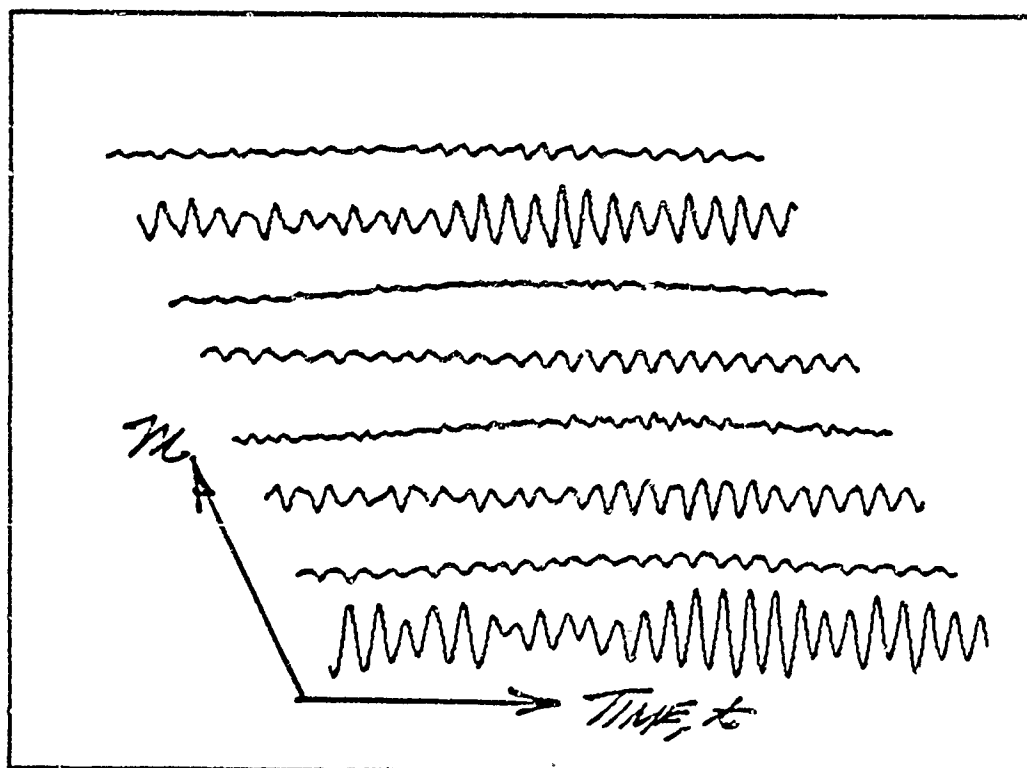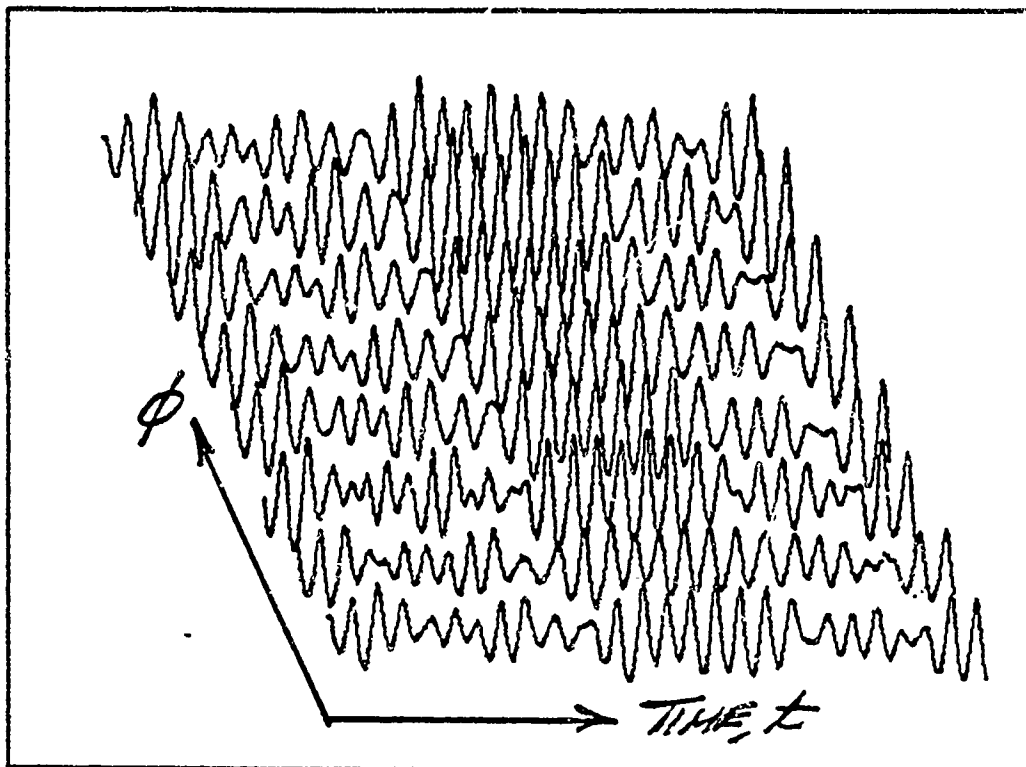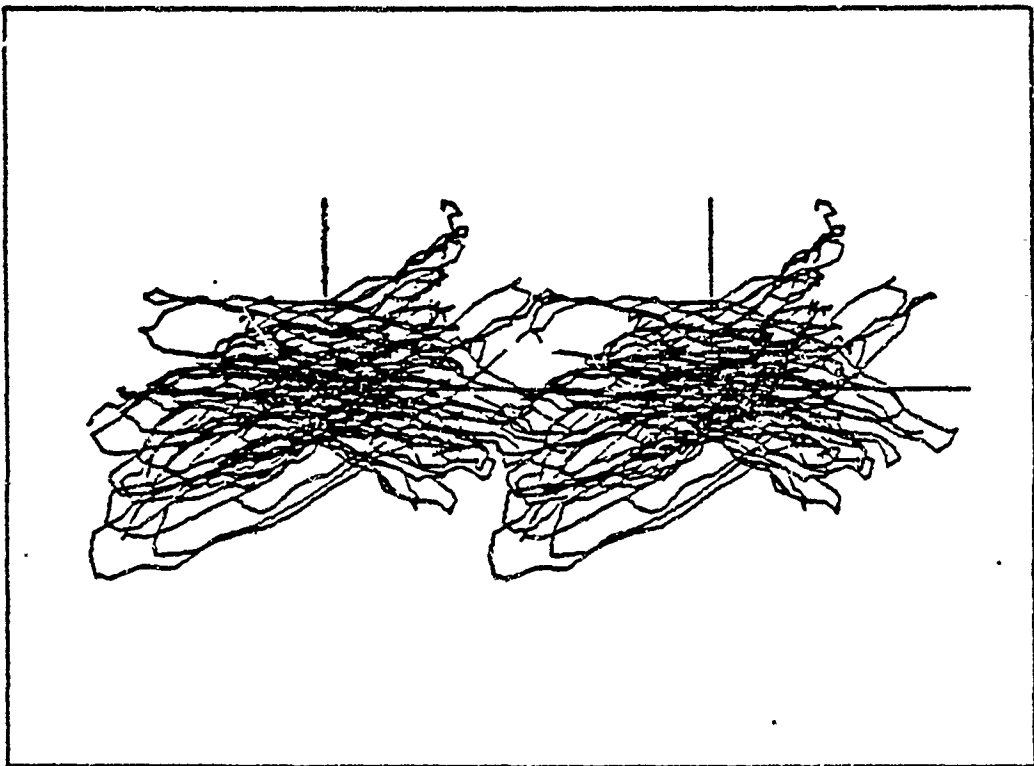
Phase Space Statistics

Based on the fact that the Navier Stokes equations involve first differences in time and that the (incompressible) pressure is determined by the instantaneous velocity field, we model the system as a noise driven Markov process. That is, the expectation of the future state of the system depends only on the present.

The conditional mean represents the temporally coherent part of the decomposed signal and is related to the temporal cross correlation function. The "fine scale" turbulence is modelled by a random vector of zero mean and unity variance. The conditional covariance can be decomposed locally into a set of eigenvectors and eigenvalues. If the conditional, joint statistics are uncorrelated one would expect the conditional eigenvectors to parallel the basis vectors of the original decomposition.

Measured Conditional Accelerations

Joint statistics are based on $a_o(t)$, horizontal axis, and on $b(t)$, vertical axis. Measurements span the region from laminar flow to fully developed (based on emergence of inertial subrange) turbulence. At $x/D = 0.2$ the conditional convariance eigenvectors are correlated by the instability; by $x/D = 0.8$ the conditional means are small compared to the conditional covariance eigenvalues (root mean square) and the conditional, joint statistics appear to be uncorrelated.
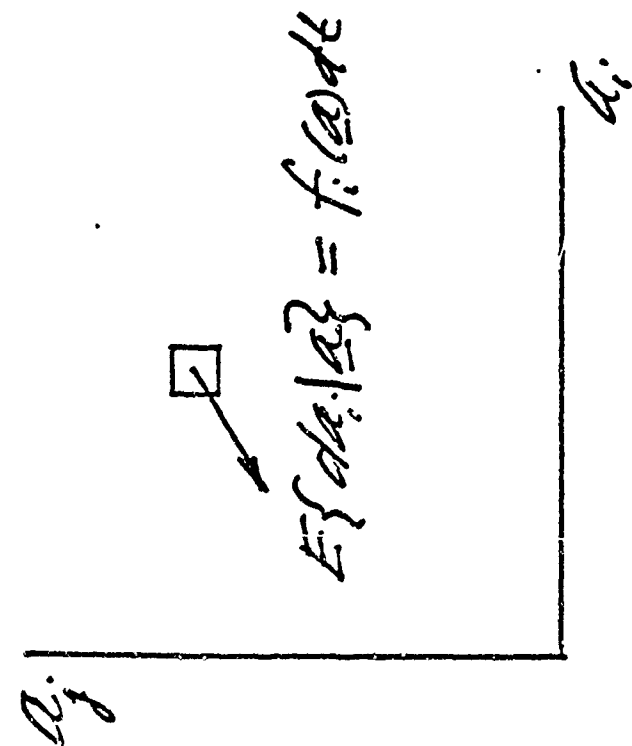
In each case the sampling rate was 50 kHz, and the joint statistics are based on 1,024,000 data points. The data was
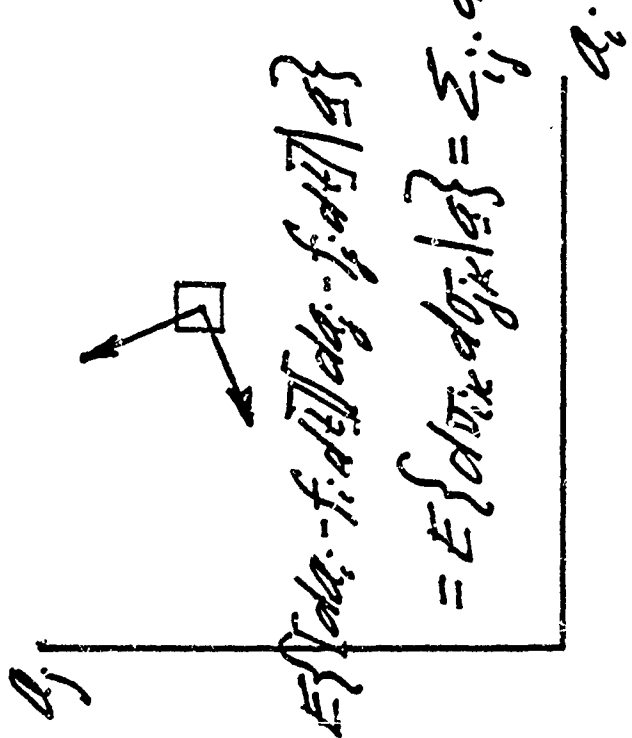
5

PHASE SPACE STATISTICS

$$u(\phi, t) = a_0(t) + \sum_m a_m(t) \cos m\phi + \sum_m b_m(t) \sin m\phi$$
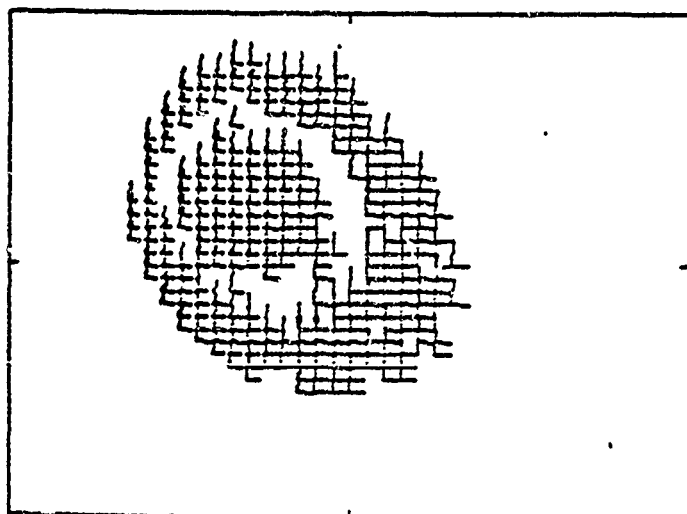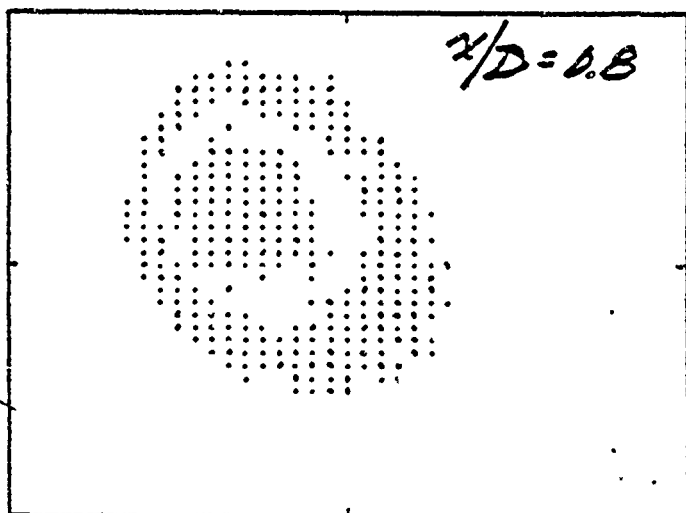
$$da_i = f_i(a)\, dt + \beta_{ik}\, d\sigma_{ik}$$
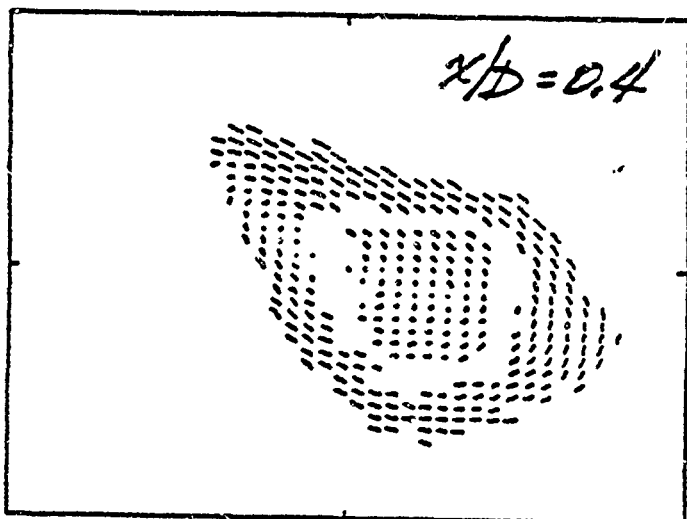
$$E\{\beta_i \cdot \beta_j\} = 0$$

$$E\{\beta_i \cdot \beta_i \cdot \beta_j\} = \delta_{ij}$$

$$E\left\{\int da_i \,|\, a\right\} = f_i(a)\, dt$$

$$E\left\{\int [da_i - f_i\, dt][da_j - f_j\, dt] \,|\, a\right\} = E\left\{\int d\sigma_{ik}\, d\sigma_{jk} \,|\, a\right\} = \sum_{ij} dt$$

$$E\{d\alpha\,|\,\alpha\}$$

$$E\{d\sigma_{ik}\,d\sigma_{jkl}\,|\,\alpha\}$$

7
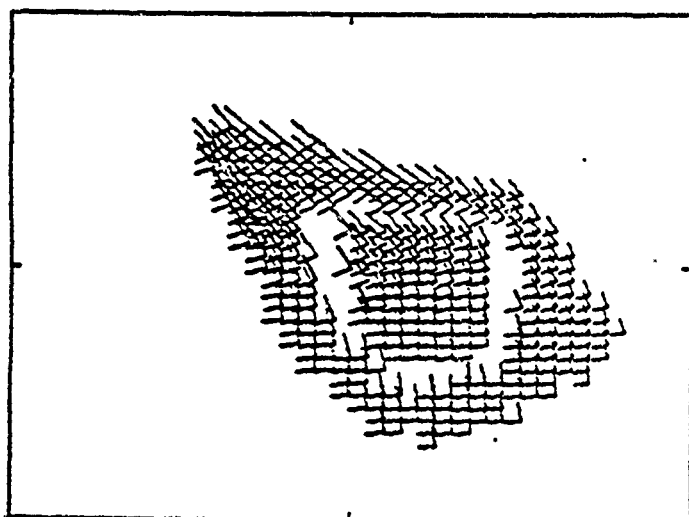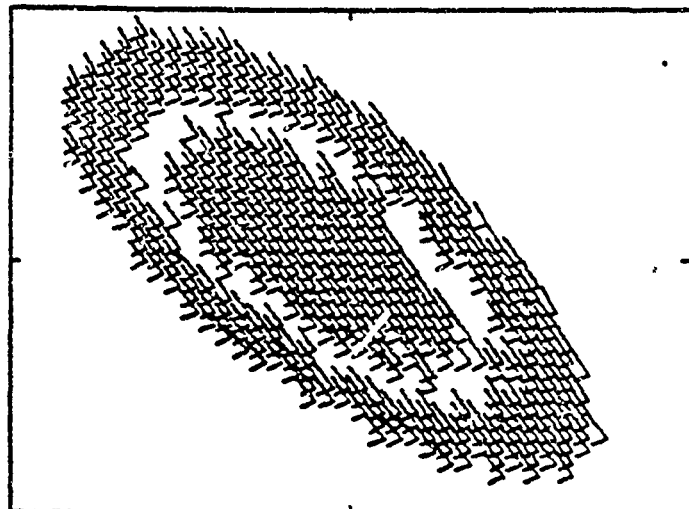
digitized in 1024 point records and de-meaned before being decomposed into Fourier modes. The display is modulated by contours of joint probability density: contours between 50-70% and between 80-100% of the peak value were selected. The joint probability distributions are evidently skewed and the display is approximately 4 x 4 standard deviations. Approximate because the scaling is based on the first 1% of the database.